

TOPICS IN CELESTIAL MECHANICS

RICHARD MOECKEL

1. THE NEWTONIAN n -BODY PROBLEM

Celestial mechanics can be defined as the study of the solution of Newton's differential equations formulated by Isaac Newton in 1686 in his *Philosophiae Naturalis Principia Mathematica*.

The setting for celestial mechanics is three-dimensional space:

$$\mathbb{R}^3 = \{q = (x, y, z) : x, y, z \in \mathbb{R}\}$$

with the Euclidean norm:

$$|q| = \sqrt{x^2 + y^2 + z^2}.$$

A *point particle* is characterized by a position $q \in \mathbb{R}^3$ and a mass $m \in \mathbb{R}^+$. A motion of such a particle is described by a curve $q(t)$ where t runs over some interval in \mathbb{R} ; the mass is assumed to be constant. Some remarks will be made below about why it is reasonable to model a celestial body by a point particle. For every motion of a point particle one can define:

$$\text{velocity: } v(t) = \dot{q}(t)$$

$$\text{momentum: } p(t) = mv(t).$$

Newton formulated the following laws of motion:

Lex.I. *Corpus omne perservare in statu suo quiescendi vel movendi uniformiter in directum, nisi quatenus a viribus impressis cogitur statum illum mutare*¹

Lex.II. *Mutationem motus proportionem esse vi motrici impressae et fieri secundem lineam qua vis illa imprimitur.*²

Lex.III *Actioni contrarium semper et aequalem esse reactionem: sive corporum duorum actiones in se mutuo semper esse aequales et in partes contrarias dirigi.*³

The first law is statement of the principle of inertia. The second law asserts the existence of a force function $F : \mathbb{R}^4 \rightarrow \mathbb{R}^3$ such that:

$$\dot{p} = F(q, t) \quad \text{or} \quad m\ddot{q} = F(q, t).$$

In celestial mechanics, the dependence of $F(q, t)$ on t is usually indirect; the force on one body depends on the positions of the other massive bodies which in turn depend on t . The third law postulates the symmetry of the mutual interaction of two bodies which will apply, in particular, to the gravitational interaction.

Date: May 4, 2020.

¹Every body continues in its quiescent state or moves uniformly in direction, unless it is compelled by impressed forces to change its state.

²The change of momentum is proportional to the motive force impressed and takes place along the line where this force is impressed.

³To every action there is always an equal and opposite reaction: the actions of two bodies on one another are always equal and aimed in opposite directions.

The *n-body problem* is about the motion of n point particles under the influence of their mutual gravitational attraction. Each particle has a mass $m_i > 0$ and position, velocity and momentum vectors $q_i, v_i, p_i \in \mathbb{R}^3$. The whole system can be described using the vectors $q, v, p \in \mathbb{R}^{3n}$ where

$$q = (q_1, q_2, \dots, q_n) \quad v = (v_1, v_2, \dots, v_n) \quad p = (m_1 v_1, m_2 v_2, \dots, m_n v_n).$$

According to Newton, the gravitational force acting on particle i due to the presence of particle j is

$$F_{ij} = \frac{G m_i m_j (q_j - q_i)}{|q_i - q_j|^3}$$

where G is a constant. Note that F_{ij} acts along the line containing the masses. It's proportional to the product of the two masses and inversely proportional to the distance between them (see Figure 1). The force produced on m_j by m_i is $F_{ji} = -F_{ij}$ by Newton's third law. By choosing the units of mass, one can arrange that $G = 1$ and this will be assumed from now on (see Exercise 1.1).

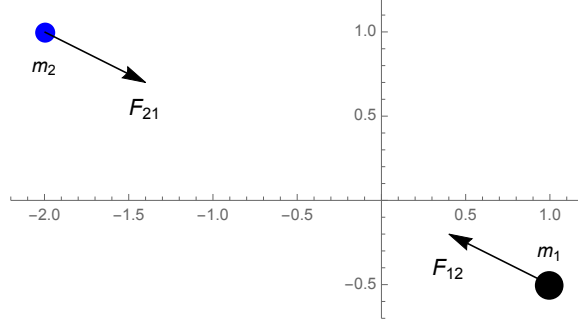


FIGURE 1. Newtonian gravitational forces.

The force on the i -th mass due to the other $n - 1$ masses is:

$$F_i = \sum_{j \neq i} F_{ij} = \sum_{j \neq i} \frac{m_i m_j (q_j - q_i)}{|q_j - q_i|^3}.$$

This can be written:

$$F_i(q) = \nabla_i U(q)$$

where

$$(1) \quad U(q) = \sum_{\substack{(i,j) \\ i < j}} \frac{m_i m_j}{|q_i - q_j|}$$

and ∇_i is the partial gradient operator:

$$\nabla_i U = \left(\frac{\partial U}{\partial x_i}, \frac{\partial U}{\partial y_i}, \frac{\partial U}{\partial z_i} \right) \in \mathbb{R}^3.$$

The function $U(q)$ will be called the *Newtonian gravitational potential function*. $V(q) = -U(q)$ is the *gravitational potential energy*. Newton's second law becomes

$$\dot{p}_i = m_i \ddot{q}_i = \nabla_i U(q) \quad i = 1, \dots, n.$$

or, more concisely

$$(2) \quad \dot{p} = \nabla U(q) \quad \text{or} \quad M \ddot{q} = \nabla U(q)$$

where ∇ is the gradient operator in \mathbb{R}^{3n} and M is the $3n \times 3n$ mass matrix

$$M = \text{diag}(m_1, m_1, m_1, \dots, m_n, m_n, m_n).$$

It is worth digressing at this point to note two important, special features of the Newtonian interparticle potential:

$$\frac{m_i m_j}{|q_i - q_j|}.$$

First of all, the presence of the factor $m_i m_j$ has the effect that the equation for the acceleration of the i -th mass,

$$\ddot{q}_i = \frac{1}{m_i} F_i$$

is independent of m_i . This corresponds to the observation, notably by Galileo, that the trajectory of a falling body is independent of its mass.

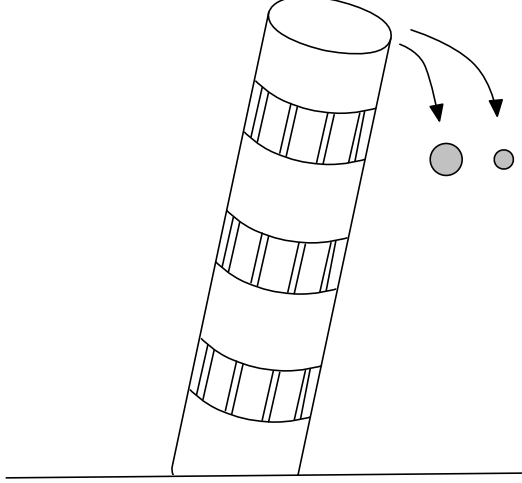


FIGURE 2. Masses falling from a tower.

Second, the fact that the potential is inversely proportional to the distance between the particles provides some justification for the modeling of celestial bodies by point particles. While such bodies are not even approximately pointlike, they are approximately spherically symmetric. It turns out that with the Newtonian potential, spherically symmetric bodies behave as if their total mass were concentrated at their centers.

To see this, consider a more general massive body, specified by giving a bounded subset $\mathcal{B} \subset \mathbb{R}^3$ together with a continuous mass density functions ρ . The gravitational force exerted by such a mass distribution on a point mass m at position q is $F = \nabla U(q)$ where

$$U(q) = \int_{\mathcal{B}} \frac{m}{|q - p|} dm$$

where the triple integral is over $p = (x, y, z) \in \mathcal{B}$ and $dm = \rho(x, y, z) dx dy dz$.

Proposition 1.1. *Suppose \mathcal{B} is a ball of radius R centered at $q_0 \in \mathbb{R}^3$ and ρ is a spherically symmetric density function. Then the mutual Newtonian potential of the ball and a mass m at any point q with $|q| > R$ is*

$$U(q) = \frac{m_0 m}{|q_0 - q|}$$

where m_0 is the total mass in the ball.

Proof. Using the symmetry of the Euclidean distance under rotations and translations, it is no loss of generality to assume $q_0 = (0, 0, 0)$ and $q = (0, 0, z)$, $z > R$. Using spherical coordinates $(x, y, z) = r(\cos \theta \sin \phi, \sin \theta \sin \phi, \cos \phi)$, the spherical symmetry means that the density function depends only on r and then

$$U(q) = \int_0^R \int_0^\pi \int_0^{2\pi} \frac{m_0 \rho(r) r^2 \sin \phi d\theta d\phi dr}{\sqrt{r^2 + z^2 - 2rz \cos \phi}}.$$

It is an exercise to carry out the first two integrals to show

$$U(q) = \frac{m_0 m}{z} \quad m_0 = \int_0^R 4\pi r^2 \rho(r) dr.$$

QED

There is an alternative proof of this result, based on the fact that $f(x, y, z) = 1/|q - p|$ is a harmonic function of $p = (x, y, z)$, that is, $f_{xx} + f_{yy} + f_{zz} = 0$. The well-known mean value theorem for harmonic functions states that the average value of a harmonic function over a sphere is equal to the value at the center of the sphere, which can be proved using the divergence theorem (see exercise 1.3). Fixing a value of r and applying this to the function $f(x, y, z) = m\rho(r)/|q - p|$ and the sphere $S_r = \{|q - q_0| = r\}$ gives

$$\int_{S_r} f = \frac{4\pi r^2 \rho(r) m}{|q_0 - q|}.$$

Then integration over $0 \leq r \leq R$ completes the proof.

Although \mathbb{R}^3 is the natural home of celestial mechanics, it is useful and interesting to consider the point-mass n -body problem in \mathbb{R}^d for any positive integer d . In this case the position vectors are $q_1, \dots, q_n \in \mathbb{R}^d$ and the vectors q, v, p are elements of \mathbb{R}^{dn} . Newton's equations (2) form a system of real-analytic, second order differential equations on the *configuration space*, $X = \mathbb{R}^{dn} \setminus \Delta$, where

$$\Delta = \{q : q_i = q_j \text{ for some } i \neq j\}$$

is the *collision set*. It can be transformed in the usual way into a first-order system in the *phase space*:

$$TX = X \times \mathbb{R}^{dn} = \{(q, v) : q \in X \text{ and } v \in \mathbb{R}^{dn}\}$$

namely:

$$(3) \quad \begin{aligned} \dot{q} &= v \\ \dot{v} &= M^{-1} \nabla U(q). \end{aligned}$$

The notation TX takes note of the fact that the phase space is the tangent bundle of X . The *Newtonian n-body problem* is to study the solutions of equations (3).

A solution to (3) is a differentiable curve $(q(t), v(t))$ where the time t lies in some interval I . Since the differential equation is given by real-analytic functions on phase space, the solutions will be real-analytic functions of time and of their

initial conditions, that is, they are given locally by convergent power series. Since the phase space is not compact, it may not be possible to extend solutions for all time $t \in \mathbb{R}$. In general the maximal interval of existence will be of the form $I = (a, b)$ with $-\infty \leq a < b \leq \infty$. By the general theory of ordinary differential equations, if $b < \infty$ then as $t \rightarrow b_-$, $(q(t), v(t))$ must leave every compact subset of $\mathbb{R}^{dn} \setminus \Delta \times \mathbb{R}^{dn}$ and similarly for $a > -\infty$. For example, this can happen if $q(t)$ converges to a collision configuration $\bar{q} \in \Delta$ (see exercise 1.5).

Exercise 1.1. Using units of kilograms for mass, meters for distance and seconds for time, the gravitational constant is $G \simeq 6.674 \times 10^{-11} \frac{m^3}{kg \cdot sec^2}$.

- i. The radius of Earth is $r_E \simeq 6.378 \times 10^6 m$ and 1 day = $24 \times 60 \times 60$ seconds.
Show that $G \simeq 1.92 \times 10^{-21} \frac{r_E^3}{kg \cdot day^2}$.
- ii. Use units r_E for distance and days for time. Define a new mass unit, call it a *chunk*, where 1 chunk = $5.2076 \times 10^{20} kg$. Show that $G \simeq 1 \frac{r_E^3}{ch \cdot day^2}$.
The mass of Earth is $M \simeq 5.972 \times 10^{24} kg$. Show that this is equivalent to $M \simeq 11468 ch$.

Exercise 1.2. Carry out the integrals to complete the proof of Proposition 1.1

Exercise 1.3. Let $f(x, y, z)$ be a harmonic function in an open set $\mathcal{U} \subset \mathbb{R}^3$ containing the origin and let

$$F(r) = \frac{1}{4\pi r^2} \int_{S_r} f(x, y, z) dA$$

be the average value of f on the sphere $S_r = \{x^2 + y^2 + z^2 = r^2\}$, for r such that the solid ball of radius r is contained in \mathcal{U} . Here dA is the surface area element on the sphere.

- i. Show that $F(r) = \frac{1}{4\pi} \int_{S_1} f(rx, ry, rz) dA$. Note that $F(0) = f(0, 0, 0)$, the value of f at the center of the sphere.
- ii. Show that $F'(r) = \frac{1}{4\pi} \int_{S_1} \nabla f(x, y, z) \cdot (x, y, z) dA$.
- iii. Use Gauss's theorem (the divergence theorem) to prove the mean value property for harmonic function in \mathbb{R}^3 .

Exercise 1.4. Let $(q(t), v(t))$, $t \in I$ be a solution of the n -body problem in \mathbb{R}^d . Let $t_0 \in I$ and assume that the initial positions $q_i(t_0)$ and initial velocities $v_i(t_0)$ all belong to $\mathbb{R}^k \times \{0\}$ for some $k < d$. Show that $q_i(t) \in \mathbb{R}^k \times \{0\}$ and $v_i(t) \in \mathbb{R}^k \times \{0\}$ for all $t \in I$. In other words, the n -body problem in \mathbb{R}^k can be viewed as an invariant set for the n -body problem in \mathbb{R}^d . Hint: First show that if $q \in \mathbb{R}^k \times \{0\}$ then also $\nabla_i U(q) \in \mathbb{R}^k \times \{0\}$. Apply the standard existence and uniqueness theory for differential equations in TX , first with $X = \mathbb{R}^{kn} \setminus \Delta$ then with $X = \mathbb{R}^{dn} \setminus \Delta$.

Exercise 1.5. (A simple collision). Consider the two-body problem in \mathbb{R}^1 with equal masses $m_1 = m_2 = 1$. Show that for a certain choice of the constant k , the functions

$$q_1(t) = (kt)^{\frac{2}{3}} \quad q_2(t) = -(kt)^{\frac{2}{3}}$$

solve Newton's equations for all $t \neq 0$. At $t = 0$ there is a collision at the origin. Strictly speaking, there are two separate solutions, one with maximal interval of existence $I = (-\infty, 0)$ and one with $I = (0, \infty)$. Show that the velocities v_i become infinite as $t \rightarrow 0$.

2. VARIATIONAL FORMULATIONS

Newton's laws of motion can be derived from the variational principles of Lagrange or Hamilton. This is of some philosophical interest, but also has the practical effect of simplifying the computation of the equations of motion in non-Cartesian coordinate systems

2.1. Lagrangian Formulation. Lagrangian mechanics is based on the principle of “least” action. This section contains some of the general theory of Lagrangian Mechanics. Let X be an open subset of a Euclidean space \mathbb{R}^m (such as the configuration space of the n -body problem where $m = 3n$) and let $TX = X \times \mathbb{R}^m$ denote the tangent bundle. A *Lagrangian* is a smooth function $L : TX \rightarrow \mathbb{R}$, that is, a smooth real-valued function $L(q, v)$. More generally, one can also allow Lagrangians $L(q, v, t)$ which depend explicitly on time. The dimension of the configuration space, m , is called the number of *degrees of freedom*.

For the n -body problem the Lagrangian will be

$$(4) \quad L(q, v) = \frac{1}{2}v \cdot Mv + U(q) = \frac{1}{2}v^T Mv + U(q)$$

where, in the second formula, v is viewed as a column vector and its transpose v^T is the corresponding row vector. The first term $K = \frac{1}{2} \sum m_i |v_i|^2$ is the *kinetic energy* and the second $U(q) = -V(q)$ where $V(q)$ is the gravitational potential energy. The recipe

$$(5) \quad \text{Lagrangian} = \text{Kinetic Energy} - \text{Potential Energy}$$

holds for many other physical systems as well.

Given a Lagrangian and a curve $q(t) \in X$, the *action* of the curve on the interval $[a, b]$ is:

$$A(q) = \int_a^b L(q(t), \dot{q}(t), t) dt.$$

Thus the action is a function on the space of curves in X . For now, it is sufficient to work with C^2 curves. A *variation* of a curve $q(t)$ on $[a, b]$ is a C^2 family of curves $q_s(t)$ in X , where $t \in [a, b]$ and $s \in (\delta, \delta)$ for some $\delta > 0$. The variation has *fixed endpoints* if $q_s(a) = q(a)$ and $q_s(b) = q(b)$. If $q_s(t)$ is a variation of q then to first order in s

$$q_s(t) = q(t) + s\alpha(t) + \dots \quad \alpha(t) = \left. \frac{\partial q_s(t)}{\partial s} \right|_{s=0}.$$

$\alpha(t)$ can be viewed a vectorfield along the curve $q(t)$ (see Figure 3). It will be called the *variation vectorfield* corresponding to the variation $q_s(t)$. Note every vectorfield $\alpha(t)$ along q is the variation vectorfield of some variation, for example $q_s(t) = q(t) + s\alpha(t)$.

The principle of least action states that if $q(t)$ is a possible motion of Lagrangian system then the *first variation* of the action should be zero, for every fixed endpoint variation. That is, for every fixed endpoint variation $q_s(t)$ satisfies

$$\delta A = \left. \frac{d}{ds} A(q_s) \right|_{s=0} = 0$$

This is a necessary but not sufficient condition for q to have the least action among all nearby curves with the same endpoints. In any case, $q(t)$ can be called a *stationary curve* or *critical curve* of A on $[a, b]$.

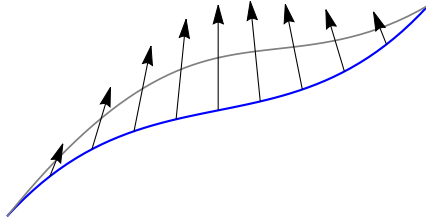


FIGURE 3. Variation of a curve and the variation vectorfield.

The following proposition is a standard result in the calculus of variations:

Proposition 2.1. *A curve, $q(t)$, is a stationary curve of A on $[a, b]$ if and only if the conjugate momentum*

$$(6) \quad p(t) = L_v(q(t), v(t), t)$$

satisfies the Euler-Lagrange (EL) equation on $[a, b]$:

$$(7) \quad \dot{p}(t) = L_q(q(t), v(t), t).$$

Before giving a proof, a digression on covectors is in order. The subscripts in this proposition denote partial derivatives with respect to the vectors $q, v \in \mathbb{R}^m$. The derivative of the real-valued function $L(q, v)$ is a linear function $DL(q, v) : \mathbb{R}^{2m} \rightarrow \mathbb{R}$ and the partial derivatives L_q, L_v are linear functions from \mathbb{R}^m to \mathbb{R} . Using other terminologies, they are *linear forms*, *one forms*, *dual vectors* or *covectors* rather than vectors. Thus the Euler-Lagrange equation is fundamentally an equation between two covectors. The space of all covectors on \mathbb{R}^m is also called the *dual space* and is denoted \mathbb{R}^{m*} .

A partial derivative covector like $p = L_v$ can be represented in coordinates as a vector of partial derivatives

$$p = (p_1, \dots, p_m) = \left(\frac{\partial L}{\partial v_1}, \dots, \frac{\partial L}{\partial v_m} \right).$$

Alternatively, it can be represented as the $1 \times m$ Jacobian matrix

$$p = [p_1 \quad \dots \quad p_m] = \left[\frac{\partial L}{\partial v_1} \quad \dots \quad \frac{\partial L}{\partial v_m} \right].$$

Ordinary vectors $w \in \mathbb{R}^m$ can also be represented in two ways, as coordinate vectors or $m \times 1$ matrices

$$w = (w_1, \dots, w_m) = \begin{bmatrix} w_1 \\ \vdots \\ w_m \end{bmatrix}.$$

Then the value of the linear function p on the vector w is

$$p(w) = p_1 w_1 + \dots + p_m w_m = (p_1, \dots, p_m) \cdot (w_1, \dots, w_m) = [p_1 \quad \dots \quad p_m] \begin{bmatrix} w_1 \\ \vdots \\ w_m \end{bmatrix}.$$

Thus, evaluating a covector on a vector amounts to taking the dot product of their coordinate vectors or multiplying their matrices.

Proof of Proposition 2.1. The action of q_s is

$$A(q_s) = \int_a^b L(q_s(t), \dot{q}_s(t), t) dt.$$

Differentiating with respect to s under the integral sign and using the chain rule gives

$$\delta A = \int_a^b L_q(q(t), v(t), t) \cdot \alpha(t) + p(t) \cdot \dot{\alpha}(t) dt$$

where $v(t) = \dot{q}(t)$, $\alpha(t)$ is the variation vectorfield and $p(t) = L_v(q(t), v(t), t)$. Since $q(t)$ is C^2 , $p(t)$ is C^1 , and the second term can be integrated by parts. Using the fact that $\alpha(a) = \alpha(b) = 0$ this gives

$$(8) \quad \delta A = \int_a^b [L_q(q(t), v(t), t) - \dot{p}(t)] \cdot \alpha(t) dt.$$

Since $\alpha(t)$ is an arbitrary C^2 fixed endpoint vectorfield along $q(t)$, the following lemma shows that the function in square brackets must vanish, which is equivalent to the Euler-Lagrange equation (7). QED

Lemma 2.1. *Suppose $f : [a, b] \rightarrow \mathbb{R}^m$ is a continuous function such that*

$$\int_a^b f(t) \cdot \alpha(t) dt = 0$$

for all C^∞ functions $\alpha : [a, b] \rightarrow \mathbb{R}^m$ with $\alpha(a) = \alpha(b) = 0$. Then $f(t) = 0$ for all $t \in [a, b]$.

Proof. Exercise 2.1. QED

Newton's equation (2) are the Euler-Lagrange equations for the Lagrangian (4). In fact, let $U(q)$ be any smooth function on an open set $X \subset \mathbb{R}^m$ and M any invertible, symmetric $m \times m$ matrix. The $1 \times m$ partial derivative matrices of the Lagrangian (4) are

$$L_v = v^T M \quad L_q = DU(q)$$

and the Euler-Lagrange equation is $\dot{v}^T M = DU(q)$. Taking transposes gives Newton's equation $M\dot{v} = \nabla U(q)$.

In this case, the Euler-Lagrange equations amount to a second order differential equation for q on X or, equivalently, a first-order differential equation for (q, v) on TX . More generally, this will be true whenever it is possible to invert the equation $p = L_v(q, v)$ defining the conjugate momentum.

Definition 2.1. *A Lagrangian $L(q, v)$ is nondegenerate if the equation $p = L_v(q, v)$ can be solved for v as a smooth function $v(q, p)$.*

The utility of the Lagrangian point of view lies in the fact that the Euler-Lagrange equations are invariant under changes of coordinates. Consider a time-independent Lagrangian $L(q, v)$ and a smooth coordinate change given by a diffeomorphism $Q = \phi(q)$, $\phi : X \rightarrow Y$ where $Y \subset \mathbb{R}^m$ is another open set. The inverse map will be written $q = \psi(Q)$. The velocity variables are related by $v = D\psi(Q)V$ and the Lagrangian becomes

$$\tilde{L}(Q, V) = L(\psi(Q), D\psi(Q)V).$$

Writing things like this in terms of the “backward” coordinate change map ψ instead of ϕ , it actually suffices to assume that ψ is a local diffeomorphism.

Proposition 2.2. *Let $\psi : Y \rightarrow X$ be a local diffeomorphism. A C^2 curve $Q(t)$ solves the Euler-Lagrange equations for \tilde{L} if and only if the corresponding curve $q(t) = \psi(Q(t))$ solves the Euler-Lagrange equations for L .*

Proof. First suppose ψ is really a diffeomorphism with inverse ϕ . It suffices to show that q is a stationary curve for the action A if and only if Q is a stationary curve for the action \tilde{A} of \tilde{L} . Suppose q is stationary for L and let $Q_s(t)$ be any fixed endpoint variation of Q . Then $q_s(t) = \psi(Q_s(t))$ is a fixed endpoint variation of q with $\dot{q}_s(t) = D\psi(Q_s(t))\dot{Q}_s(t)$. The actions satisfy

$$A(q_s) = \int_a^b L(q_s, \dot{q}_s) dt = \int_a^b L(\psi(Q_s), D\psi(Q_s)\dot{Q}_s) dt = \int_a^b \tilde{L}(Q_s, \dot{Q}_s) dt = \tilde{A}(Q_s)$$

It follows that $\delta\tilde{A}(Q) = \delta A(q) = 0$, so Q is stationary for \tilde{A} . Reversing the roles of q, Q completes the proof when ψ is a diffeomorphism.

To handle the case of a local diffeomorphism, let $t_0 \in [a, b]$ and let U, V be neighborhoods of $q(t_0), Q(t_0)$ such that $\psi : V \rightarrow U$ is a diffeomorphism. There is some interval $I = [c, d]$ with $t_0 \in I \subset [a, b]$ such that $q(t) \in U, Q(t) \in V$ for all $t \in I$. The previous proof applies to fixed endpoint variations on the interval I , so at time t_0 , q solve the EL equations for L if and only if Q solves the EL equations for \tilde{L} . Since t_0 is arbitrary, the proof is complete. QED

Actually, this result is still true for time-dependent Lagrangians and time-dependent coordinate changes (see exercise 2.5). Its main practical consequence is that to find the transformed differential equations, it suffices to transform the Lagrangian and then compute the Euler-Lagrange equation in the new variables. Here is a simple example – the central force problem in the plane.

Example 2.1. Consider a point particle with mass m and position vector $q \in \mathbb{R}^2$ subjected to a force $F(q) = f(|q|)q$ where f is a real-valued function. Thus the force vector is always pointing toward or away from the “center”, $q = 0$. Suppose further that $F(q) = \nabla U(|q|)$ for some potential function depending only on $|q|$. Newton’s equations are the Euler-Lagrange equations for the Lagrangian

$$L(q, v) = \frac{m}{2}|v|^2 + U(|q|).$$

Let r, θ be the usual polar coordinates in the plane. Then the backward coordinate change is a local diffeomorphism away from the origin:

$$q = r(\cos \theta, \sin \theta) \quad v = \dot{r}(\cos \theta, \sin \theta) + r\dot{\theta}(-\sin \theta, \cos \theta)$$

and the transformed Lagrangian is

$$\tilde{L}(r, \theta, \dot{r}, \dot{\theta}) = \frac{m}{2}(\dot{r}^2 + r^2\dot{\theta}^2) + U(r).$$

The conjugate momentum vector is

$$p = (p_r, p_\theta) = (L_{\dot{r}}, L_{\dot{\theta}}) = (m\dot{r}, mr^2\dot{\theta})$$

and the Euler-Lagrange equations are

$$\begin{aligned} \dot{p}_r &= m\ddot{r} = L_r = U'(r) + 2r\dot{\theta}^2 \\ \dot{p}_\theta &= 0. \end{aligned}$$

The zero in the second equation comes from the fact that the \tilde{L} is independent of the position variable θ . It follows that

$$p_\theta = r^2 \dot{\theta} = C$$

for some constant, C and the equations become

$$(9) \quad m\ddot{r} = U'(r) + \frac{2C^2}{r^3} \quad \dot{\theta} = \frac{C}{r^2}.$$

Using the coordinate invariance property of the Euler-Lagrange equations, it is also possible to generalize to Lagrangian systems on manifolds. If X is an m -dimensional manifold then it is covered by a system of local coordinate patches diffeomorphic to open subsets in \mathbb{R}^m . Using local coordinate, the tangent bundle TX is parametrized by variables (q, v) as above and a Lagrangian $L : TX \rightarrow \mathbb{R}$ takes the form $L(q, v)$ as above. Assuming the Lagrangian is nondegenerate, the Euler-Lagrange equations define a first order system of differential equations in each coordinate patch. Proposition 2.2 shows that these locally defined differential equations fit together consistently to give a differential equation on TX . In practice, it is better to use some tricks to avoid local coordinates.

Example 2.2. Consider a pendulum consisting of a mass m attached to a rigid rod of length l swinging in a vertical plane, say the (x, z) plane. The configuration manifold is the circle $X = \{(x, z) : x^2 + z^2 = l^2\}$. Instead of using local coordinates, X can be parametrized by an angle θ using $(x, z) = l(\sin \theta, -\cos \theta)$ and then the velocity is $(\dot{x}, \dot{z}) = l(\cos \theta, \sin \theta)\dot{\theta}$ (the parametrization is such that $\theta = 0$ represents the bottom of the circle). Assume that the gravitational force is given by $F = (0, -mg)$ where g is constant. This is the gradient of $U(z) = -mgz$. The Lagrangian is of the standard form (5)

$$L = \frac{1}{2}m(\dot{x}^2 + \dot{z}^2) - mgz = \frac{1}{2}ml^2\dot{\theta}^2 + mgl \cos \theta$$

and the EL equation is

$$\ddot{\theta} + \frac{g}{l} \sin \theta = 0.$$

For a spherical pendulum, that is, not confined to the plane, the configuration manifold is $X = \{(x, y, z) : x^2 + y^2 + z^2 = l^2\}$. This time there is no global parametrization. Spherical coordinates

$$(x, y, z) = l(\sin \theta \cos \phi, \sin \theta \sin \phi, -\cos \theta)$$

cover the sphere but have singularities at $\{\theta = 0\}$. Stereographic projections $(x, y, z) = l(2u, 2v, \pm(1 - u^2 - v^2))/(1 + u^2 + v^2)$ could be used to give nonsingular local coordinates omitting only $(0, 0, \pm l)$. An alternative is to find a Lagrangian system on $T\mathbb{R}^3$ for which TX is invariant and whose Lagrangian has the right values on TX .

Let $q = (x, y, z)$ and $v = \dot{q}$ and consider the “homogenized” Lagrangian

$$L(q, v) = \frac{1}{2} \frac{ml^2|v|^2}{|q|^2} - \frac{mglz}{|q|}.$$

If $(q, v) \in TX = \{|q| = l, q \cdot v = 0\}$ then the homogenizing factors cancel out and $L(q, v)$ give the correct standard Lagrangian (5). Moreover, TX is an invariant set for the EL equations of L . It follows that restricting L to TX gives the correct solutions for the spherical pendulum (see exercise 2.2).

The method used in this example is justified by the following proposition, whose proof is exercise 2.3

Proposition 2.3. *Let $L : T\mathbb{R}^m \rightarrow \mathbb{R}$ be a nondegenerate Lagrangian and let $X \subset \mathbb{R}^m$ be submanifold such that TX is invariant under the EL equations of L . Let $\tilde{L} : TX \rightarrow \mathbb{R}$ be the restriction of L to TX . Suppose a curve $(q(t), v(t)) \in TX$ solves the EL equations for L . Then it solves the EL equations for \tilde{L} (in every local coordinate system).*

Exercise 2.1. Prove lemma 2.1. Hint: For each $t_0 \in (a, b)$ consider a variation vectorfield $\alpha(t) = b(t)f(t_0)$ where $b(t)$ is a real-valued C^∞ bump function vanishing outside a small neighborhood of t_0 .

Exercise 2.2. Consider the spherical pendulum of Example 2.2.

- i. Find the Lagrangian $L(\theta, \phi, \dot{\theta}, \dot{\phi})$ in spherical coordinates and verify that $p_\phi = \frac{\partial L}{\partial \dot{\phi}}$ is constant along solutions of the EL equations. Show that there are simple periodic solutions where the pendulum moves on the circles $\theta(t) = c$.
- ii. Find the Lagrangian $L(u, v, \dot{u}, \dot{v})$ using the stereographic local coordinate system $(x, y, z) = l(2u, 2v, u^2 + v^2 - 1)/(1 + u^2 + v^2)$.
- iii. Show that TX is an invariant set for the EL equations of the homogenized Lagrangian, that is, if $|q| = l$ and $q \cdot v = 0$ at a certain time t_0 then these equations continue to hold for all time. Hint: Find the EL equations and calculate the time derivatives of $|q|^2$ and $q \cdot v$ along a solution.

Exercise 2.3. Prove Proposition 2.3. Hint: q is a critical curve for variations q_s in \mathbb{R}^m and, in particular, for variations in X .

Exercise 2.4. Show that for any Lagrangian $L(q, v)$ which does not depend explicitly on t , the function $H(q, v) = p \cdot v - L(q, v)$ is constant along solutions of the Euler-Lagrange equations. Show that for the Lagrangian (4),

$$H(q, v) = \frac{1}{2}v^T M v - U(q) = \text{Kinetic energy} + \text{Potential energy} = \text{Total Energy}.$$

Exercise 2.5. Show that Proposition 2.2 can be generalized to the case where $L = L(q, v, t)$, $q = \psi(Q, t)$ and $\tilde{L}(Q, V, t) = L(\psi(Q, t), D\psi(Q, t)V + \psi_t(Q, t), t)$ where $D\psi$ still denotes the derivative with respect to Q .

2.2. Hamiltonian Formulation. There is an alternative variational formulation of mechanics where the velocity v is replaced by the momentum p and the Lagrangian by the Hamiltonian. For simplicity, only the time-independent case will be discussed here, but everything generalizes to the case of time-dependent Lagrangians and Hamiltonians.

Let X be an open subset of \mathbb{R}^m and consider a Lagrangian $L : TX \rightarrow \mathbb{R}$ of the form

$$L(q, v) = \frac{1}{2}v^T M v + U(q)$$

where M is an invertible $m \times m$ matrix. The tangent bundle of X is just the product space

$$TX = X \times \mathbb{R}^m = \{(q, v) : q \in X, v \in \mathbb{R}^m\}.$$

Using matrix representations, the conjugate momentum covector $p = L_v(q, v) \in \mathbb{R}^{m*}$ and the velocity $v \in \mathbb{R}^m$ are related by

$$p = v^T M \quad v = M^{-1}p^T.$$

The transformation $(x, v) \mapsto (x, p)$ can be viewed as a diffeomorphism $TX \simeq T^*X$ where

$$T^*X = X \times \mathbb{R}^{m*} = \{(q, p) : q \in X, p \in \mathbb{R}^{m*}\}$$

is the *cotangent bundle* of X .

More generally, for any nondegenerate Lagrangian, one can solve the equation $p = L_v(q, v)$ for $v = v(q, p)$. Then define the *Hamiltonian function* $H : T^*X \rightarrow \mathbb{R}$ by

$$(10) \quad H(x, p) = p \cdot v - L(q, v)|_{v=v(q, p)}$$

where the \cdot denotes multiplication of $1 \times m$ and $m \times 1$ matrices or, equivalently, the result of evaluating the covector p on the vector v . If $L(q, v) = \frac{1}{2}v^T M v + U(q)$, as in the n -body problem, then

$$H(q, p) = \frac{1}{2}p M^{-1} p^T - U(q).$$

$$(11) \quad \text{Hamiltonian} = \text{Kinetic Energy} + \text{Potential Energy} = \text{Total Energy}.$$

The process of going from $L(q, v)$ to $H(q, p)$ is sometimes called the *Legendre transform*. One can recover the Lagrangian from the Hamiltonian by

$$(12) \quad L(q, v) = p \cdot v - H(q, p)|_{p=p(q, v)}$$

where $p(q, v) = L_v(q, v)$.

Proposition 2.4. *Let L be a nondegenerate Lagrangian and let $H(q, p)$ be the corresponding Hamiltonian. Then a curve $(q(t), v(t)) \in TX$ solves the Euler-Lagrange equation for L if and only if the curve $(q(t), p(t)) \in T^*X$ solves Hamilton's equations for H :*

$$(13) \quad \begin{aligned} \dot{q} &= H_p(q, p) \\ \dot{p} &= -H_q(q, p). \end{aligned}$$

Proof. Differentiating (10) with respect to p gives

$$H_p(q, p) = \frac{\partial}{\partial p} [p \cdot v(q, p) - L(q, v(q, p))] = v + [p - L_v(q, v(q, p))] \frac{\partial v}{\partial p}.$$

The quantity in square brackets vanishes by definition of $v(q, p)$ so $H_p(q, p) = v = \dot{q}$ which is the first of Hamilton's equations.

Similarly, differentiating (10) with respect to q gives

$$H_q(q, p) = -L_q(q, v(q, p)) + [p - L_v(q, v(q, p))] \frac{\partial v}{\partial q} = -L_q(q, p).$$

Setting this equal to $-\dot{p}$ is equivalent to both the Euler-Lagrange equation and to the second of Hamilton's equations. QED

Since p is a covector, the partial derivative $H_p(q, p)$ is a linear function $\mathbb{R}^{m*} \rightarrow \mathbb{R}$, that is, it is an element of the dual space of the dual space. Such a function is naturally identified with an ordinary vector. Thus the first equation in (13) is an equation between vectors while the second is between covectors.

The form of Hamilton's equations lends itself to a short proof of the conservation of energy. Compare exercise 2.4.

Proposition 2.5. *If $(q(t), p(t))$ solves Hamilton's equations (13) then the total energy $H(q(t), p(t)) = h$ is constant.*

Proof. By the chain rule

$$\begin{aligned} \frac{d}{dt} H(q(t), p(t)) &= H_q(q(t), p(t))\dot{q}(t) + H_p(q(t), p(t))\dot{p}(t) \\ &= H_q(q(t), p(t)) \cdot H_p(q(t), p(t)) - H_p(q(t), p(t)) \cdot H_q(q(t), p(t)) = 0. \end{aligned}$$

QED

Hamilton's equations make sense for any smooth function $H : T^*X \rightarrow \mathbb{R}$, even if it does not arise as the Legendre transform of a Lagrangian. In fact the domain does not have to be T^*X but could be any open subset $Z \subset \mathbb{R}^m \times \mathbb{R}^{m*}$. Motivated by (12), define the action of a curve $(q(t), p(t)) \in Z$, $t \in [a, b]$ as

$$(14) \quad A(q, p) = \int_a^b p(t)\dot{q}(t) - H(q(t), p(t)) dt.$$

This is the basis of a variational interpretation of Hamilton's equations. For this q and p are allowed to vary independently.

Proposition 2.6. *Let $H : Z \rightarrow \mathbb{R}$ be a smooth Hamiltonian, where Z is open in $\mathbb{R}^m \times \mathbb{R}^{m*}$. Then a C^1 curve $(q(t), p(t)) \in T^*X$ solves Hamilton's equations (13) if and only if it is stationary under all fixed endpoint variations (q_s, p_s) .*

Proof. Let (q_s, p_s) be a C^1 family of curves in TX and let $(\alpha(t), \beta(t)) = \frac{d}{ds}(q_s, p_s)|_{s=0}$ be the variation vectorfield. Then differentiating under the integral sign and integrating by parts gives

$$\delta A = \frac{d}{ds} A(q_s, p_s)|_{s=0} = \int_a^b [\beta(t) \cdot (\dot{q} - H_p(q, p)) - (\dot{p} + H_q(q, p)) \cdot \alpha(t)] dt$$

where, as usual, \cdot denotes evaluation of a covector on a vector. Since $\alpha(t)$ and $\beta(t)$ can be arbitrary vectorfields along (q, p) , Lemma 2.1 shows that both parentheses must vanish. QED

As before, the payoff for this variational approach is invariance under changes of coordinates. But now one can allow coordinate changes which mix up the configuration and momentum variables. Suppose the new coordinates (Q, P) are related to the old coordinates by $(q, p) = \psi(Q, P) = (q(Q, P), p(Q, P))$ where $\psi : W \rightarrow Z$ is a local diffeomorphism. The Hamiltonian transforms easily to $\tilde{H}(Q, P) = H(q(Q, P), p(Q, P))$ and the action integral becomes

$$A(q, p) = \int_a^b p(Q, P) \overline{q(Q, P)} - \tilde{H}(Q, P) dt.$$

To relate this to $\tilde{A}(Q, P)$, the integrals of $p(t)\dot{q}(t) = P(t)\dot{Q}(t)$ should be equal, at least up to a constant depending on the endpoints. This can be expressed using differential forms. Consider the *canonical one-form*

$$pdq = p \cdot dq = p_1 dq_1 + \dots + p_m dq_m.$$

Then for any curve, the integral of $p(t)\dot{q}(t)$ can be viewed as the line integral of pdq .

Definition 2.2. *Let Z, W be open sets in $\mathbb{R}^m \times \mathbb{R}^{m*}$ and let $\psi : W \rightarrow Z$ be a local diffeomorphism $(q, p) = \psi(Q, P) = (q(Q, P), p(Q, P))$. Then ψ is exact symplectic if $pdq = PdQ + dS(Q, P)$ for some smooth function $S(Q, P)$. ψ is symplectic if it is exact symplectic in some neighborhood of each $(Q, P) \in W$.*

Those familiar with differential forms will recognize that the condition for ψ to be symplectic is equivalent to equality of the two-forms

$$dp \wedge dq = dp_1 \wedge dq_1 + \dots + dp_m \wedge dq_m = dP_1 \wedge dQ_1 + \dots + dP_m \wedge dQ_m = dP \wedge dQ.$$

Proposition 2.7. *If $(q, p) = \psi(Q, P)$ is symplectic then $(q(t), p(t))$ solves Hamilton's equations for $H(q, p)$ if and only if $(Q(t), P(t))$ solves Hamilton's equations for $\tilde{H}(Q, P) = H(q(Q, P), p(Q, P))$.*

Proof. It suffices to consider a neighborhood of each $t_0 \in [a, b]$. As in the proof of Proposition 2.2, this reduces the problem to the case where ψ is a diffeomorphism and one can also assume that it is exact symplectic. Suppose (q, p) solves Hamilton's equations and let (Q_s, P_s) be any variation of (Q, P) . Then $(q_s, p_s) = \psi(Q_s, P_s)$ is a variation of (q, p) and so the first variation $\delta A(q, p) = 0$. But

$$A(q_s, p_s) = \int_a^b p_s \cdot \dot{q}_s - H(q_s, p_s) dt = \int_a^b P_s \cdot \dot{Q}_s - \tilde{H}(Q_s, P_s) dt + \int_a^b dS(Q_s, P_s) dt.$$

The first integral on the right is $\tilde{A}(Q_s, P_s)$ and the second is $S(Q_s(b), P_s(b)) - S(Q_s(a), P_s(a))$ which is a constant, independent of s . Differentiating with respect to s at $s = 0$ gives

$$\delta \tilde{A}(Q, P) = \delta A(q, p) = 0.$$

So (Q, P) is a stationary curve and therefore solves Hamilton's equations for $\tilde{H}(Q, P)$.

QED

For Lagrangians on TX the most general coordinate changes were of the form $q = \psi(Q), v = D\psi(Q)V$ where the velocity variables transform by the derivative. In other words, tangent vectors V at Q map forward to tangent vectors v at q by $v = D\psi(Q)V$. On the other hand, if $q = \psi(Q)$ is a local diffeomorphism, then covectors at q are mapped to covectors at Q by the pullback operation $P = pD\psi(Q)$ or $p = PD\psi(Q)^{-1}$. This turns out to be exact symplectic.

Proposition 2.8. *Let $\psi : Y \rightarrow X$ be a local diffeomorphism, where X, Y are open subsets of \mathbb{R}^m . Then the transformation*

$$(q(Q, P), p(Q, P)) = (\psi(Q), PD\psi(Q)^{-1})$$

is exact symplectic.

Proof. Since $q = \psi(Q)$ the chain rule gives $dq = D\psi(Q)dQ$. Then

$$pdq = PD\psi(Q)^{-1} \cdot D\psi(Q)dQ = PdQ.$$

QED

Symplectic maps of this form are sometimes called *point transformations*. On the other hand, here is an example of a useful symplectic map which mixes up the position and momentum variables.

Example 2.3. (Action-angle variables for the harmonic oscillator.) Consider the motion of a simple spring moving on the x -axis. Newton's equation is $m\ddot{x} = -kx$ where $m > 0$ is the mass and $k > 0$ is the spring constant. It can be viewed as a Lagrangian or Hamiltonian system with

$$L(x, v) = \frac{1}{2}mv^2 - \frac{1}{2}kx^2 \quad H(x, p) = \frac{1}{2m}p^2 + \frac{1}{2}kx^2$$

where $v = \dot{x}, p = mv$. First, the linear transformation $x = X/(mk)^{\frac{1}{4}}, p = P(mk)^{\frac{1}{4}}$ has $pdx = PdX$ and the new Hamiltonian is

$$\tilde{H}(X, P) = \frac{1}{2}\omega(X^2 + P^2) \quad \omega = \sqrt{\frac{k}{m}}.$$

Next introduce *symplectic polar coordinates* (θ, τ) where

$$(X, P) = \sqrt{2\tau}(\cos \theta, -\sin \theta).$$

So θ is the *clockwise* angle in the (X, P) plane and, instead of the usual radius, $\tau = \frac{1}{2}(X^2 + P^2)$. Note that

$$\begin{aligned} PdX &= -\sqrt{2\tau} \sin \theta (\cos \theta / \sqrt{2\tau} d\tau - \sqrt{2\tau} \sin \theta d\theta) = -\sin \theta \cos \theta d\tau + 2\tau \sin^2 \theta d\theta \\ &= \tau d\theta + dS(\theta, \tau) \end{aligned}$$

where $S = -\tau \sin \theta \cos \theta$. Thus (θ, τ) are indeed symplectic coordinates. The new Hamiltonian is simply

$$K(\theta, \tau) = \omega\tau$$

and Hamilton's equations are

$$\dot{\theta} = K_\tau = \omega \quad \dot{\tau} = -K_\theta = 0.$$

Figure 4 shows phase portraits for the harmonic oscillator in the original (x, p) coordinates and in action-angle coordinates, (θ, τ) . For any Hamiltonian system in the plane, solution must move along level curves of the Hamiltonian and it is only necessary to add arrows to get the phase portrait.

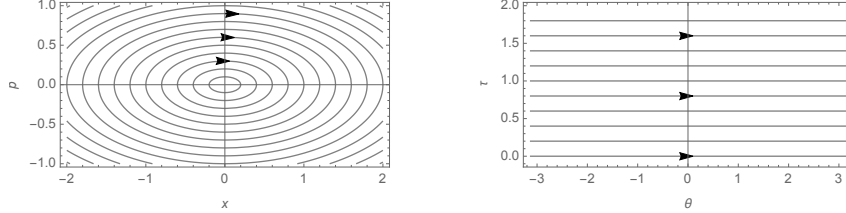


FIGURE 4. Phase portraits for the harmonic oscillator.

Hamiltonian's like $K(\theta, \tau) = \omega\tau$ from Example 2.3 give the simplest kind of Hamiltonian differential equations. To generalize, consider a Hamiltonian $H : \mathbb{R}^m \times \mathbb{R}^{m*} \rightarrow \mathbb{R}$ of the form $H(\theta, \tau) = K(\tau)$ where $\theta = (\theta_1, \dots, \theta_m) \in \mathbb{R}^m$ and $\tau = (\tau_1, \dots, \tau_m) \in \mathbb{R}^{m*}$. The notation is meant to suggest that θ_i are angular variables. Hamilton's equations are

$$\dot{\theta} = \omega(\tau) \quad \dot{\tau} = 0 \quad \omega(\tau) = K_\tau.$$

The momentum variables τ_i are constant along solutions. Fixing their values $\tau = c$ defines an m -dimensional torus \mathcal{M}_c . On this torus the angles change with constant speed and $\theta(t) = \theta(0) + t\omega(c)$.

Another consequence of the coordinate invariance of Hamilton's equations is the possibility of defining Hamiltonian systems on manifolds. Any manifold X of dimension m has a cotangent bundle T^*X of dimension $2m$ equipped with local coordinate systems (q, p) as above. The coordinate change maps are exact symplectic,

so function $H : T^*X \rightarrow \mathbb{R}$ gives rise to a well-defined differential equation. More generally, one can consider any manifold of dimension $2m$ which has such a family of coordinate systems. The development of these general ideas is a long story and is not really needed below. A good reference is [3].

Exercise 2.6. Show that Proposition 2.4 can be generalized to the case of a time-dependent Lagrangian $L(q, v, t)$ and Hamiltonian $H(q, p, t)$.

Exercise 2.7. Show that Proposition 2.5 is not true for general time-dependent Hamiltonians $H(q, p, t)$.

Exercise 2.8. Show that Proposition 2.7 can be generalized to the time-dependent case where $H = H(q, p, t)$, $q = q(Q, P, t)$, $p = p(Q, P, t)$ and

$$\tilde{H}(Q, P, t) = H(q(Q, P, t), p(Q, P, t), t).$$

Exercise 2.9. Consider the planar pendulum of Example 2.2. For the Lagrangian $L(\theta, \dot{\theta})$, carry out the Legendre transformation to find the corresponding Hamiltonian $H(\theta, p_\theta)$, where $p_\theta = L_{\dot{\theta}}$. Similarly, for the spherical pendulum with the Lagrangian $L(\theta, \phi, \dot{\theta}, \dot{\phi})$ in spherical coordinates, find the corresponding Hamiltonian $H(\theta, \phi, p_\theta, p_\phi)$.

Exercise 2.10. Let (q, p) be coordinates in $\mathbb{R} \times \mathbb{R}^* \simeq \mathbb{R}^2$.

- i. Show that a linear map $q = aQ + bP, p = cQ + dP$ is exact symplectic if and only if $ad - bc = 1$, that is, if and only if the matrix $\begin{bmatrix} a & b \\ c & d \end{bmatrix}$ has determinant 1. Hint: Calculate $pdq - PdQ$ and recall the criterion for a differential $fdQ + gdP$ to be dS for some function $S(Q, P)$.
- ii. Similarly, show that a smooth map of the plane $\psi(Q, P) = (q(Q, P), p(Q, P))$ is an exact symplectic local diffeomorphism if and only if $\det D\psi(Q, P) = 1$ for all (Q, P) .

3. SYMMETRIES AND INTEGRALS

The n -body problem has several constants of motion which arise from the symmetries of the system. Since the Newtonian potential function $U(q)$ is a function of the Euclidean distances $r_{ij} = |q_i - q_j|$, it is invariant under simultaneous translations, rotations and reflections of the n position vectors in \mathbb{R}^d . Let $A \in \mathbf{O}(d)$ be any $d \times d$ orthogonal matrix A and $b \in \mathbb{R}^d$ any vector. If $q \in \mathbb{R}^{dn} \setminus \Delta$ is a configuration, let $Aq + b$ denote the configuration with position vectors $Aq_i + b \in \mathbb{R}^d$.

Proposition 3.1. *Let $q(t)$, $t \in I$, be a solution of the n -body problem (2). Then $Q(t) = Aq(t) + b$ is also a solution. In fact, the same is true when $b = kt + l$ is a linear function of time with $k, l \in \mathbb{R}^d$.*

Proof. The potential energy satisfies $U(Q) = U(Aq_1 + b, Aq_2 + b, \dots) = U(q_1, q_2, \dots)$ for all $A \in \mathbf{O}(d)$, $b \in \mathbb{R}^d$ and $q_i \in \mathbb{R}^d \setminus \Delta$. Differentiation with respect to q_i gives

$$D_i U(Q) A = D_i U(q)$$

by the chain rule. Here $D_i U$ is the partial derivative with respect to q_i as a linear map $\mathbb{R}^d \rightarrow \mathbb{R}^1$ which can be represented as a d -dimensional row vector. The partial gradient vector $\nabla_i U$ is the d -dimensional column vector $D_i U^T$, where T denotes

the transpose. Orthogonality of A implies $A^T = A^{-1}$ and so the partial gradients satisfy

$$\nabla_i U(Q) = A \nabla_i U(q).$$

Now let $Q_i(t) = Aq_i(t) + b$, with $b = kt + l$. Then for all $t \in I$

$$m_i \ddot{Q}(t) = m_i A \ddot{q}_i(t) = A m_i \ddot{q}(t) = A \nabla_i U(q(t)) = \nabla_i U(Q(t)).$$

This shows that $Q(t)$ is a solution, as claimed. QED

3.1. Translation symmetry and total momentum. Symmetry gives rise to several *constants of motion* or *integrals*. The simplest is the total momentum

$$p_{tot} = m_1 \dot{q}_1 + \dots + m_n \dot{q}_n = m_1 v_1 + \dots + m_n v_n.$$

Proposition 3.2. *Let $q(t)$, $t \in I$, be a solution of the n -body problem (2). Then $p_{tot}(t)$ is constant.*

Proof. Translation symmetry of U means $U(q_1 + b, \dots, q_n + b) = U(q_1, \dots, q_n)$. Differentiation with respect to b gives

$$\nabla_1 U(q) + \dots + \nabla_n U(q) = 0.$$

Since $\nabla_i U(q) = m_i \ddot{q}_i = m_i \dot{v}_i$, this implies

$$\dot{p}_{tot}(t) = m_1 \dot{v}_1(t) + \dots + m_n \dot{v}_n(t) = 0$$

as required. QED

The *center of mass* of the configuration q is the vector

$$(15) \quad c = \frac{1}{m} (m_1 q_1 + \dots + m_n q_n) \in \mathbb{R}^d \quad m = m_1 + \dots + m_n.$$

Note that $m \dot{c} = p_{tot}$ hence

Corollary 3.1. *The center of mass moves in a straight line in \mathbb{R}^d with constant velocity $\dot{c} = p_{tot}/m$.*

Note that if $p_{tot} = 0$, the center of mass is constant. Using simple translations of coordinates, one can always reduce to the case $c = p_{tot} = 0$.

Proposition 3.3. *Let $q(t)$, $t \in I$ be any solution of the n -body problem with total momentum p_{tot} . Then there is a constant vector $c_0 \in \mathbb{R}^d$ such that the solution $Q(t) = q(t) - p_{tot}t/m - c_0$ has total momentum 0 and center of mass at the origin.*

Proof. $q(t) - p_{tot}t/m$ has total momentum zero, so its center of mass c_0 is constant. Subtracting c_0 gives the required solution. QED

It follows from this discussion that $c = p_{tot} = 0$ defines an invariant subset of the phase space. It is given by the linear equations

$$(16) \quad \begin{aligned} m_1 q_1 + \dots + m_n q_n &= 0 \\ m_1 v_1 + \dots + m_n v_n &= 0. \end{aligned}$$

Let $X \subset \mathbb{R}^{dn}$ be the subspace of dimension $d(n-1)$ given by either one of these equations. Then the invariant set $(X \setminus \Delta) \times X$ of dimension $2d(n-1)$ will be called the *translation reduced phase space*. Proposition 3.3 shows that there is no loss of generality in focussing on solutions in this reduced space.

It's possible to explicitly carry out this reduction of dimension by introducing a basis for the subspace X . From the Lagrangian point of view, Proposition 2.3 shows

that the new differential equations will be the EL equations for the restriction of the Lagrangian to TX . In order to get nice reduced equations, this basis should be chosen to make the reduced Lagrangian as simple as possible.

Example 3.1. (The two-body problem) Consider the two-body problem in \mathbb{R}^d . Instead of coordinates $q_1, q_2 \in \mathbb{R}^d$, introduce new variables $x, c \in \mathbb{R}^d$ where

$$x = q_2 - q_1 \quad c = \frac{1}{m}(m_1 q_1 + m_2 q_2).$$

c is the center of mass and x is the position of q_2 relative to q_1 . The inverse formulae are

$$q_1 = c - \nu_2 x \quad q_2 = c + \nu_1 x$$

where $\nu_1 = \frac{m_1}{m_1 + m_2}$, $\nu_2 = \frac{m_2}{m_1 + m_2}$. The velocities $v_i = \dot{q}_i$, \dot{c} and $u = \dot{x}$ are related by the same formulas. Transforming the Lagrangian

$$L(q, v) = \frac{1}{2}(m_1|v_1|^2 + m_2|v_2|^2) + \frac{m_1 m_2}{|q_2 - q_1|}$$

gives, after some simplification,

$$\tilde{L} = \frac{1}{2}(m|\dot{c}|^2 + \mu_1|u|^2) + \frac{m_1 m_2}{|x|}$$

where $\mu_1 = \frac{m_1 m_2}{m_1 + m_2}$. Note that the kinetic energy is still in diagonal form. Since $c = \dot{c} = 0$ is an invariant set, the differential equation on the reduced phase space is the EL equation for the reduced Lagrangian

$$L_{red}(x, u) = \frac{1}{2}(\mu_1|u|^2) + \frac{m_1 m_2}{|x|}.$$

Since the collision set is the origin $x = 0$, reduced phase space is TX where $X = \mathbb{R}^d \setminus 0$.

Example 3.2. Now consider the three-body problem in \mathbb{R}^d . Instead of coordinates $q_1, q_2, q_3 \in \mathbb{R}^d$, Jacobi introduced new variables $x_1, x_2, c \in \mathbb{R}^d$ where

$$x_1 = q_2 - q_1 \quad x_2 = q_3 - \nu_1 q_1 - \nu_2 q_2 \quad c = \frac{1}{m}(m_1 q_1 + m_2 q_2 + m_3 q_3).$$

c is the center of mass, x_1 is the position of q_2 relative to q_1 and x_2 is the position of q_3 relative to the center of mass of q_1, q_2 . The inverse formulae are

$$q_1 = c - \nu_2 x_1 - \frac{m_3}{m} x_2 \quad q_2 = c + \nu_1 x_1 - \frac{m_3}{m} x_2 \quad q_3 = c + \frac{m_1 + m_2}{m} x_2$$

The velocities $v_i = \dot{q}_i$, \dot{c} and $u_i = \dot{x}_i$ are related by the same formulas.

Transforming the Lagrangian $L(q, v)$ gives, after some simplification,

$$\tilde{L} = \frac{1}{2}(m|\dot{c}|^2 + \mu_1|u_1|^2 + \mu_2|u_2|^2) + U(x_1, x_2)$$

where $\mu_1 = \frac{m_1 m_2}{m_1 + m_2}$, $\mu_2 = \frac{(m_1 + m_2)m_3}{m}$ and

$$U(x_1, x_2) = \frac{m_1 m_2}{|x_1|} + \frac{m_1 m_3}{|x_2 + \nu_2 x_1|} + \frac{m_2 m_3}{|x_2 - \nu_1 x_1|}.$$

Once again, the kinetic energy is in diagonal form.

Now the reduced equations on the invariant manifold TX are the EL equations of the restriction to $\{c = \dot{c} = 0\}$:

$$L_{red}(x, u) = \frac{1}{2}(\mu_1|u_1|^2 + \mu_2|u_2|^2) + U(x).$$

Exercise 3.4 shows how to generalize Jacobi coordinates to the n -body problem.

3.2. Rotation symmetry and angular momentum. The invariance of the potential under rotations lead to the *angular momentum* integral. This will be discussed in the general context of Lagrangian mechanics. Consider a nondegenerate Lagrangian $L(q, v)$ defined on TX where $X \subset \mathbb{R}^m$ is an open set. Let G denote a symmetry group acting on the configuration space X . That is, each element g of the group determines a diffeomorphism of X . For each $q \in X$, let $g(q)$ be the image of q under g . The velocities will be transformed by the derivative map Dg . G acts as a symmetry of the Lagrangian L if $L(g(q), Dg(q)v) = L(q, v)$ for all $(q, v) \in TX$ and all $g \in G$.

Example 3.3. For the n -body problem in \mathbb{R}^d , the rotation group $G = \mathbf{SO}(d)$ acts as a symmetry group. If $A \in \mathbf{SO}(d)$ is a rotation matrix, the action of A on $q = (q_1, \dots, q_n) \in \mathbb{R}^{dn}$ is $A(q) = (Aq_1, \dots, Aq_n)$. Also, $DA(q)v = (Av_1, \dots, Av_n)$. So the position vectors and velocity vectors of all of the bodies are rotated simultaneously as in Proposition 3.1. That proposition shows that A maps solutions to solutions and it clearly also preserves the Lagrangian

$$L(q, v) = \frac{1}{2} \sum m_i |v_i|^2 + U(q).$$

Consider a one-parameter group of symmetries, that is, a curve $g_s \in G$, $s \in \mathbb{R}$, with $g_0 = id$ and $g_{s+t} = g_s \cdot g_t$ for all $s, t \in \mathbb{R}$, where \cdot denotes the group operation. For example, in $\mathbf{SO}(d)$ there is a one-parameter group of rotations acting in the usual way on any fixed plane in \mathbb{R}^d while fixing the vectors orthogonal to the plane. More generally, let a be any antisymmetric $d \times d$ matrix. Then the matrix exponential $A(s) = \exp(sa)$ is a one-parameter group of rotations. In fact, every one-parameter group in $\mathbf{SO}(d)$ is of this form. Every one-parameter group acting on X determines a *symmetry vectorfield* or *infinitesimal symmetry* on X by

$$\chi(q) = \frac{d}{ds} g_s(q)|_{s=0}.$$

The space of antisymmetric $d \times d$ matrices is denoted $\mathbf{so}(d)$. The notation comes from Lie theory; $\mathbf{SO}(d)$ is a Lie group and $\mathbf{so}(d)$ is its Lie algebra.

Example 3.4. For a one-parameter group of rotations $A(s) \in \mathbf{SO}(d)$ acting on \mathbb{R}^{dn} via $A(s)(q) = (A(s)q_1, \dots, A(s)q_n)$ the symmetry vectorfield is $\chi(q) = (aq_1, \dots, aq_n)$ where a is the antisymmetric matrix $\frac{d}{ds} A(s)|_{s=0}$.

The following proposition is the simplest version of *Nöther's theorem* relating symmetries of a Lagrangian to constants of motion for the EL equations.

Proposition 3.4. *Suppose g_s is one-parameter group of symmetries of the Lagrangian $L(q, v)$ and $\chi(q)$ be the symmetry vectorfield. Let $p(q, v) \in \mathbb{R}^{m*}$ be the conjugate momentum covector. Then the function $C : TX \rightarrow \mathbb{R}$*

$$C(q, v) = p(q, v) \cdot \chi(q)$$

is constant along solutions of the EL equations.

Proof. Let $(q(t), v(t))$ be a solution of the EL equations. Then

$$\frac{d}{dt} C(q, v) = \dot{p} \cdot \chi(q) + p \cdot D\chi(q)\dot{q} = L_q(q, v) \cdot \chi(q) + p(q, v) \cdot D\chi(q)v.$$

It must be shown that this vanishes.

Since g_s is a symmetry of the Lagrangian, $L(g_s(q), Dg_s(q)v) = L(q, v)$ for all q, v, s . Differentiating with respect to s at $s = 0$ and using the chain rule gives

$$0 = L_q(q, v) \cdot \chi(q) + p(q, v) \cdot \left(\frac{d}{ds} Dg_s(q)|_{s=0} \right) v.$$

It remains to show that the derivative in parentheses is $D\chi(q)$. But

$$\frac{d}{ds} Dg_s(q)|_{s=0} = D \frac{d}{ds} g_s(q)|_{s=0} = D\chi(q)$$

by reversing the order of differentiation and by the definition of $\chi(q)$. QED

To describe this in \mathbb{R}^d , let $\alpha, \beta \in \{1, 2, \dots, d\}$ be two of the d coordinate indices.

Proposition 3.5. *Let $q(t)$, $t \in I$, be a solution of the n -body problem (2). Then for every pair of indices α, β , $C_{\alpha\beta}(t)$ is constant where*

$$C_{\alpha\beta} = \sum_i (q_{i\alpha} p_{i\beta} - q_{i\beta} p_{i\alpha}) = \sum_i m_i (q_{i\alpha} v_{i\beta} - q_{i\beta} v_{i\alpha}).$$

Proof. For simplicity, consider the case $(\alpha, \beta) = (1, 2)$. Let $A(s)$ denote the rotation matrix which rotates by s radians in the (α, β) coordinate plane while fixing all other coordinates. Then $A(s)$ is the matrix obtained from the $d \times d$ identity matrix by replacing the $(1, 2)$ block by $\begin{bmatrix} \cos s & -\sin s \\ \sin s & \cos s \end{bmatrix}$. The corresponding antisymmetric matrix $a = A'(0)$, is the matrix with $(1, 2)$ block given $\begin{bmatrix} 0 & -1 \\ 1 & 0 \end{bmatrix}$ and all other entries equal to 0 and the symmetry vectorfield is $\chi(q) = (aq_1, \dots, aq_n)$.

Nöther's theorem shows that

$$C_{\alpha\beta} = p \cdot \chi(q) = \sum p_i \cdot aq_i = \sum p_i \cdot (-q_{i2}, q_{i1}, 0, \dots, 0) = \sum (p_{i2}q_{i1} - p_{i1}q_{i2})$$

is constant. QED

Note that $C_{\alpha\alpha} = 0$ and $C_{\beta\alpha} = -C_{\alpha\beta}$ so there are at most $\binom{d}{2}$ independent angular momentum constants. The symbol C denotes the tensor with components $C_{\alpha\beta}$. For the planar problem, with $d = 2$, there is only one component and C reduces to the scalar $C = C_{12} = \sum m_i (q_{i1} v_{i2} - q_{i2} v_{i1})$. If $d = 3$ there are three independent components which can be viewed either the components of an *angular momentum vector*

$$C = (C_{32}, C_{13}, C_{21}) = (C_1, C_2, C_3).$$

or of an antisymmetric 3×3 matrix

$$C = \begin{bmatrix} 0 & -C_3 & C_2 \\ C_3 & 0 & -C_1 \\ -C_2 & C_1 & 0 \end{bmatrix}.$$

The angular momentum vector can be written using the cross product in \mathbb{R}^3 as

$$C = \sum m_i q_i \times v_i$$

or, more generally, using wedge products in \mathbb{R}^d (see Exercise 3.2).

Instead of describing the angular momentum componentwise, one can instead define a function

$$C(q, v; a) = p(q, v) \cdot aq \quad a \in \mathbf{so}(d).$$

In other words, the angular momentum can be viewed as a map $C : TX \times \mathbf{so}(d) \rightarrow \mathbb{R}$. The linear maps $\mathbf{so}(d) \rightarrow \mathbb{R}$ form the dual space $\mathbf{so}(d)^*$ of the vectorspace $\mathbf{so}(d)$. Thus, yet another point of view is to say that the angular momentum is a map $C : TX \rightarrow \mathbf{so}(d)^*$ assigning to each $(q, v) \in TX$ the linear function $C(q, v; \cdot) \in \mathbf{so}(d)^*$.

Exercise 3.1. (A more interesting collision). Consider the two-body problem in \mathbb{R}^d with equal masses $m_1 = m_2 = 1$. Let u, b, c be arbitrary vectors in \mathbb{R}^d with $|u| = 1$. Show that there is a solution of the form

$$q_1(t) = u(kt)^{\frac{2}{3}} + bt + c \quad q_2(t) = -u(kt)^{\frac{2}{3}} + bt + c$$

where k is the constant from Exercise 1.5. For $d = 2$, $u = (1, 0)$, $b = (1, 1)$ and $c = (0, 0)$, plot the resulting parametrized curves in the plane.

Exercise 3.2. (Angular momentum as a bivector). Define the outer product or tensor product of vectors $u, v \in \mathbb{R}^d$ by regarding both vectors as $d \times 1$ column vectors and setting $u \otimes v = uv^T$ where the superscript T denotes the transpose. Thus $u \otimes v$ is a $d \times d$ matrix. Next define the wedge product as $u \wedge v = u \otimes v - v \otimes u$, an antisymmetric $d \times d$ matrix. Finally, define a *bivector* as a linear combination of wedge products.

- i. Show that the angular momentum can be written $C(q, v) = \sum m_i q_i \wedge v_i$.
- ii. Show that $C(q, v) = \sum C_{\alpha\beta} e_\alpha \wedge e_\beta$ where e_J are the standard basis vectors in \mathbb{R}^d and where the sum runs over all indices (α, β) with $1 \leq \alpha < \beta \leq d$.
- iii. Consider a coordinate change $Q_i = Aq_i, V_i = Av_i$ where $A : \mathbb{R}^d \rightarrow \mathbb{R}^d$ is a linear map. Show that $C(Q, V) = AC(q, v)A^T$.

Exercise 3.3. (Scaling symmetry). Suppose $q(t)$ is a solution of (2) for masses m_i and consider the function $Q(t) = aq(bt)$ where $a > 0$ and $b \neq 0$ are constants. This represents a rescaling of the position variables by a and the time variable by b .

- i. Show that $Q(t)$ solves equation (2) for masses $\tilde{m}_i = cm_i$ where $c = a^3b^2$. In particular, if $a^3b^2 = 1$, $Q(t)$ is a new solution with the same masses.
- ii. Assuming that $a^3b^2 = 1$, determine how the energies H and angular momenta C of the two solutions are related and show that the quantities $HC_{\alpha\beta}^2$ are invariant.
- iii. Show that “without loss of generality”, one may assume that the total mass is $m_1 + \dots + m_n = 1$ and that the energy is $H = 1, -1$ or 0 .

Exercise 3.4. This exercise shows how to define Jacobi-like coordinates for the n -body problem. The goal is to replace $q_1, \dots, q_n \in \mathbb{R}^d$ by new variables x_1, \dots, x_{n-1}, c where c is the center of mass in such a way that the kinetic energy term in the new Lagrangian is diagonal. First consider the problem with $d = 1$, that is the n -body problem on the line, so $q = (q_1, \dots, q_n) \in \mathbb{R}^n$.

Let $M = \text{diag}(m_1, m_2, \dots, m_n)$ be the $n \times n$ mass matrix and let P be an $n \times n$ matrix whose columns are M -orthogonal, that is, $P^T M P = D$ where $D = \text{diag}(d_1, \dots, d_n)$ is a diagonal matrix with $d_i > 0$. Define new coordinates $x = (x_1, \dots, x_n) \in \mathbb{R}^n$ by $q = Px, x = P^{-1}q$. Note that the velocities $v = \dot{q}, u = \dot{x}$ are related by $v = Pu, u = P^{-1}v$. Also, if the last row of P^{-1} is $(m_1, \dots, m_n)/m$ then the last new coordinate is $x_n = c$.

- i. For the case $n = 3$ from Example 3.4, what are the matrices P, P^{-1}, D ?
- ii. Show that for the n -body problem with $d = 1$ the kinetic energy is $K = \frac{1}{2} \sum d_i |u_i|^2$. Explain why the formula continues to hold for $d > 1$.

- iii. For $n = 4$ there are several different versions of Jacobi coordinates. Show that there is a set of Jacobi coordinates with $x_1 = q_2 - q_1$, $x_2 = q_4 - q_3$ and x_3 the vector connecting the centers of mass of the pairs. What is the new Lagrangian?
- iv. Find another set of Jacobi coordinates when $n = 4$ with x_1, x_2 as in Example 3.4. What is the new Lagrangian? Hint: x_3 continues the pattern set by x_1, x_2 .

4. THE TWO-BODY PROBLEM AND THE KEPLER PROBLEM

The two-body problem is the simplest nontrivial case, and the only one which can be explicitly solved. It is worth looking at several ways to attack the problem and to spend some time getting a good understanding of the solutions. Without loss of generality, one may assume that the center of mass is at the origin and the total momentum is zero:

$$m_1 q_1 + m_2 q_2 = m_1 v_1 + m_2 v_2 = 0.$$

Let $X \subset \mathbb{R}^{2d}$ be the d -dimensional subspace defined by either of these equations. The translation-reduced phase space is $(X \setminus \Delta) \times X$ which has dimension $2d$.

Example 3.1 described how to parametrize the subspace X to obtain a reduced Lagrangian system. With $q = q_2 - q_1$ and $v = \dot{q}$, the reduced Lagrangian is

$$L_{2bp} = \frac{1}{2} \mu_1 |v|^2 + U(q) \quad U(q) = \frac{m_1 m_2}{|q|}$$

where $\mu_1 = \frac{m_1 m_2}{m_1 + m_2}$ which simplified slightly by canceling a factor of μ_1 to get

$$L = \frac{1}{2} |v|^2 + U(q) \quad U(q) = \frac{m}{|q|}$$

where $m = m_1 + m_2$ is the total mass. Note that multiplying a Lagrangian by a constant has no effect on the Euler-Lagrange equation. The Euler-Lagrange equations for L are equivalent to the first order system

$$(17) \quad \begin{aligned} \dot{q} &= v \\ \dot{v} &= -\frac{m q}{|q|^3} = \nabla U(q) \end{aligned}$$

where

$$U(q) = \frac{m}{r} \quad r = |q|.$$

Using these coordinates, the singular set becomes $\Delta = \{q = 0\}$ and the reduced phase space is $(\mathbb{R}^d \setminus 0) \times \mathbb{R}^d$. The system (17) is called the *Kepler problem* in \mathbb{R}^d . It can be viewed as the problem of the motion of a point of mass 1 attracted to a point of mass $m = m_1 + m_2$ which is fixed at the origin. Then the angular momentum tensor C and the energy H are given by

$$(18) \quad C_{\alpha, \beta} = q_\alpha v_\beta - q_\beta v_\alpha \quad H(q, v) = \frac{|v|^2}{2} - \frac{m}{|q|} = h.$$

The relation between the Kepler problem and the two-body problem is illustrated in Figure 5. Given a solution $q(t)$ of the Kepler problem, the corresponding positions of the two bodies with center of mass at the origin are

$$q_1 = -\frac{m_2}{m} q \quad q_2 = \frac{m_1}{m} q.$$

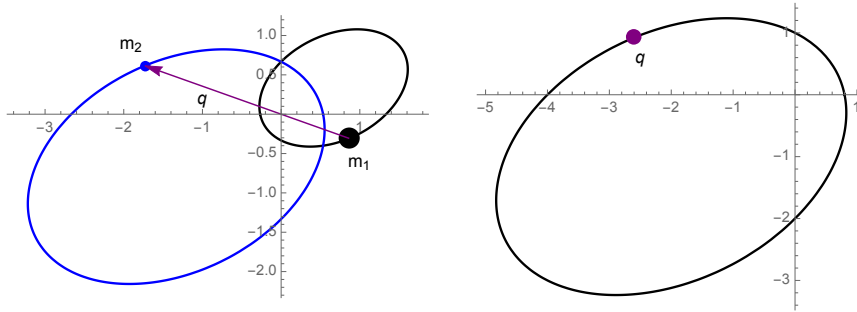


FIGURE 5. Elliptical orbit of the planar two-body problem and the corresponding orbit for the Kepler problem.

Although the Kepler problem has been set up in \mathbb{R}^d , it turns out that the motion is always planar.

Proposition 4.1. *Every solution $q(t)$ of the Kepler problem moves in a fixed plane in \mathbb{R}^d , namely, the plane through the origin containing its initial position and velocity vectors.*

Proof. Using rotational symmetry one may assume without loss of generality that the initial position q_0 and initial velocity v_0 lie in the plane $P = \mathbb{R}^2 \times \{0\} \subset \mathbb{R}^d$. In the phase space $\mathbb{R}^d \setminus 0 \times \mathbb{R}^d$ the subspace $P \setminus 0 \times P$ is invariant. To see this, note that for $q \in P$, the force vector $\frac{-mq}{r^3}$ is also in P . If v is in P as well, then the EL vectorfield $(\dot{q}, \dot{v}) = (v, \frac{-mq}{r^3})$ is tangent to $P \times P$. Then as in exercise 1.4, the uniqueness theorem for ordinary differential equations implies that $P \setminus 0 \times P$ is invariant. In particular, $q(t) \in P \setminus 0$ for all t such that the solution exists. QED

Example 4.1. Circular solutions. Before looking into the general solution of the Kepler problem, it's interesting to explore some of the simplest ones. Consider the Kepler problem in \mathbb{R}^2 and look for periodic solutions which move on a circle with constant angular speed. In other words, try to find a solution of the form $q(t) = r_0(\cos \omega t, \sin \omega t)$ where r_0, ω are constant. The velocity is $v = r_0\omega(-\sin \omega t, \cos \omega t)$ and $v' = r_0\omega^2(-\cos \omega t, -\sin \omega t) = -\omega^2q$. Comparison with (17) shows that this is a solution if and only if $r_0^3\omega^2 = m$. So given any r_0 , there is such a circular periodic solution. The energy, angular momentum and period are

$$h = -\frac{m}{2r_0} \quad C = \pm\sqrt{mr_0} \quad T = 2\pi\sqrt{\frac{r_0^3}{m}}.$$

Exercise 4.1. According to Exercise 1.1 the mass of the Earth is $m \approx 11468$ in units such that $G = 1$, distance is measured in Earth radii and time in days. Assuming that the motion of a satellite is modeled by the Kepler problem with this mass, what are the possible periods for circular earth satellites? What radius will give a geostationary satellite, that is, a satellite with a period of $T = 1$ day?

4.1. The Laplace-Runge-Lenz vector and orbital elements. As Kepler observed, $q(t)$ generally sweeps out a conic section in its plane of motion, that is, an ellipse, hyperbola or parabola. Perhaps the simplest way to show this is to use the

Laplace-Runge-Lenz vector (or LRL vector). The d -dimensional LRL vector, A , is defined as

$$(19) \quad A = |v|^2 q - (q \cdot v)v - \frac{mq}{r}.$$

Proposition 4.2. *The LRL vector $A(q(t), v(t))$ is constant along every solution of the Kepler problem.*

The proof is Exercise 4.2.

The angular momentum and energy (18) are also constant of motion. Using Lagrange's identity

$$|v|^2 |q|^2 = (q \cdot v)^2 + \sum_{\alpha < \beta} (q_\alpha v_\beta - q_\beta v_\alpha)^2$$

it is easy to check that A, C, h are related by

$$(20) \quad |A|^2 = m^2 + 2h|C|^2$$

where $|C|^2 = \sum_{\alpha < \beta} C_{\alpha\beta}^2$.

Using the LRL vector, it is easy to derive an equation for the path swept out by a solution $q(t)$. This path lies in the two-dimensional plane P spanned by q, v and the LRL vector (19) also lies in this plane. Using a rotation in \mathbb{R}^d , one may reduce to the case $q, v, A \in \mathbb{R}^2$, that is, the planar Kepler problem. Choose a Cartesian coordinate system in P and write $q = (x, y), v = (u, w)$. Then the LRL vector becomes $A = (\alpha, \beta)$ where

$$(21) \quad \begin{aligned} \alpha &= Cw - \frac{mx}{r} = C\dot{y} - \frac{mx}{r} \\ \beta &= -Cu - \frac{my}{r} = -C\dot{x} - \frac{my}{r} \\ C &= C_{12} = xw - yu. \end{aligned}$$

Proposition 4.3. *Let $q(t) = (x(t), y(t))$ be a solution to the planar Kepler problem (17) with velocity vector $v(t) = (u(t), w(t))$ and LRL vector $A = (\alpha, \beta)$. Then $q(t)$ moves on the curve*

$$(22) \quad mr = C^2 - \alpha x - \beta y$$

and if $C \neq 0$, the velocity moves on the circle (called the hodograph)

$$(23) \quad \left(u + \frac{\beta}{C}\right)^2 + \left(w - \frac{\alpha}{C}\right)^2 = \frac{m^2}{C^2}.$$

Proof. It follows from (21) that

$$(24) \quad \alpha x + \beta y = C(xw - yu) - m \frac{x^2 + y^2}{r} = C^2 - mr$$

where $r = \sqrt{x^2 + y^2}$ which implies (22).

On the other hand, it also follows that

$$(\alpha - Cw)^2 + (\beta + Cu)^2 = m^2$$

which gives (23) if $C \neq 0$

QED

The curve (22) is a conic section. To see this, recall that a conic section in the plane can be defined by an equation of the form $r = ed$ where r is the distance of an arbitrary point (x, y) on the curve to a fixed point in the plane (the focus) and d is the distance to a fixed line (the directorix). The ratio $e = r/d$ is called the *eccentricity* of the conic. Now the distance from a point (x, y) to the line with equation $ax + by + c = 0$ is $d = |ax + by + c|/\sqrt{a^2 + b^2}$. It follows that (22) describes a conic with

$$\begin{aligned} \text{Focus: } & (0, 0) \\ \text{Directorix: } & ax + \beta y - C^2 = 0 \\ \text{Eccentricity: } & e = \frac{\sqrt{\alpha^2 + \beta^2}}{m} = \frac{|A|}{m}. \end{aligned}$$

There are two exceptional cases. If $\alpha = \beta = 0$ but $C \neq 0$ the equation (22) describes a circle with center $(0, 0)$ and radius C/m . If $C = 0$, then $(\alpha, \beta) \neq (0, 0)$, the focus lies on the directorix, and equation (22) reduces to $\beta x - \alpha y = 0$, the line orthogonal to the directorix. Otherwise, the curve is an ellipse if $0 < e < 1$, one branch of a hyperbola if $e > 1$ or a parabola if $e = 1$. Equation (20) shows that the elliptical case arises when the energy $h < 0$, the hyperbolic case when $h > 0$ and the parabolic case when $h = 0$.

In the case of a circle or ellipse, the orbit is a closed curve in the plane which suggests that the solution $(q(t), v(t))$ in phase space is a periodic function of time. To see this, note that as $C \neq 0$, the velocity is never zero so $q(t)$ keeps moving around the orbit and must return to its initial position after some time T . Meanwhile the velocity moves on the hodograph circle (which encloses the origin in this case). From geometry, it's clear that distinct points on the circle or ellipse have distinct tangent directions which give distinct points on the hodograph. It follows that $v(t)$ also returns to its initial value after time T so $(q(t), v(t))$ is a periodic solution. The problem of finding formulas determining $q(t), v(t)$ and T will be deferred to the next section.

Using polar coordinates, $q = (x, y) = r(\cos \theta, \sin \theta)$, the equation (24) can be written

$$(25) \quad r = \frac{C^2}{m + \alpha \cos \theta + \beta \sin \theta} = \frac{C^2}{m + |A| \cos(\theta - \varpi)}$$

where $A = (\alpha, \beta) = |A|(\cos \varpi, \sin \varpi)$. It follows that the minimum distance r to the focus occurs when $\theta = \varpi$, that is, in the direction of the LRL vector, A (see Figure 6). The minimal distance is given by

$$r_{min} = \frac{C^2}{m + |A|} = \frac{C^2}{m(1 + e)}.$$

The closest point to the center is called the *pericenter* or if the center of attraction represents the sun, the *perihelion*. The angle ϖ is the *longitude of the pericenter* (the use of the strange symbol ϖ , called "varpi", is traditional).

In the case of an ellipse, the maximum value of r occurs at the *apocenter* or *aphelion* which occurs in the direction of $-A$. Adding these gives the length of the major axis of the ellipse and half that is the *major semiaxis*, a :

$$a = \frac{1}{2}(r_{min} + r_{max}) = \frac{1}{2} \left(\frac{C^2}{m + |A|} + \frac{C^2}{m - |A|} \right) = \frac{m}{|2h|}.$$

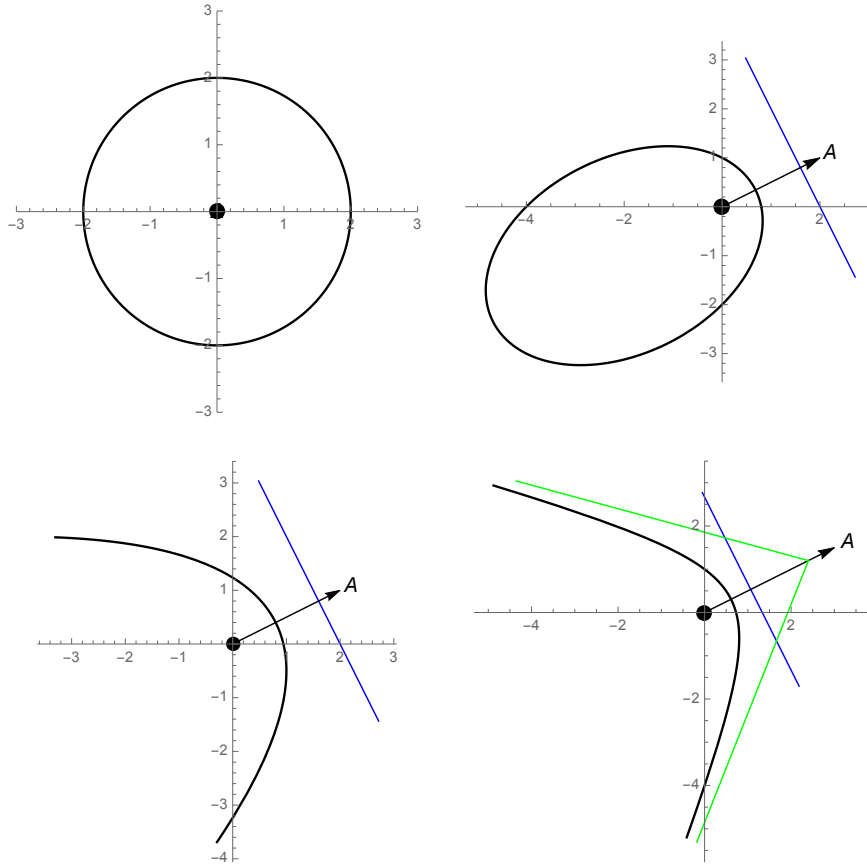


FIGURE 6. Some orbits of the Kepler problem and their LRL vectors.

For the hyperbola the major semiaxis is defined as the distance from the pericenter to the center and it turns out to be given by the same formula. It seems there is no sensible definition of the major semiaxis for a parabola. Another useful parameter is the *semilatus rectum*, p , which is the radius of the points on the conic where (x, y) is perpendicular to A . It is given by

$$p = \frac{|C|^2}{m}.$$

The parameters describing the shape and orientation of the conic are called the *orbital elements*. It's clear from (22) that an orbit of the planar Kepler problem is uniquely determined by $|C|^2$ and $A = |A|(\cos \varpi, \sin \varpi)$. It is easy to see that these could be found in terms of three of the orbital elements described above. Namely, the longitude of the pericenter ϖ , the eccentricity e and one or the other of the size parameters: the major semiaxis, a , the minimal distance r_{min} or the semilatus rectum p . r_{min} and p work in all cases while the major semiaxis works when $h \neq 0$. The following summarizes a few of the formulas.

Proposition 4.4. *The orbital elements of the conic section describing a solution of the planar Kepler problem with LRL vector $A = |A|(\cos \varpi, \sin \varpi)$ are*

$$\begin{aligned}
 \text{Major semiaxis: } a &= \frac{m}{|2h|} \\
 \text{Eccentricity: } e &= \frac{|A|}{m} = \sqrt{1 + \frac{2h|C|^2}{m^2}} \\
 \text{Longitude of pericenter: } \varpi & \\
 \text{Semilatus rectum: } p &= \frac{|C|^2}{m} \\
 \text{Radius of pericenter: } r_{\min} &= \frac{|C|^2}{m + |A|}
 \end{aligned}
 \tag{26}$$

Specifying a, e, ϖ determines an orbit of the planar Kepler problem, but one more parameter is needed to specify the position of the moving mass along the orbit. If the orbit is not circular then the pericenter is uniquely determined. For a circular one, an arbitrary point could be chosen.

Definition 4.1. *The true anomaly, $\nu(t)$, is the angle between the pericenter and $q(t)$, that is $\nu = \theta - \varpi$. For a circular or elliptical orbit, let T be the period and define the mean angular velocity $n = \frac{2\pi}{T}$. Then the mean anomaly, $M(t)$ is $M(t) = n(t - \tau)$ where τ is the time at pericenter.*

Clearly knowing either ν or M is enough to determine the position of $q(t)$ along its orbit. How to find them will be discussed in the next section. For now just note the following version of the formula (25):

$$r = \frac{C^2}{m + |A| \cos \nu} = \frac{p}{1 + e \cos \nu}.
 \tag{27}$$

Since the spatial case, $d = 3$, is the most important, it is useful to have a way to describe a Kepler orbit there. Two more orbital elements are needed to specify the plane of the orbit. It is traditional to use two angles even if there is no sensible way to do this which works in all cases. Suppose some Cartesian coordinates (x, y, z) have been chosen for \mathbb{R}^3 . For example, to describe orbits in the solar system the usual choice is to make the (x, y) plane be the ecliptic, that is, the plane of the earth's orbit. The z axis is chosen so that the motion of the earth looks counter-clockwise when viewed from a position with $z > 0$. The choice for the positive x -axis is the first point of Aries, which gives the location of the Sun on the Spring equinox.

The angular momentum tensor $C_{\alpha\beta}$ can be viewed as a vector

$$C = (C_1, C_2, C_3) = (q_2 v_2 - q_3 v_1, q_3 v_1 - q_1 v_3, q_1 v_2 - q_2 v_1) = q \times v$$

where $q \times v$ is the cross product. It's orthogonal to the plane of motion, which is spanned by q, v . The three-dimensional LRL vector can also be expressed using cross products

$$A(q, v) = v \times C - \frac{mq}{r} = v \times (q \times v) - \frac{mq}{r}$$

and it lies in the plane of motion.

Assuming that $C \neq (0, 0, 0)$, the vector $C/|C|$ provides a unit normal vector to the orbit. Define the *inclination*, ι of an orbit to be the angle between $C/|C|$

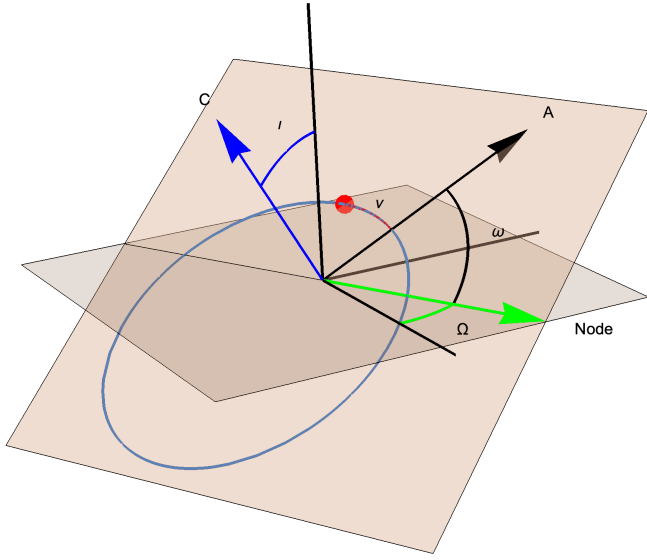


FIGURE 7. Orbital elements for the spatial Kepler problem.

and the positive z -axis, that is,

$$\cos \iota = \frac{C_3}{|C|} \quad \sin \iota = \frac{\sqrt{C_1^2 + C_2^2}}{|C|}.$$

For example, an orbit in the (x, y) -plane has inclination $\iota = 0$. If the inclination is not zero, then the vector $(-C_2, C_1, 0)$ points along the line of intersection of the (x, y) plane with the plane of motion. The ray in this direction is called the *ascending node*. For such orbits, one can define another angle, the *longitude of the ascending node*, Ω , such that

$$(\cos \Omega, \sin \Omega) = \frac{(-C_2, C_1)}{\sqrt{C_1^2 + C_2^2}} = \frac{(-C_2, C_1)}{|C| \sin \iota}.$$

Ω is not defined, or could be viewed as arbitrary, for orbits in the (x, y) -plane. In any case, knowing both ι and Ω will determine the plane of the orbit.

Finally, to describe the orbit within the plane of motion, one can still use the planar elements a or p and e and it only remains to specify the location of the perihelion within the plane of motion. The traditional way, which works when $\iota \neq 0$ is to first define another angle, ω , as the angle between the ascending node and the perihelion. Since A points to the pericenter and using the fact that $A \cdot C = 0$

Planet	a	e	ι	T
Earth	149.6	0.017	0.0	365.2
Venus	108.2	0.007	3.4	224.7
Mars	227.9	0.094	1.9	687.0
Jupiter	778.6	0.049	1.3	4331
Saturn	1433.5	0.057	2.5	10747

TABLE 1. Orbital elements from the solar system. Major semiaxis, a , is in millions of km., inclination in degrees and period in days.

one can show

$$\cos \omega = \frac{A_2 C_1 - A_1 C_2}{|A||C| \sin \iota} \quad \sin \omega = \frac{-A_1 C_1 - A_2 C_2}{|A||C| \sin \iota}.$$

ω is called the *argument of the pericenter*. Alternatively, one can define the *longitude of the pericenter* in the spatial case as

$$\varpi = \Omega + \omega.$$

Note that ϖ is the sum of angles in different planes. This has the advantage that, in the limit as $\iota \rightarrow 0$, it can be shown that it reduces to the planar longitude of the perihelion, that is, the angle between A and the x -axis. Either ϖ or, in the nonplanar case, ω can be used to specify the pericenter. Then ν or M give the position of the mass along the orbit. See Figure 7.

The following table gives some orbital elements of planets in the solar system [23].

To summarize, reasonable choices of orbital elements in the spatial case are

$$a \text{ or } p \quad e \quad \varpi \text{ or } \omega \quad \iota \quad \Omega \quad \nu \text{ or } M.$$

Exercise 4.2. Prove Proposition 4.2.

Exercise 4.3. Show that for a hyperbolic solution of the Kepler problem, let σ denote the angle between the asymptotes. σ can be described as a *scattering angle* which measures how much the path of a moving particle is affected by passing near the attracting center. Show that the scattering angle is

$$\sigma = 2 \arctan(\sqrt{2h}|C|/m) = 2 \arctan \sqrt{e^2 - 1}.$$

Thus among the Kepler orbits with given mass m and energy $H > 0$, all scattering angle with $0 < \sigma < \pi$ are possible.

4.2. Solution using Souriau's method. Here is another interesting and remarkably simple way to solve the Kepler problem which is due to Souriau [24]. In addition to giving formulas for the orbit, it leads to formulas for the position along the orbit.

Let $q(t)$ be a solution of the Kepler problem in \mathbb{R}^d with energy constant h . The independent variable t will be replaced by another parameter $u(t)$. By definition, $u(t)$ and its inverse function $t(u)$ satisfy

$$\dot{u}(t) = \frac{1}{r(t)} \quad t'(u) = r(u) \quad r = |q|.$$

This defines $u(t)$ up to an additive constant. For any function $f(t)$, write $f(u)$ for $f(t(u))$ and $f'(u)$ for the derivative with respect to u . The derivatives with respect to the two timescales are related by $f' = r\dot{f}$.

Using the new timescale, the differential equations of the Kepler problem are

$$(28) \quad \begin{aligned} q' &= rv \\ v' &= -\frac{mq}{r^2} \\ t' &= r. \end{aligned}$$

It is also straightforward and useful to calculate

$$r' = q \cdot v \quad q'' = (q \cdot v)v - \frac{mq}{r}.$$

The energy equation is still

$$\frac{1}{2}|v|^2 - \frac{m}{r} = h.$$

Let Z be the “spacetime” vector $Z(u) = (t(u), q(u)) \in \mathbb{R}^{d+1}$. Then a simple calculation gives

$$(29) \quad \begin{aligned} Z &= (t, q) \\ Z' &= (r, rv) \\ Z'' &= (q \cdot v, (q \cdot v)v - \frac{mq}{r}) \\ Z''' &= (2hr + m, 2hrv) = 2hZ' + (m, 0) \\ Z'''' &= 2hZ''. \end{aligned}$$

The energy equation was used to simplify Z''' . The result of this remarkable calculation is that Z'' satisfies a simple linear differential equation.

Proposition 4.5. *Let $q(t)$ be a solution of the Kepler problem with energy h and let*

$$(30) \quad X = Z'' = (q \cdot v, (q \cdot v)v - \frac{mq}{r}) \quad Y = Z''' = (2hr + m, 2hrv).$$

Then with respect to the timescale u , $X(u)$ satisfies the linear differential equations $X'' = 2hX$ and $X(u), Y(u)$ satisfy the first order linear system

$$(31) \quad X' = Y \quad Y' = 2hX.$$

It is easy to solve this linear system. In the negative energy case, $h < 0$, let $\omega = \sqrt{-2h}$ and the second order equation for X becomes $X'' = -\omega^2 X$. This is just the equation of a $(d+1)$ -dimensional harmonic oscillator and the solution is

$$(32) \quad \begin{aligned} X &= C_1 \cos \omega u + C_2 \sin \omega u \\ Y &= -\omega C_1 \sin \omega u + \omega C_2 \cos \omega u \end{aligned}$$

where $C_1, C_2 \in \mathbb{R}^{d+1}$ are arbitrary constant vectors.

Similarly if $h > 0$ the solution is

$$(33) \quad \begin{aligned} X &= C_1 \cosh \omega u + C_2 \sinh \omega u \\ Y &= \omega C_1 \sinh \omega u + \omega C_2 \cosh \omega u \end{aligned}$$

where $\omega = \sqrt{2h}$.

Equations (30) can be viewed as an elaborate change of coordinates or conjugacy, $(X, Y) = \psi(q, v)$, which maps the orbits of the Kepler problem with energy H onto

a submanifold of $\mathbb{R}^{d+1} \times \mathbb{R}^{d+1}$. To find the image of ψ , it is convenient to split the vectors $X, Y \in \mathbb{R}^{d+1}$ as $X = (X_0, \hat{X}), Y = (Y_0, \hat{Y})$ with $X_0, Y_0 \in \mathbb{R}^1$ and $\hat{X}, \hat{Y} \in \mathbb{R}^d$. Then ψ is given by

$$(34) \quad X_0 = q \cdot v \quad \hat{X} = (q \cdot v)v - \frac{mq}{r} \quad Y_0 = 2hr + m \quad \hat{Y} = 2hrv$$

With the help of the energy equation, one can check that the following constraints equations hold

$$(35) \quad \begin{aligned} -2hX_0^2 + |\hat{X}|^2 &= m^2 \\ -2hY_0^2 + |\hat{Y}|^2 &= -2hm^2 \\ -2hX_0Y_0 + \hat{X} \cdot \hat{Y} &= 0. \end{aligned}$$

Proposition 4.6. *For $h \neq 0$, let $\mathcal{M}(h) = \{(q, v) : q \neq 0, H(q, v) = h\}$ and $\mathcal{N}(h) = \{(X, Y) : Y \neq (m, 0), (35) \text{ hold}\}$ and let $(X, Y) = \psi(q, v)$ be the mapping defined by (34). Then $\psi : \mathcal{M}(h) \rightarrow \mathcal{N}(h)$ is a diffeomorphism.*

Proof. Since $r = |q| \neq 0$ in $\mathcal{M}(h)$, the image of ψ is contained in $\{Y \neq (m, 0)\}$. Solving equations (34) for q, v gives the inverse map

$$(36) \quad r = \frac{Y_0 - m}{2h} \quad q = \frac{1}{2hm}(X_0\hat{Y} - (Y_0 - m)\hat{X}) \quad v = \frac{\hat{Y}}{Y_0 - m}$$

which is well-defined when $H \neq 0$ and $Y \neq (m, 0)$. The image point $(q, v) = \psi^{-1}(X, Y)$ has $r \neq 0$ and one can check that it has energy h , as required. QED

Applying ψ^{-1} to the general solution formulas for $X(u), Y(u)$ gives the solutions to the Kepler problem as function of u . Note that the constant vectors in equations (32) and (33) are given by $C_1 = X(0), \omega C_2 = Y(0)$. One can choose the origin of the new timescale parameter u such that $r'(0) = q(0) \cdot v(0) = 0$ which implies $C_1 = X(0) = (0, \hat{X}(0))$. Then it follows that

$$C_1 = (0, -\frac{mq_0}{r_0}) \quad \omega C_2 = (2hr_0 + m, 2hr_0v_0)$$

where r_0, q_0, v_0 are the initial values of r, q, v at $u = 0$. Substituting these into (32) and (33) and applying ψ^{-1} gives nice formulas for the solutions of the Kepler problem.

In the negative energy case, the result can be written (after quite a bit of simplification)

$$\begin{aligned} r &= a(1 - e \cos E) \\ q &= -ae \frac{q_0}{r_0} + a \cos E \frac{q_0}{r_0} + b \sin E \frac{v_0}{|v_0|} \end{aligned}$$

with

$$\omega = \sqrt{-2h} \quad E = \omega u \quad a = \frac{m}{-2h} \quad e = \frac{a - r_0}{a} \quad b = a\sqrt{1 - e^2}.$$

The use of the variable E instead of u is traditional. It's called the *eccentric anomaly*.

From our assumption that $q_0 \cdot v_0 = 0$, it follows that q_0/r_0 and $v_0/|v_0|$ are orthogonal unit vectors. Then it is easy to see that the formula for $q(E)$ is a parametric equation for an ellipse in the plane spanned by these vectors and the lengths of the principle axes are a and b . The constant term in the formula just shifts the center of the ellipse along the direction of the major axis which moves

the focus to the origin. r takes its minimal value at $E = u = 0$ which therefore represents the pericenter.

The corresponding formulas for the positive energy case are

$$r = a(e \cosh E - 1)$$

$$q = ae \frac{q_0}{r_0} - a \cosh E \frac{q_0}{r_0} + b \sinh E \frac{v_0}{|v_0|}$$

where now $h > 0$ and

$$\omega = \sqrt{2h} \quad E = \omega u \quad a = \frac{m}{2h} \quad e = \frac{a + r_0}{a} \quad b = a\sqrt{e^2 - 1}.$$

This is a parametric representation of a hyperbola, as expected. This time E is called the *hyperbolic anomaly*.

There are also parametric formulas for the time $t(u)$ as a function of the parameter u . Recall that, by definition, $t'(u) = r(u)$. So $t(u)$ can be found by integrating the formula for $r(u)$. Choosing the initial value $t(0) = 0$ gives the formulas

$$t(u) = \frac{a}{\omega}(\omega u - e \sin \omega u) \quad h < 0$$

$$t(u) = \frac{a}{\omega}(e \sinh \omega u - \omega u) \quad h > 0.$$

These can be written

$$(37) \quad \begin{aligned} nt(E) &= E - e \sin E & h < 0 \\ nt(E) &= e \sinh E - E & h > 0 \end{aligned}$$

where $n = \omega/a$. In the negative energy case, this is called *Kepler's equation*. There are no simple formulas for the inverse functions $u(t)$ or $E(t)$. Nevertheless, these formulas together with the formulas for $q(u)$, $r(u)$ give an explicit parametric solution to the Kepler problem. For example, they can be used to plot the graphs of $r(t)$ without finding a formula for it (see Figure 9).

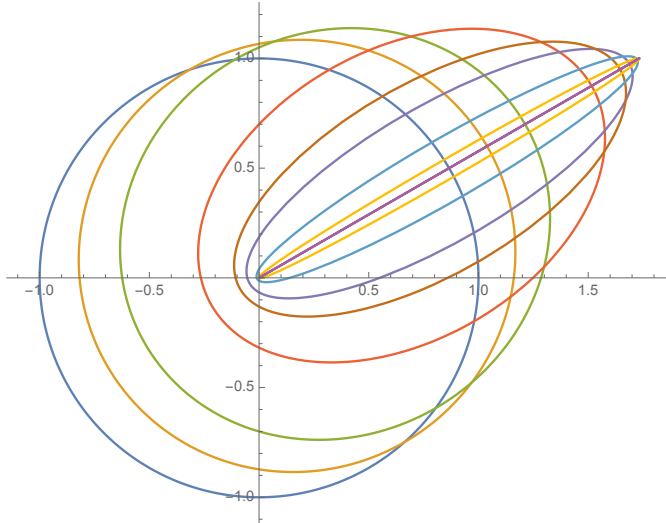


FIGURE 8. Some elliptic orbits of the Kepler problem, all with the same energy. All have the same period and major semiaxis.

From the formula for $h < 0$, it is easy to read off the periods of the elliptic orbits. Both the period and the major semiaxis depend only on the value of h (see Figure 8).

Proposition 4.7. *For the Kepler problem with energy $h < 0$, every solution is periodic with the same period $T(h)$ and moves on an elliptical path with the same major semiaxis $a(h)$ where*

$$a(h) = \frac{m}{2h} \quad T(h) = \frac{2\pi m}{|2h|^{\frac{3}{2}}} = \frac{2\pi a^{\frac{3}{2}}}{\sqrt{m}}.$$

Proof. The formula for $a(h)$ is already established. The parametric formula $q(E)$ is clearly periodic with period 2π . As E varies over one period, $t(E)$ increases by $T = 2\pi/n = \frac{2\pi a}{\omega}$ and this is the period with respect to t . Using the formula for a and $\omega = \sqrt{|2h|}$ the other formulas for T follow. QED

The proof shows that $n = 2\pi/T$ is the mean angular velocity as in Definition 4.1. So nt is the mean anomaly and the Kepler equation 37 can be written

$$M = E - e \sin E.$$

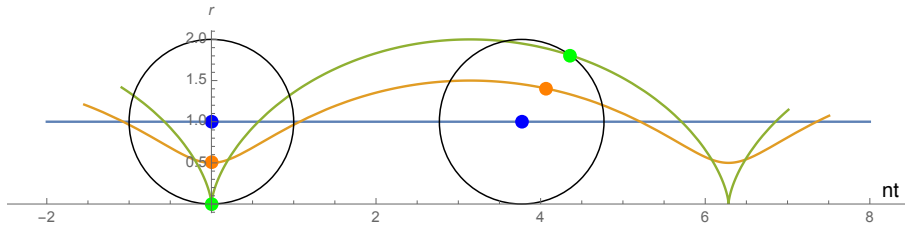


FIGURE 9. Radius versus nt for some elliptic orbits of the Kepler problem with eccentricities $0, \frac{1}{2}, 1$. For $0 < e < 1$ graphs are trochoids while for $e = 1$ it's a cycloid (see exercise 4.8).

Exercise 4.4. Verify equations (29) and (35).

Exercise 4.5. According to the last equation in Proposition 4.7 the ratio a^3/T^2 should be the same for all solutions of the Kepler problem with a given central mass, m . For the solar system, this is known as Kepler's third law. Using the data from Table 4.1, check the validity of this prediction.

Exercise 4.6. If $h = 0$ the vector $Z = (t, q)$ satisfies $Z'''' = 0$ and it follows that Z is a cubic polynomial, $Z(u) = C_0 + C_1 u + C_2 u^2 + C_3 u^3$ for some constant vectors $C_i \in \mathbb{R}^{d+1}$. Evaluate the constants to show that under the assumptions $t_0 = q_0 \cdot v_0 = 0$

$$\begin{aligned} t(u) &= r_0 u + \frac{1}{6} m u^3 \\ r(u) &= r_0 + \frac{1}{2} m u^2 \\ q(u) &= q_0 + r_0 v_0 u - \frac{m q_0}{2 r_0} u^2. \end{aligned}$$

Exercise 4.7. For $h = 0$ there is no need to extend into \mathbb{R}^{d+1} . Let $Z = q$ instead of (t, q) . Then (29) shows that $Z''' = 0$. Let

$$(38) \quad X = Z'' = q'' = (q \cdot v)v - \frac{mq}{r} \quad Y = Z' = rv.$$

Show that (38) defines a diffeomorphism $\psi : \mathcal{M}(0) \rightarrow \mathcal{N}(0)$ where $\mathcal{M}(0) = \{(q, v) : q \neq 0, H(q, v) = 0\}$ and $\mathcal{N}(0) = \{(X, Y) : Y \neq 0, |X| = m\}$ hold } such that the new differential equations are $X' = 0, Y' = X$. Hint: Find ψ^{-1} .

Exercise 4.8. For the Kepler problem with energy $h < 0$, the graph of the distance to the attracting center $r(nt) = |q(nt)|$ as a function of nt is a trochoid, that is, the curve swept out by a point inside a circular disk as the disk rolls along a line. The graph is given parametrically by $nt = E - e \sin E, r = a(1 - e \cos E)$. Show that this is the curve swept out by a point p at radius ae inside a disk of radius a as it rolls along the nt axis as in Figure 9. Hint: After the disk has rolled through an angle θ , what is the position of the center ? What is the position of p ?

4.3. Regularization, Conjugacy to a Geodesic Flow, and Hidden Symmetry. This section describes several of the deeper consequences of the coordinate and timescale transformations of the last section. According to Proposition 4.6, the change of coordinates $(X, Y) = \psi(q, v)$ maps the Kepler problem with fixed energy h onto the submanifold $\mathcal{N}(h) = \{(X, Y) : Y \neq (m, 0), (35) \text{ hold}\} \subset \mathbb{R}^{d+1} \times \mathbb{R}^{d+1}$. The deleted points $Y = (m, 0), X_0 = 0, |\hat{X}| = m$ represent collision states. Attempting to apply the inverse map (36) gives $q = 0$. Also, for nearby points which satisfy (35) velocity satisfies

$$|v| = \frac{|\hat{Y}|}{|Y_0 - m|} = \frac{-2h(Y_0 + m)}{|\hat{Y}|}.$$

As $Y \rightarrow (m, 0)$, it follows that $|v| \rightarrow \infty$.

But from the point of view of the differential equations for (X, Y) , the points with $Y = (m, 0)$ are nonsingular. Thus the singular Kepler problem has been embedded into a smooth system with no singularities. Allowing solutions $(X(u), Y(u))$ to pass through $Y = (m, 0)$ provides a way to extend solutions of the Kepler problem through collision in way which is compatible with the nearby noncollision solutions. This extension is called a *regularization* of the Kepler problem. The one described here is close to that of Moser [19].

For example, consider a solution of (30) with initial conditions $X(0) = (0, \hat{X}(0))$, $Y(0) = (m, 0) = 0$ where $|\hat{X}| = m$. This satisfies the constraint equations (30) for every value of the energy h . For simplicity, consider a solution with energy $h = -\frac{1}{2}$. If $\hat{X}(0) = m\xi$ where ξ is a unit vector, then the constants C_i in the solution (32) are $C_1 = (0, m\xi), \omega C_2 = (m, 0)$ and the solution is

$$X_0(u) = m \sin u \quad \hat{X}(u) = m \cos u \xi \quad Y_0(u) = m \cos u \quad \hat{Y}(u) = -m \sin u \xi$$

Applying ψ^{-1} gives a regularized solution of the Kepler problem

$$\begin{aligned} q(u) &= m\xi(1 - \cos u) & v(u) &= \frac{\xi \sin u}{m(1 - \cos u)} \\ r(u) &= m(1 - \cos u) & t(u) &= m(u - \sin u). \end{aligned}$$

This solution moves periodically on the line segment from the origin to $m\xi$ bouncing off the singularity at the origin at $u = 0, \pm 2\pi, \dots$. At these times, the velocity is

infinite. The graph of the radius as a function of the time t is like the cycloid in Figure 9.

Figure 8 shows several elliptic orbits of the Kepler problem with the same energy and different eccentricities $0 \leq e \leq 1$. As $e \rightarrow 1$ the ellipses converge to a line segment associated to a regularized solution. In this way, one can see that the bouncing behavior of the regularized solution is a continuous, natural extension of these nearby, nonsingular solutions.

Next, it will be shown that the regularized Kepler problem is equivalent to the familiar problem of geodesics on a sphere or hyperboloid. First consider the negative energy case. Using the notation $\omega = \sqrt{-2h}$, the constraint equations (30) can be written as

$$\omega^2 X_0^2 + |\hat{X}|^2 = m^2 \quad \omega^2 Y_0^2 + |\hat{Y}|^2 = \omega^2 m^2 \quad \omega^2 X_0 Y_0 + \hat{X} \cdot \hat{Y} = 0.$$

Define new, rescaled variables $Q, P \in \mathbb{R}^{d+1}$ by

$$Q_0 = \frac{1}{m} Y_0 \quad \hat{Q} = \frac{1}{\omega m} \hat{Y} \quad P_0 = -\frac{\omega^2}{m} X_0 \quad \hat{P} = -\frac{\omega}{m} \hat{X}.$$

Then the differential equations (31) become

$$Q' = P \quad P' = -\omega^2 Q$$

and the constraint equations become (35) become

$$|Q|^2 = Q_0^2 + |\hat{Q}|^2 = 1 \quad |P|^2 = P_0^2 + |\hat{P}|^2 = \omega^2 \quad Q \cdot P = Q_0 P_0 + \hat{Q} \cdot \hat{P} = 0.$$

These are the differential equations for the geodesic flow on the unit sphere in \mathbb{R}^{d+1} . $Q(u)$ describes the point on the sphere and $P(u) = Q'(u)$ is its velocity vector which is always perpendicular to $Q(u)$ and has constant speed $|P(u)| = \omega$. In what follows, the term “geodesic flow” will always refer to geodesics with some fixed constant speed. Note that the condition $Y \neq (m, 0)$ of Proposition 4.6 becomes $Q = (Q_0, \hat{Q}) \neq (1, 0)$ here.

Proposition 4.8. *The Kepler problem in \mathbb{R}^d with fixed energy $h < 0$ is conjugate to the open subset of the geodesic flow on the unit sphere in \mathbb{R}^{d+1} consisting of all geodesics which never pass through the point $Q = (Q_0, \hat{Q}) = (1, 0)$. The regularized Kepler problem is conjugate to the full geodesic flow.*

For example, the regularized, planar Kepler problem ($d=2$) is conjugate to the geodesic flow on the unit sphere $\mathbb{S}^2 \subset \mathbb{R}^3$. The geodesics are the great circles. Thus these coordinate changes have the remarkable effect of mapping all of the elliptical orbits with a given energy, as in Figure 8 onto the great circles on the sphere. The regularized collision orbits which sweep out line segments in the plane are mapped to the geodesics passing through the special point $Q = (1, 0)$ which, by a convenient change of perspective, will be called the “North Pole”. Viewed in the sphere, these are in no way special.

An immediate corollary of this discussion is the realization that the Kepler problem has an unexpectedly large group of symmetries. While it is clear that the Kepler problem in \mathbb{R}^d is invariant under orthogonal transformation in \mathbb{R}^d it now appears that

Corollary 4.1. *The regularized Kepler problem in \mathbb{R}^d with a fixed negative energy admits the symmetry group $\mathbf{O}(d+1)$, the orthogonal group in \mathbb{R}^{d+1} .*

For example, the planar Kepler problem is clearly invariant under rotations and reflections of the plane. But this is only a one-dimensional group. In fact, there is an action of the three-dimensional group of rotations and reflections in space. This is sometimes called a *hidden symmetry* of the Kepler problem.

To explore this phenomenon further, consider how the rotations of \mathbb{R}^3 transform the Kepler ellipses of the planar problem. First note that the rotation group of the plane, $\mathbf{SO}(2)$ preserves the distance to the origin, r and simply rotates all of the elliptical orbits around the origin. Since $r = (Y_0 - m)/(2h) = m(1 - Q_0)/\omega^2$, the corresponding rotations of the sphere are those which preserve the Q_0 coordinate, that is, the rotations around the North Pole. On the other hand, rotations in $\mathbf{SO}(3)$ which move the North Pole will have a nontrivial effect on the elliptical orbits. This is best seen in an animation, but Figure 10 shows the effect of the rotations around the point $(0, 0, 1)$ on the great circle geodesics and the corresponding Keplerian orbits. All of the ellipses on the right side of the figure are the images of the circular geodesic under the action of the hidden symmetry group.

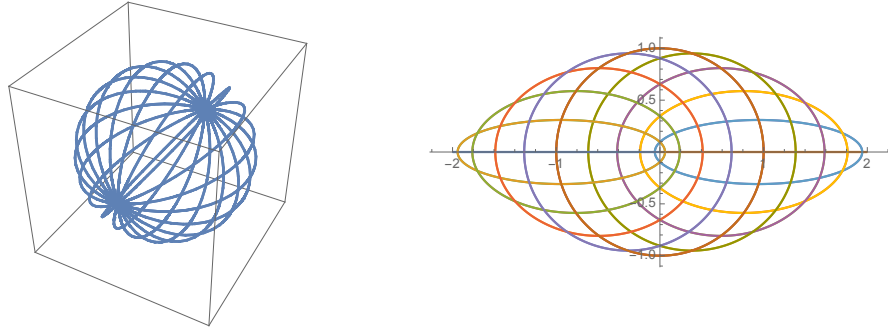


FIGURE 10. Action of a family of rotations in $\mathbf{SO}(3)$ on the great circles in \mathbb{S}^2 and on the corresponding planar Kepler orbits.

Next suppose $h > 0$ and set $\omega = \sqrt{2h}$. This time, the constraint equations (30) can be written as

$$-\omega^2 X_0^2 + |\hat{X}|^2 = m^2 \quad -\omega^2 Y_0^2 + |\hat{Y}|^2 = -\omega^2 m^2 \quad -\omega^2 X_0 Y_0 + \hat{X} \cdot \hat{Y} = 0.$$

The rescaled variables $Q, P \in \mathbb{R}^{d+1}$ by

$$Q_0 = \frac{1}{m} Y_0 \quad \hat{Q} = \frac{1}{\omega m} \hat{Y} \quad P_0 = -\frac{\omega^2}{m} X_0 \quad \hat{P} = -\frac{\omega}{m} \hat{X}$$

satisfy

$$Q' = P \quad P' = \omega^2 Q$$

with

$$-Q_0^2 + |\hat{Q}|^2 = -1 \quad -P_0^2 + |\hat{P}|^2 = \omega^2 \quad -Q_0 P_0 + \hat{Q} \cdot \hat{P} = 0.$$

These are the differential equations for the geodesic flow on a hyperboloid of two sheets in \mathbb{R}^{d+1} . Equation 34 shows that, in this case, $Y_0 > 0$ and hence $Q_0 > 0$ so only the “top” sheet of the hyperboloid is relevant.

Proposition 4.9. *The Kepler problem in \mathbb{R}^d with fixed energy $h > 0$ is conjugate to the open subset of the geodesic flow on the top sheet of a unit hyperboloid in \mathbb{R}^{d+1} consisting of all geodesics which never pass through the point $Q = (Q_0, \hat{Q}) = (1, 0)$. The regularized Kepler problem is conjugate to the full geodesic flow.*

The geodesics on the hyperboloid are just the “great hyperboloids” obtained by intersecting the hyperboloid with two-dimensional planes through the origin.

The analogy between the negative and positive energy cases can be made stronger by using the Minkowski metric and norm in \mathbb{R}^{d+1}

$$\langle V, W \rangle = -V_0 W_0 + \hat{V} \cdot \hat{W} \quad \|V\|^2 = -V_0^2 + |\hat{V}|^2.$$

Then the constraints can be written

$$\|Q\|^2 = -1 \quad \|P\|^2 = \omega^2 \quad \langle Q, P \rangle = 0.$$

So the hyperboloid is just a unit “sphere” with respect to the Minkowski metric. The symmetry group of the positive energy Kepler problem is $\mathbf{O}(1, d)$, that is, the linear transformations of \mathbb{R}^{d+1} which preserve the Minkowski metric. This group contains orthogonal group $\mathbf{O}(d)$ as the subgroup mapping $0 \times \mathbb{R}^d$ to itself, but the full group is much larger. So once again, there are hidden symmetries.

Corollary 4.2. *The regularized Kepler problem in \mathbb{R}^d with a fixed positive energy admits the symmetry group $\mathbf{O}(1, d)$.*

The analogy extends to the case $h = 0$ as well where one gets the geodesics in \mathbb{R}^d , that is, straight line motions at constant speed.

Proposition 4.10. *The Kepler problem in \mathbb{R}^d with fixed energy $h = 0$ is conjugate to the open subset of the geodesic flow on Euclidean space \mathbb{R}^d consisting of all geodesics which never pass through the point $Q = 0$. The regularized Kepler problem is conjugate to the full geodesic flow. The symmetry group is the Euclidean group $\text{Euc}(d)$.*

The proof is a bit different (see exercise 4.9). Once again, the symmetry group is unexpectedly large. For example, while the Kepler problem in the plane is obviously symmetry under rotations of the plane, this is not so for translations. Figure 11 shows a family of geodesics in the plane obtained by translation and the corresponding family of parabolic orbits.

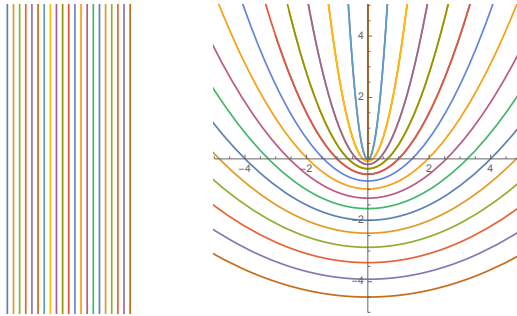


FIGURE 11. Action of a family of translations in $\text{Euc}(2)$ on the lines in \mathbb{R}^2 and on the corresponding planar Kepler orbits.

Exercise 4.9. Use Exercise 4.7 to prove Proposition 4.10.

4.4. Central force problems, reduction, invariant tori. It is illuminating to consider the Kepler problem as a special case of a central force problem, an approach going back to Newton. Imagine changing the potential of the Kepler problem to some other function $U(q) = F(r)$ depending only on the radius $r = |q|$. In this case, the force function

$$\nabla U(q) = \frac{F'(r)}{r} q$$

always points toward or away from the origin. This is called a *central force* problem. For example, one could take a *power-law* potential

$$U(q) = F(r) = \frac{m}{r^\alpha} \quad r = |q|$$

where $\alpha > 0$. It will be seen that the Kepler case $\alpha = 1$ has extra structure.

The differential equation are

$$(39) \quad \begin{aligned} \dot{q} &= v \\ \dot{v} &= \nabla U(q) = \frac{F'(r)}{r} q. \end{aligned}$$

The symmetry arguments showing that angular momentum tensor is constant apply here too. Also, there is an energy constant

$$(40) \quad \frac{1}{2}|v|^2 - U(q) = \frac{1}{2}|v|^2 - F(r) = h.$$

The same proof as for the Kepler problem shows that all of the motions of a central force problem are actually planar.

Proposition 4.11. *Every solution $q(t)$ of a central force problem moves in a fixed plane in \mathbb{R}^d , namely, the plane through the origin containing its initial position and velocity vectors.*

Assuming that the motion plane is really \mathbb{R}^2 , the flow takes place in the four-dimensional phase space $\{(q, v) : q \neq 0\} \subset \mathbb{R}^4$. One can introduce polar coordinates as in Example 2.1 to get a Lagrangian

$$\tilde{L} = \frac{1}{2}(\dot{r}^2 + r^2\dot{\theta}^2) + F(r).$$

The EL equations are

$$\dot{p}_r = F'(r) + 2r^2\dot{\theta} \quad \dot{p}_\theta = 0$$

where $p_r = \tilde{L}_r = \dot{r}$, $p_\theta = r^2\dot{\theta}$. The fact that p_θ is constant can be seen as a special case of Nöther's theorem where the symmetry is the translation of the angle $\theta \mapsto \theta + s$, $s \in \mathbb{R}$. Since translation of θ corresponds to rotation in the plane, it is no surprise that p_θ is just the planar angular momentum. Indeed, viewing the problem as a unit mass attracted to the origin, the angular momentum scalar is

$$C = q_1 v_2 - q_2 v_1 = r^2\dot{\theta}.$$

Using the symmetry of the problem under rotations, it's possible to reduce to only two dimensions. This reduction process will first be discussed for a general Lagrangian $L(q, v)$ on TX where X is an open set in \mathbb{R}^m and suppose that L does not depend on the last configuration variable q_m . In other words, $L = L(q_1, \dots, q_{m-1}, v_1, \dots, v_m)$. In this case q_m is sometimes called a *cyclic variable*. The m -th Euler-Lagrange equation is $\dot{p}_m = 0$ so p_m is a constant of motion. The

following result shows how to construct a reduced Lagrangian system after fixing a value for p_m .

Proposition 4.12. *Let $L(q, v)$ be a Lagrangian such that q_m is a cyclic variable. Let $(\hat{q}, \hat{v}) = (q_1, \dots, q_{m-1}, v_1, \dots, v_{m-1})$ and suppose the equation $p_m = L_{v_m}(q, v)$ can be inverted to get v_m as a function $v_m(\hat{q}, \hat{v}, p_m)$. If $q(t)$ is a solution of the Euler-Lagrange equations for L with $p_m = \mu \in \mathbb{R}$ then $\hat{q}(t)$ is a solution of the Euler-Lagrange equations for the reduced Lagrangian*

$$(41) \quad L_\mu(\hat{q}, \hat{v}) = L(\hat{q}, \hat{v}, v_m(\hat{q}, \hat{v}, \mu)) - \mu \cdot v_m(\hat{q}, \hat{v}, \mu).$$

Moreover, q_m, v_m can be reconstructed by integrating the equation $\dot{q}_m = v_m = v_m(\hat{q}(t), \hat{v}(t), \mu)$.

Proof. Exercise 4.10. QED

The reduced Lagrangian L_μ is sometimes called the *Routhian*.

Example 4.2. For the central force problem, fix a value $p_\theta = C$ for the angular momentum. The equation $p_\theta = r^2\dot{\theta} = C$ can be solved for $\dot{\theta} = C/r^2$ and the Routhian is

$$(42) \quad L_C(r, \dot{r}) = \frac{1}{2}(\dot{r}^2 + r^2(C/r^2)^2) + F(r) - C(C/r^2) = \frac{1}{2}\dot{r}^2 - \frac{C^2}{2r^2} + F(r).$$

For each fixed C , one can study this equation in the (r, \dot{r}) phase space. If a solution $r(t)$ is found then recover $\theta(t)$ can be recovered by integration

$$\theta(t) = \theta(0) + \int_0^t \frac{C}{r(s)^2} ds.$$

Setting $w = \dot{r}$, the reduced Lagrangian (42) can be written

$$L_C(r, w) = \frac{1}{2}w^2 - V_C(r) \quad V_C(r) = \frac{C^2}{2r^2} - F(r).$$

$V_C(r)$ is called the *reduced* or *amended* potential energy (this is really the potential energy – note the minus sign in the Lagrangian). The energy constant is

$$H_C(r, w) = \frac{1}{2}w^2 + V_C(r) = h.$$

Plotting the level curves of H_C in the (r, w) plane produces the phase portrait of the reduced system.

Figure 12 shows typical amended potentials for the power-law potentials $F(r) = mr^{-\alpha}$ for the Kepler problem $\alpha = 1$ and for $\alpha = 3$ where the amended potentials are

$$(43) \quad V_C(r) = \frac{C^2}{2r^2} - \frac{m}{r^\alpha}.$$

The shape of the corresponding graph for $0 < \alpha < 2$ resembles the Kepler case while the shape for $\alpha > 2$ is like the case $\alpha = 3$. It is clear from (43) that $V(r)$ changes sign at $r = r_0$ and has exactly one critical point $r = r_{crit}$ where

$$r_0 = \left(\frac{C^2}{2m} \right)^{\frac{1}{2-\alpha}} \quad r_{crit} = \left(\frac{C^2}{\alpha m} \right)^{\frac{1}{2-\alpha}}.$$

The critical point is a minimum or a maximum of the potential energy according to whether $\alpha < 2$ or $\alpha > 2$.

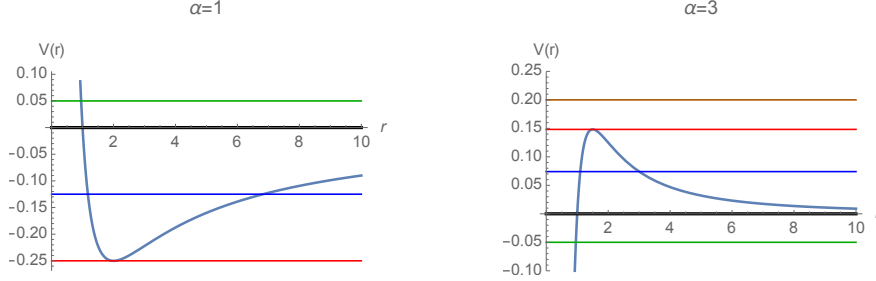


FIGURE 12. Amended potential energies for some $r^{-\alpha}$ power-law central force problems with $m = 1$, $C = \sqrt{2}$. Also shown are some lines $V = h$ for several values of the energy.

From the graph of $V_C(r)$ one obtains the phase portraits in the (r, w) halfplane by plotting the curve $w^2 = 2(h - V_C(r))$ for various values of h . These curves are clearly symmetric under reflection through the w -axis and their projections lie over the interval or intervals where $V_C(r) \leq h$. In Figure 12, these intervals are those such that the graph is below the corresponding horizontal line at height h . The results for $\alpha = 1, 3$ are shown in Figure 13.

For the Kepler problem (left) there is an equilibrium point at $(r_{crit}, 0) = (C^2/m, 0)$ with energy $h = -m^2/(2C^2)$ (red). Energies $h < -m^2/(2C^2)$ are not possible for fixed C . The equilibrium of the reduced system means that for the corresponding solution the radius r is constant. Though not shown in the figure, one can imagine the angle $\theta(t)$ increasing or decreasing. In fact, the angular momentum equation shows that $\dot{\theta} = C/r_{crit}^2$ which is also constant. The corresponding solutions are just the circular solutions of the Kepler problem. For energies $-m^2/(2C^2) < h < 0$ there is a family of periodic solutions (blue) such that $r(t)$ oscillates over some interval $[r_1, r_2]$. This is the radial behavior of the elliptic Kepler orbits. For energies $h \geq 0$, the radius decreases from infinity, reaches a minimum and then increases to infinity again (black and green). This is the radial behavior of the parabolic and hyperbolic solutions. The phase portrait is similar for all α with $0 < \alpha < 2$ but there are significant differences in the angular behavior which will be explored later.

For $\alpha = 3$ (right) the (r, w) phase portrait is completely different. There is an equilibrium point at $(r_{crit}, 0)$ (red) which will correspond to a circular periodic solution. But now it's a saddle point and the corresponding energy level curve has branches tending to infinity and branches which fall into the singularity ($r(t) \rightarrow 0$). In fact there are lots of solutions which have this fate in forward or backward time, or both. Apparently there are no bounded solutions other than the circular one. The picture is similar for all $\alpha > 2$.

The passage from dynamics in the four-dimensional $(r, \theta, w, \dot{\theta})$ space to the two-dimensional (r, w) halfplane is a process of *reduction* by symmetry. After fixing the angular momentum C , $\dot{\theta} = C/r^2$ is uniquely determined and θ can be ignored. A more sophisticated point of view is to say that the (r, w) halfplane is a quotient space of the fixed angular momentum manifold under the action of the rotational

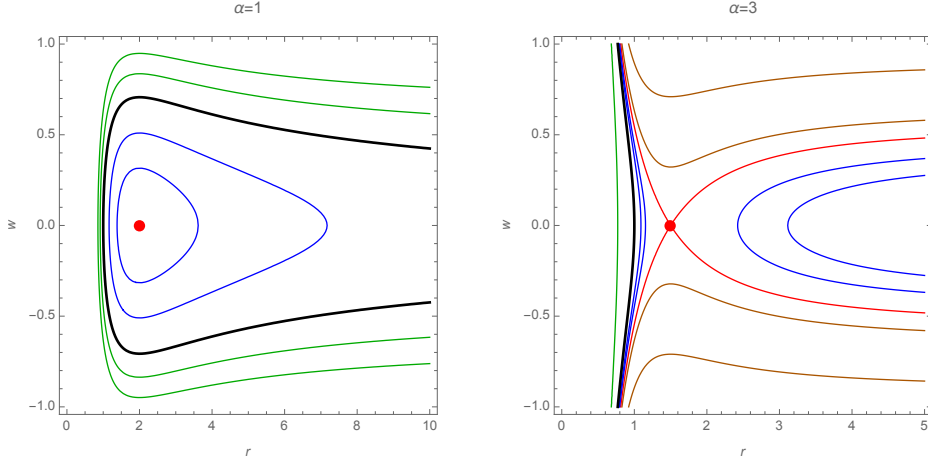


FIGURE 13. Phase plots in the (r, w) halfplane corresponding to the potentials in Figure 12.

symmetry group $\mathbf{SO}(2)$. More precisely, define submanifolds of the phase space

$$\begin{aligned}\mathcal{M}(C) &= \{(r, \theta, w, \dot{\theta}) : r > 0, r^2\dot{\theta} = C\} \\ \mathcal{M}(h, C) &= \{(r, \theta, w, \dot{\theta}) : r > 0, r^2\dot{\theta} = C, \frac{1}{2}w^2 + \frac{C^2}{2r^2} - F(r) = h\}.\end{aligned}$$

Clearly $\mathcal{M}(C)$ is three-dimensional while $\mathcal{M}(h, C) \subset \mathcal{M}(C)$ is a two-dimensional surface. In the most interesting cases, $\mathcal{M}(h, C)$ will be diffeomorphic to a torus $\mathbb{T}^2 = \mathbb{S}^1 \times \mathbb{S}^1$. Now by simply ignoring the θ variable and keeping the same equations, one obtains quotient manifolds $\tilde{\mathcal{M}}(C) = \mathcal{M}(C)/\mathbf{SO}(2)$ and $\tilde{\mathcal{M}}(h, C) = \mathcal{M}(h, C)/\mathbf{SO}(2)$ whose dimensions are, respectively, two and one. $\tilde{\mathcal{M}}(C)$ is just the (r, w) halfplane and $\tilde{\mathcal{M}}(h, C)$ are the level curves of reduced energy as in Figure 13.

The opposite process to reduction is reconstruction. Given the motion $r(t)$ of the radius, how can one find $q(t)$? The answer is to use the angular momentum constant to recover $\theta, \dot{\theta}$. Since $C = r^2\dot{\theta}$ has been fixed in advance, one can determine $\theta(t)$ by integration

$$\theta(t) = \theta(0) + \int_0^t \frac{C ds}{r(s)^2}.$$

Once $\theta(t)$ is found, then the orbit in \mathbb{R}^2 is $q(t) = r(t)(\cos \theta(t), \sin \theta(t))$. For example, Figure 14 shows two orbits for the power law potential with $\alpha = 1.5$ and two choices of the energy. Instead of the simple, periodic ellipses of the Kepler problem, the curves wind around the origin many times without returning to their initial positions. It can be shown that orbits like this may never close up and instead fill in an annular region $r_1 \leq r \leq r_2$ densely.

The most interesting cases are the periodic orbits for $0 < \alpha < 2$ and energies $V_{min} < h < 0$, where $V_{min} = V(r_{crit})$ (blue curves in Figure 13 (left)). For $C > 0$, $\theta(t)$ is increasing and so $q(t)$ moves counterclockwise around the origin as $r(t)$ oscillates over an interval $[r_1(h), r_2(h)]$. In the phase space, the corresponding solution move on an *invariant torus*. Fix a value of $C \neq 0$ and an energy h in

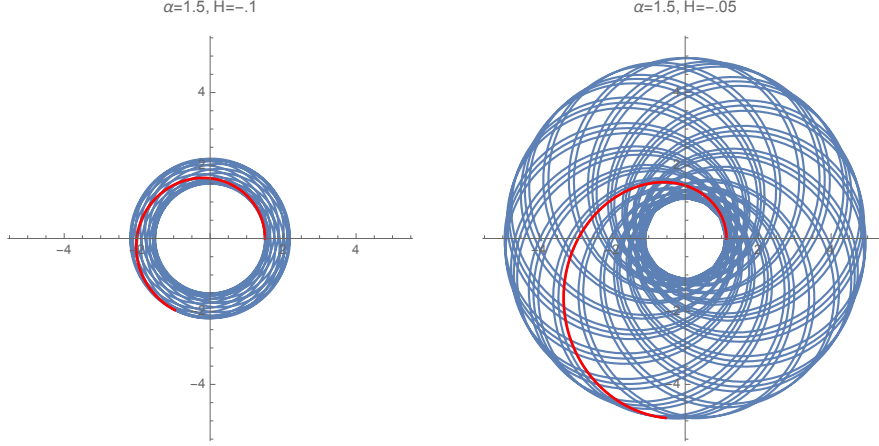


FIGURE 14. Two orbits for the power law potential with $\alpha = 1.5$ and energies $h = -0.1, -0.05$. The red curves show half of a radial period.

this range. Then the quotient manifold $\tilde{\mathcal{M}}(h, C)$ is a simple closed curve, so is diffeomorphic to \mathbb{S}^1 . In the corresponding unreduced manifold $\mathcal{M}(h, C)$, $\dot{\theta} = C/r^2$ is uniquely determined while the angle θ is arbitrary. Thinking of θ as parametrizing another circle, it follows that $\mathcal{M}(h, C)$ is diffeomorphic to $\mathbb{S}^1 \times \mathbb{S}^1$, that is, to a two-dimensional torus \mathbb{T}^2 . Invariant tori in phase space are a common feature of many mechanics problems

To understand the flow on such a torus, the crucial point is to determine how much $\theta(t)$ changes as $r(t)$ goes once around the curve $\tilde{\mathcal{M}}(h, C)$. Let $\Phi(h, C, \alpha)$ denote this change in $\theta(t)$ over one period of the oscillation of r . For the Kepler problem with $\alpha = 1$ this is just the change in the polar angle in going once around the ellipse which is clearly exactly 2π for all solutions. In other words $\Phi(h, C, 1) = 2\pi$ for $-C^2/m < h < 0$. Thus the invariant tori for the Kepler problem are filled with periodic solutions which close up after going once around in the radial direction and once around in the θ direction (see Figure 15 (left)).

On the other hand, for $\alpha \neq 1$, it turns out that the value of $\Phi(h, C, \alpha)$ varies with h, C . On some of the tori, $\Phi(h, C, \alpha) = 2\pi \frac{p}{q}$ will be a rational multiple of 2π . Then all of the solutions on the torus will be periodic, closing up after going q times around $\tilde{\mathcal{M}}(h, C)$ and p times around in the θ direction. On other tori, suppose $\Phi(h, C, \alpha) = 2\pi\omega$ for some irrational number α . In this case, the solutions on the torus never close up and, in fact, each solution is dense in the torus as in Figure 15 (right). From this point of view, one can say that Figure 14 shows the projections of solutions on two different invariant tori onto the configuration space. The tori project to annuli and a solution which is dense in the torus will project to a curve which is dense in the annulus.

It's possible to parametrize a torus using two angles and then the flow can be depicted in two dimensions. For the tori considered here, one angle will be θ . The other could be a time parameter on the curve $\tilde{\mathcal{M}}(h, C)$. Each such curve is a periodic solution of the reduced system in the (r, w) plane. If $T(h, C)$ is the period



FIGURE 15. Projections of invariant tori. Six orbits on a Kepler torus (left) and one orbit from the power law with $\alpha = 1.5$ (right). The Kepler torus is filled with simple periodic orbit; orbits on the other torus could be dense.

then the variable $\tau = 2\pi t/T$ runs from 0 to 2π during one period. The angular variables (τ, θ) parametrize the torus $\mathcal{M}(h, C)$. Figure 16 shows the flow using these variables for the solution in Figure 14 (left). If $C > 0$, all solutions have τ and θ monotonically increasing. There will be a Poincaré map from $\tau = 0$ to $\tau = 2\pi$ which is a rigid rotation of the circle given by $\theta \mapsto \theta + \Phi(h, C)$. The well-known Kronecker theorem shows that if $\Phi = 2\pi\omega$ with ω irrational, then every orbit of this circle rotation is dense in the circle. It follows that the corresponding solution curve is dense in the torus (exercise 4.11).

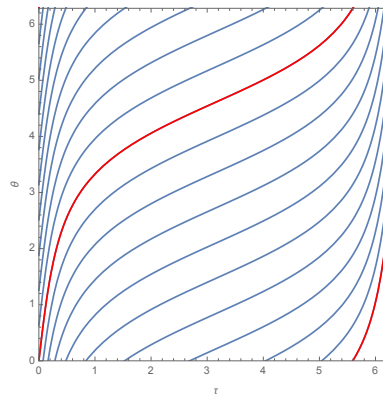


FIGURE 16. Flow on a torus in angular variables (τ, θ) . The torus corresponds to the solution in Figures 14 and 15 (left). One period or τ is shown in red and the corresponding change in θ is $\Phi = 2\pi\omega$ with $\omega \simeq 1.46573 \dots$

Exercise 4.10. Prove Proposition 4.12.

Exercise 4.11. Consider the torus flow on $\mathcal{M}(h, C)$ using angular parameters (τ, θ) and the corresponding Poincaré map of the circle $\tau = 0 \bmod 2\pi$. Show that if a solution has a dense orbit for the Poincaré map then the orbit in the torus is also dense.

5. PERTURBATION THEORY

Several real-life problems in celestial mechanics which can be viewed as a two-body problem plus a small perturbing force. This section describes two examples, the motion of a satellite around the Earth and the precession and nutation of the Earth itself. Both are based on the fact that the Earth is not spherically symmetric but has an equatorial bulge. It will be modeled as an “oblate spheroid”, that is, a rigid body whose mass distribution is not spherically symmetric but is symmetric under rotation around an axis. The potential will be approximated by using a Legendre expansion.

5.1. Rigid bodies, inertia tensor and MacCullagh’s formula. To describe a solid body in \mathbb{R}^3 , let $Q = (X, Y, Z)$ be a set of *body coordinates* in a copy of \mathbb{R}^3 . The solid is specified by a compact set $\mathcal{B} \subset \mathbb{R}^3$ together with a continuous mass density function ρ . The total mass and center of mass of the body are given by

$$m = \int_{\mathcal{B}} \rho(Q) dV \quad \bar{Q} = \frac{1}{m} \int_{\mathcal{B}} Q \rho(Q) dV$$

where the integrals are triple integrals with respect to Q . Assume that the origin of the body coordinates is chosen so that $\bar{Q} = 0$. The *inertia tensor* of \mathcal{B} is the 3×3 matrix

$$(44) \quad \mathcal{I} = \int_{\mathcal{B}} (|Q|^2 I - Q \cdot Q^T) \rho(Q) dV.$$

Here I is the 3×3 identity matrix and Q is viewed as a column vector so $Q \cdot Q^T$ is also 3×3 . Now \mathcal{I} is a symmetric, positive definite matrix so it is possible to choose the axes of the body coordinate system so that

$$\mathcal{I} = \text{diag}(A, B, C) \quad 0 \leq A \leq B \leq C.$$

Then the X, Y, Z axes are called the principle axes and A, B, C are the principle moments of inertia.

Example 5.1. Suppose \mathcal{B} is the spheroid $\frac{X^2}{a^2} + \frac{Y^2}{a^2} + \frac{Z^2}{c^2} \leq 1$ with constant density ρ_0 . So a is the radius at the equator and c is the radius at the poles. The moments of inertia are

$$A = B = \frac{4\pi}{15} \rho_0 a^2 c (a^2 + c^2) = \frac{1}{5} m(a^2 + c^2) \quad C = \frac{8\pi}{15} \rho_0 a^4 c = \frac{2}{5} m a^2$$

where $m = \frac{4\pi}{3} \rho_0 a^2 c$ is the total mass.

An equatorial bulge would mean $a > c$ and $A < C$. The effect of the bulge can be measured using one of the dimensionless ratios

$$\epsilon = \frac{C - A}{C} = \frac{a^2 - c^2}{2a^2} \quad J_2 = \frac{C - A}{ma^2} = \frac{a^2 - c^2}{5a^2}.$$

Both of these quantities make sense even if the density is not constant. For the Earth

$$\epsilon \simeq 0.00323 \quad J_2 \simeq 0.0010826.$$

If $u \in \mathbb{R}^3$ is a unit vector and $Q \in \mathbb{R}^3$ then

$$u^T(|Q|^2 I - Q \cdot Q^T)u = |Q|^2|u|^2 - (Q \cdot u)^2 = |Q|^2 \sin^2 \gamma = d^2$$

where γ is the angle between Q and u and d is the distance from Q to the axis determined by u . This is called the *moment of inertia* of Q with respect to u . Hence the *total moment of inertia* of \mathcal{B} with respect to the axis u is

$$(45) \quad \mathcal{I}(u) = u^T \mathcal{I}u = \int_{\mathcal{B}} |Q|^2 \sin^2 \gamma \rho(Q) dV = Au_1^2 + Bu_2^2 + Cu_3^2.$$

The *total moment of inertia* of \mathcal{B} with respect to the origin is defined as

$$(46) \quad \mathcal{I}_0 = \int_{\mathcal{B}} |Q|^2 \rho(Q) dV = \frac{1}{2}(A + B + C).$$

The Legendre polynomials $P_n(c)$ are defined as the coefficients in the expansion

$$\frac{1}{\sqrt{1 + x^2 - 2xc}} = \sum_{n=0}^{\infty} P_n(c)x^n = 1 + cx + \frac{1}{2}(3c^2 - 1)x^2 + \dots$$

For $q, Q \in \mathbb{R}^3$, $|q - Q|^2 = r^2 + R^2 - 2rR \cos \gamma$ where $r = |q|$, $R = |Q|$ and $rR \cos \gamma = q \cdot Q$. Then $|q - Q| = r\sqrt{1 + x^2 - 2xc}$ where $x = R/r$ and $c = \cos \gamma$ and

$$(47) \quad \frac{1}{|q - Q|} = \frac{1}{r} \sum_{n=0}^{\infty} \left(\frac{R}{r}\right)^n P_n(\cos \gamma) = \frac{1}{r} + \frac{R}{r^2} \cos \gamma + \frac{R^2}{2r^3} (3 \cos^2 \gamma - 1) + \dots$$

Consider the gravitational interaction of a rigid body \mathcal{B} and a point particle of mass 1 at position q . The gravitational potential of \mathcal{B} at q is given by

$$U(q) = \int_{\mathcal{B}} \frac{\rho(Q)dV}{|q - Q|} \simeq \frac{m}{r} + \frac{1}{r^2} \int_{\mathcal{B}} R \cos \gamma \rho(Q) dV + \frac{1}{r^3} \int_{\mathcal{B}} R^2 P_2(\gamma) \rho(Q) dV + \dots$$

where the integrals are over $Q \in \mathcal{B}$ and where the expansion (47) was used. Dropping the higher order terms leads to a convenient approximation to the potential. Note that $rR \cos \gamma = q \cdot Q$ and integration shows that the second term in the approximation is $r^{-3}q \cdot \bar{Q} = 0$ by choice of the body coordinate system.

To evaluate the third term, write $P_2(\cos \gamma) = \frac{1}{2}(3 \cos^2 \gamma - 1) = 1 - \frac{3}{2} \sin^2 \gamma$ and recall (46) to get

$$\begin{aligned} \int_{\mathcal{B}} R^2 P_2(\gamma) \rho(Q) dV &= \mathcal{I}_0 - \frac{3}{2} \mathcal{I}(q/r) \\ &= \frac{1}{2} (A + B + C - 3(A(x/r)^2 + B(y/r)^2 + C(z/r)^2)) \end{aligned}$$

Thus the interaction potential between the rigid body and the point mass m located at position $q = (x, y, z)$ in body coordinates satisfies

$$(48) \quad U(q) \simeq \frac{m}{r} + \frac{1}{2r^3} (A + B + C - 3(A(x/r)^2 + B(y/r)^2 + C(z/r)^2))$$

which is known as *MacCullagh's formula*. If $A = B$ this can be written in several useful ways

$$\begin{aligned}
 (49) \quad U(q) &\simeq \frac{m}{r} + \frac{1}{2r^3}(C - A)(1 - 3(z/r)^2) \\
 &= \frac{m}{r} + \frac{1}{2r^3}(C - A)(1 - 3\cos^2\gamma) \\
 &= \frac{m}{r} \left(1 + J_2 \frac{a^2}{2r^2} (1 - 3\cos^2\gamma) \right).
 \end{aligned}$$

Exercise 5.1. Verify the formulas in Example 5.1.

5.2. Motion of an Earth satellite. In this section, MacCullagh's formula will be used to approximate the motion of a small satellite around the Earth. Assume that the Earth is an oblate spheroid, symmetric about the z axis in \mathbb{R}^3 and that, apart from its rotation about this axis, it remains fixed. Choose the units of distance so that the equatorial radius of the Earth is $a = 1$ and let the unit of time be one day. As in Exercise 1.1, the mass of the Earth will be $m \simeq 11468$.

If $q = (x, y, z)$ is the position of the satellite, its motion will be governed by a perturbed Kepler problem with Lagrangian

$$L = \frac{1}{2}|v|^2 + U(q) \quad U(q) \simeq \frac{m}{r} + \frac{\delta m}{2r^3}(1 - 3\cos^2\gamma).$$

where $\delta = J_2 \simeq 0.001$ and $\cos\gamma = z/r$. Note that, as for the Kepler problem, the mass m has been canceled out of the equation. To avoid hitting the Earth, only solutions with $r(t) > 1$ should be allowed.

First consider the effect of the perturbation on an equatorial satellite, that is, a solution with $z(t) = 0$. This is a central force problem in \mathbb{R}^2 with

$$U(q) = F(r) = \frac{m}{r} + \frac{\delta m}{2r^3}.$$

After section 4.4, one expects that the bounded solutions will move on invariant tori. Fixing an angular momentum C leads to a reduced system

$$L_c(r, w) = \frac{1}{2}w^2 - V_C(r) \quad V_C(r) = \frac{C^2}{2r^2} - \frac{m}{r} - \frac{\delta m}{2r^3}.$$

For $m = 11468$, $C = 200$ and $\delta = 0.1$, Figure 17 shows the behavior of $q(t)$ for two of the resulting solutions over a time period of 30 days. It can be described as an approximately elliptical path which slowly *precesses*. The motion of the satellite is counter-clockwise and so is the precession, so the precession is called *prograde* as opposed to *retrograde*.

Moving on to the nonplanar motions provides an opportunity to introduce some typical tools of perturbation theory – Delaunay variables and the averaging method. Recall that the elliptical orbits of the Kepler problem can be described by orbital elements

$$a, e, \omega, \iota, \Omega, M$$

as in Section 4.1. One can view the orbital elements as a new set of coordinates. The mean anomaly $M = n(t - \tau)$ increases with constant speed while all of the other elements remain constant. For the perturbed Kepler problem, one expects that these other elements will change slowly.

It's possible to find the differential equations for the orbital elements but they are rather complicated. It's easier to make use of a slightly different set of variables.

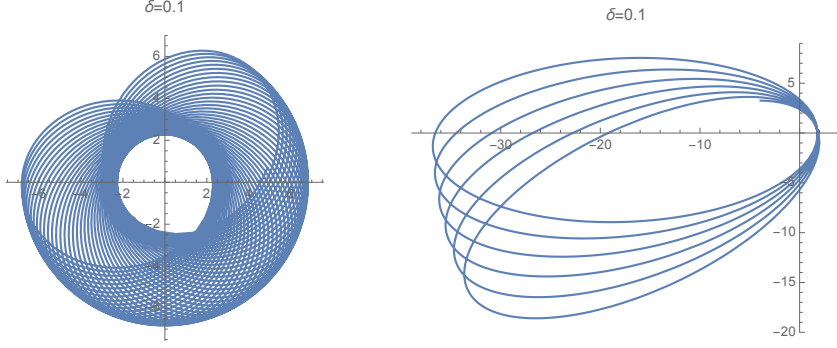


FIGURE 17. Two satellite orbits around an oblate planet with $J_2 = 0.1$. They resemble elliptical orbits of the Kepler problem with a slow prograde precession. For the Earth, with $J_2 \simeq 0.001$ the precession is much slower.

Definition 5.1. *The Delaunay variables for the nonplanar, elliptical orbits of the Kepler problem are $M, \omega, \Omega, L, G, H$ where*

$$(50) \quad L = \sqrt{ma} \quad G = \sqrt{ma(1 - e^2)} \quad H = G \cos \iota.$$

Note that L, H are not the Lagrangian and Hamiltonian. The physical meaning of the variables L, G, H can be found using (26). Namely

$$(51) \quad L = \frac{m}{\sqrt{-2h}} \quad G = |C| \quad H = C_3$$

where h is the energy and $C = (C_1, C_2, C_3)$ is the angular momentum.

The reason for preferring Delaunay variables to the usual orbital elements is explained by the following result.

Proposition 5.1. *The Delaunay variables are symplectic coordinates, that is, the map $(q, p) \mapsto (M, \omega, \Omega, L, G, H)$ is symplectic.*

The proof is rather involved. A readable reference is [12].

The differential equations for the Delaunay variables are Hamilton's equations for the Hamiltonian $\mathcal{H}(M, \omega, \Omega, L, G, H)$ which is obtained by expressing the energy function in terms of these variables. For the unperturbed Kepler problem, (51) shows that $\mathcal{H}(M, \omega, \Omega, L, G, H) = -\frac{m^2}{2L^2}$. Hamilton's equations are simply

$$\dot{M} = \mathcal{H}_L = -\frac{m^2}{L^3} \quad \dot{\omega} = \dot{\Omega} = \dot{L} = \dot{G} = \dot{H} = 0.$$

As a check, recall that $M(t) = n(t - \tau)$ so $\dot{M} = n$ where $n = 2\pi/T = (|2h|)^{\frac{3}{2}}/m$. This agrees with

$$-\frac{m^2}{L^3} = -m^2(m/\sqrt{-2h})^{-3} = \frac{|2h|^{\frac{3}{2}}}{m}.$$

For the perturbed Kepler problem describing the satellite motion, the Hamiltonian will be

$$\mathcal{H}(M, \omega, \Omega, L, G, H) = -\frac{m^2}{2L^2} + F(M, \omega, \Omega, L, G, H)$$

where F is the non-Keplerian part of the potential energy. The catch is that this must be expressed in terms of the Delaunay variables. For example, for the satellite problem in Cartesian coordinates,

$$F = \frac{\delta m}{2r^3} (1 - 3 \cos^2 \gamma)$$

where γ is the angle between $q = (x, y, z)$ and $(0, 0, 1)$. To express this in terms of the Delaunay variables, consider a right spherical triangle determined by the projections to the unit sphere of $q = (x, y, z)$, its projection to the equator $(x, y, 0)$ and the ascending node. Referring to Figure 7 shows that the “hypotenuse” of the triangle is an arc of angular size $\omega + \nu$ where ω is the angle between the ascending node and the pericenter and ν is the angle from the pericenter to q . The vertical side of the triangle is an arc of size $\frac{\pi}{2} - \gamma$ and the angle opposite this side is the inclination, ι . Now the spherical generalization of the planar rule $b = c \sin \theta$ for a right triangle with hypotenuse c and side b opposite to θ is $\sin b = \sin c \sin \theta$. It follows that

$$\cos \gamma = \sin\left(\frac{\pi}{2} - \gamma\right) = \sin(\omega + \nu) \sin \iota$$

and

$$F = \frac{\delta m}{2r^3} (1 - 3 \sin^2(\omega + \nu) \sin^2 \iota).$$

While ω, ι can easily be expressed in Delaunay variables, ν is problematical. However, the next step will be to average the perturbation.

When $\delta = 0$, the perturbation vanishes and the orbit does not evolve and the satellite motion is periodic. For small δ one expects the orbit to change significantly only on time intervals much longer than one period. Intuitively, it makes sense to consider a new perturbing function obtained by averaging the real perturbation over one satellite period. This type of procedure can be justified to some extent [3], but this will not be discussed here. For an elliptical Kepler orbit of period T , the average will be

$$\bar{F} = \frac{1}{T} \int_0^T \frac{\delta m}{2r^3} (1 - 3 \sin^2(\omega + \nu(t)) \sin^2 \iota) dt.$$

Using $C = r^2 \dot{\theta} = r^2 \dot{\nu}$, this can be written as an average with respect to ν

$$\begin{aligned} \bar{F} &= \frac{2\pi}{T|C|} \frac{1}{2\pi} \int_0^{2\pi} \frac{\delta m}{2r} (1 - 3 \sin^2(\omega + \nu) \sin^2 \iota) d\nu \\ &= \frac{\delta m n}{p|C|} \frac{1}{4\pi} \int_0^{2\pi} (1 + e \cos \nu) (1 - 3 \sin^2(\omega + \nu) \sin^2 \iota) d\nu \end{aligned}$$

where $r(\nu) = p/(1 + e \cos(\omega + \nu))$ as in (27) and $n = 2\pi/T$ is the mean angular speed. The terms involving $\cos \nu$ integrate to zero and the integral of $\sin(\omega + \nu)^2$ is π . After eliminating $\sin \iota$ in favor of $\cos \iota$ the averaged perturbing potential is

$$\bar{F} = \frac{\delta m n}{4p|C|} (1 - 3 \cos^2 \iota).$$

Finally, to express this in terms of Delaunay variables, note that $\cos \iota = H/G$ and $p = |C|^2/m = G^2/m$. Hence

$$\bar{F}(M, \omega, \Omega, L, G, H) = \frac{\delta m^2 n}{4G^3} (1 - 3 \frac{H^2}{G^2}).$$

Proposition 5.2. *According to the approximate, averaged equations, the motion of an earth satellite can be described as follows. The orbit is approximately elliptical with the elements a, e, ι remaining constant while the ascending node Ω and the ω precess slowly at rates given approximately by*

$$\dot{\omega} = \frac{3\delta n(5\cos^2 \iota - 1)}{4p^2} \quad \dot{\Omega} = -\frac{3\delta n \cos \iota}{2p^2}.$$

where $p = a(1 - e^2)$ and $n = 2\pi/T = \sqrt{m}/a^{\frac{3}{2}}$.

Proof. Using Delaunay variables, the Hamiltonian is

$$\mathcal{H}((M, \omega, \Omega, L, G, H) = -\frac{m^2}{2L^2} + \frac{\delta m^2}{4G^3}(1 - 3\frac{H^2}{G^2}).$$

Since \mathcal{H} does not depend on the angular variables M, ω, Ω , Hamilton's differential equations show that the momentum variables L, G, H are all constant. Recalling their definition in terms of orbital elements (50), it follows that a, e, ι are also constant. On the other hand Hamilton's equations for ω, Ω are

$$\dot{\omega} = \mathcal{H}_G = \frac{3\delta m^2 n(5H^2 - G^2)}{4G^6} \quad \dot{\Omega} = \mathcal{H}_H = -\frac{3\delta m^2 n H}{2G^5}.$$

Setting $G = \sqrt{mp} = \sqrt{ma(1 - e^2)}$ and $G \cos \iota$ gives the formulas in the proposition.

QED

Note that $\dot{\Omega} < 0$ which means that the precession of the plane of the orbit is retrograde with respect to the orbit itself. Meanwhile, within the plane of motion, the perihelion position is precessing in a direction which is prograde if $\cos^2 \iota < \frac{1}{5}$ and retrograde if $\cos^2 \iota > \frac{1}{5}$. $\iota = \arccos(\sqrt{1/5}) \simeq 63.435^\circ$ is called the *critical inclination*. The speed of these precessions will depend on the size of the orbit as measured by the semilatus rectum p .

Example 5.2. For the Earth, $m \approx 11468$ and $\delta = J_2 = 0.00108$. Recall that the units have been chosen so that the Earth's radius is 1 and time is in days. Consider a nearly circular satellite orbit with $a \simeq p$. The period will be $T \simeq 0.0587a^{\frac{3}{2}}$ days. The mean angular speed is $n \approx 107/a^{\frac{3}{2}}$ radians per day. Then the speeds of precession in degrees per day are

$$\dot{\Omega} \simeq -\frac{9.9638 \cos \iota}{a^{\frac{7}{2}}} \quad \dot{\omega} \simeq \frac{4.9819(5 \cos^2 \iota - 1)}{a^{\frac{7}{2}}}.$$

For a low, equatorial orbit with $a \simeq 1$ this means the plane of motion precesses at about -10 degrees per day while perihelion angle precesses at about 5 degree per day. On the other hand, here is some real satellite data.

On a certain day, the international space station had orbital elements $a \simeq 1.0653, e \simeq 0.004516, \iota \simeq 51.64^\circ, \Omega \simeq 354.15^\circ, \omega \simeq 156.907^\circ$. After about 10.32 days the elements were $a \simeq 1.0658, e \simeq 0.00055, \iota \simeq 51.64^\circ, \Omega \simeq 303.08^\circ, \omega \simeq 216.22^\circ$. The predicted and (observed) changes in Ω, ω in degrees per day are

$$\Delta\Omega \simeq -4.96 \quad (-4.45) \quad \Delta\omega \simeq 3.71 \quad (5.16).$$

The space station is in a low orbit and is, perhaps, subjected to a significant amount of drag. It makes about 15 revolutions per day.

On the other hand, the satellite GPS 32 has a much higher orbit. The elements on a certain day were $a \simeq 4.1613, e \simeq 0.00353, \iota \simeq 54.8210^\circ, \Omega \simeq 183.117^\circ, \omega \simeq 216.985^\circ$ and after 10 days they were $a \simeq 4.1613, e \simeq 0.00356, \iota \simeq 54.8218^\circ, \Omega \simeq$

$182.721^\circ, \omega \simeq 217.127^\circ$. The predicted and (observed) changes in Ω, ω in degrees per day are

$$\Delta\Omega \simeq -0.0391 \quad (-0.0396) \quad \Delta\omega \simeq 0.0223 \quad (0.0176).$$

This satellite makes about 2 revolutions per day.

6. RESTRICTED THREE-BODY PROBLEM

This section discusses a special case of the three-body problem where one of the masses is much smaller than the other. In some popular applications the three bodies are the Sun, Jupiter and an asteroid or the Sun, the Earth and the Moon or the Earth, the Moon and a spacecraft.

Consider the three-body problem where two of the masses m_1, m_2 are much larger than the third mass m_3 . In the limit as $m_3 \rightarrow 0$, the motion of the two *primaries*, m_1, m_2 are not affected by the small mass, so they will move on an orbit of the two-body problem. The simplest case is to assume they are in a circular orbit, say counterclockwise. By a choice of units, one may assume that $m_1 + m_2 = 1$ and that the major semiaxis of the orbit is $a = |q_2 - q_1| = 1$. Note that requiring three normalizations $G = m_1 + m_2 + m_3 = a = 1$ uses up all of the freedom in the choice of units. From Example 4.1 or Proposition 4.7, the period of the resulting orbit is $T = 2\pi$ and choosing a convenient origin for time, t , the two primary masses move on circles according to

$$q_1(t) = -\mu(\cos t, \sin t, 0) \quad q_2(t) = (1 - \mu)(\cos t, \sin t, 0)$$

where $m_1 = 1 - \mu, m_2 = \mu, 0 \leq \mu \leq 1$.

Now the third mass will move under the gravitational influence of the primaries. Cancelling a factor of m_3 from both sides of Newton's equation gives

$$\ddot{q}_3 = -\frac{(1 - \mu)(q_3 - q_1)}{r_{13}^3} - \frac{\mu(q_3 - q_2)}{r_{23}^3}.$$

where $r_{13} = |q_3 - q_1(t)|$. Note that this is the EL equation for the time-dependent Lagrangian

$$L(q_3, v_3, t) = \frac{1}{2}|v_3|^2 + \frac{1 - \mu}{r_{13}} + \frac{\mu}{r_{23}}.$$

The next step is to introduce rotating coordinates to make the position vectors of the primaries fixed. Let $R(t)$ be the rotation matrix

$$(52) \quad R(t) = \begin{bmatrix} \cos t & -\sin t & 0 \\ \sin t & \cos t & 0 \\ 0 & 0 & 1 \end{bmatrix}$$

which represents a counterclockwise rotation by t so that $q_1(t) = R(t)(-\mu, 0, 0)$ and $q_2(t) = R(t)(1 - \mu, 0, 0)$. Define a new position vector $q(t) \in \mathbb{R}^3$ by $q_3(t) = R(t)q(t)$. The derivative $\dot{q}(t)$ satisfies

$$v_3(t) = R(t)\dot{q}(t) + \dot{R}(t)q(t) = R(t)(\dot{q}(t) + Kq(t)) \quad K = R^{-1}\dot{R} = \begin{bmatrix} 0 & -1 & 0 \\ 1 & 0 & 0 \\ 0 & 0 & 0 \end{bmatrix}.$$

This change of variables converts the time-dependent Lagrangian $L(q_3, v_3, t)$ to

$$L(q, \dot{q}) = \frac{1}{2}|\dot{q} + Kq|^2 + \frac{1 - \mu}{r_{13}} + \frac{\mu}{r_{23}}$$

where, since the Euclidean distance is invariant under rotations,

$$r_{13} = |q - (\mu, 0, 0)| \quad r_{23} = |q - (1 - \mu, 0, 0)|.$$

Let $q = (x, y, z)$ and $\dot{q} = (u, v, w)$. Then

$$(53) \quad L(q, v) = \frac{1}{2}(u^2 + v^2 + w^2) + (xv - yu) + V(x, y, z)$$

where

$$(54) \quad V(x, y, z) = \frac{1}{2}(x^2 + y^2) + \frac{1 - \mu}{\sqrt{(x + \mu)^2 + y^2 + z^2}} + \frac{\mu}{\sqrt{(x + \mu - 1)^2 + y^2 + z^2}}.$$

This Lagrangian system is called the *circular, restricted three-body problem* or CR3BP. The EL equations are

$$(55) \quad \begin{aligned} \dot{x} &= u & \dot{u} &= V_x + 2v \\ \dot{y} &= v & \dot{v} &= V_y - 2u \\ \dot{z} &= w & \dot{w} &= V_z. \end{aligned}$$

For example, the conjugate momentum $p_x = L_u = u - y$ so $\dot{p}_x = \dot{u} - v = L_x = V_x + v$.

As in Exercise 2.4, there is an “energy” constant

$$H(x, y, z, u, v, w) = (p_x, p_y, p_z) \cdot (u, v, w) - L(x, y, z, u, v, w) = h$$

where the conjugate momenta of x, y, z are

$$p_x = L_u = u - y \quad p_y = L_v = v - x \quad p_z = L_z = w.$$

This gives

$$(56) \quad H(x, y, z, u, v, w) = \frac{1}{2}(u^2 + v^2 + w^2) - V(x, y, z) = h.$$

There is Hamiltonian version of the CR3BP where the Hamiltonian is obtained from this energy function by replacing the velocities by the momenta, but this will not be used here.

Since $V(x, y, z)$ is a function of z^2 , it follows that $V_z(x, y, 0) = 0$. Then it follows from (55) that $\{z = w = 0\}$ is an invariant set for the CR3BP, consisting of all states where the position and velocity of m_3 lie in the plane $\mathbb{R}^2 \times 0$. Setting $z = w = 0$ gives a Lagrangian system called the *planar, circular, restricted three-body problem* or PCR3BP.

Although h will be called the energy, it is not the same as the energy of the original three-body problem or even the scaled energy of the third body. Thinking of the third body as a unit mass and taking kinetic energy plus potential energy in the nonrotating frame would give

$$h_3 = \frac{1}{2}|v_3|^2 - \frac{1 - \mu}{r_{13}} - \frac{\mu}{r_{23}} = \frac{1}{2}(u^2 + v^2 + w^2) + (xv - yu) + \frac{1}{2}(x^2 + y^2) - \frac{1 - \mu}{r_{13}} - \frac{\mu}{r_{23}}.$$

On the other hand, the third component of the angular momentum of the third body in the nonrotating frame works out to be

$$c_3 = (xv - yu) + x^2 + y^2.$$

So the constant h in (56) is

$$h = h_3 - c_3.$$

The constant $-2h$, called the *Jacobi constant*, is often used but h will be retained here.

6.1. Hill's Regions and Lagrange Points. The Lagrangian system (55) has configuration space $X = \mathbb{R}^3 \setminus \{P_1, P_2\}$ where $P_1 = (-\mu, 0, 0), P_2 = (1 - \mu, 0, 0)$ are the positions of the primaries. The phase space $TX = X \times \mathbb{R}^3$ has dimension six and the energy levels

$$\mathcal{M}(h) = \{(q, \dot{q}) : H(q, \dot{q}) = h\}$$

have dimension 5. For the PCR3BP, the phase space has dimension 4, the energy level dimension 3. It turns out that fixing the energy puts some restrictions on the position q . Namely, rewriting (56) shows that $V(x, y, z) + h = \frac{1}{2}(u^2 + v^2 + z^2) \geq 0$. For $h \geq 0$, this is no restriction but for $h < 0$ may be.

Definition 6.1. *The Hill's region corresponding to energy h is the projection of $\mathcal{M}(h)$ to the configuration space*

$$\mathcal{H}(h) = \{q : V(q) + h \geq 0\}.$$

The boundary $Z(h) = \partial\mathcal{H}(h) = \{V(q) = -h\}$ is the zero-velocity surface or, for the planar problem, the zero-velocity curve.

If $q \in \mathcal{H}(h)$ then the set of admissible velocities (u, v, w) forms a sphere of radius $\sqrt{2V(x, y, z) + h}$ which shrinks to the point $(0, 0, 0)$ for $q \in Z(h)$. For the planar problem the velocities (u, v) form circles. Thus the energy manifold $\mathcal{M}(h)$ lies over its projection $\mathcal{H}(h)$ as a kind of degenerate sphere or circle bundle.

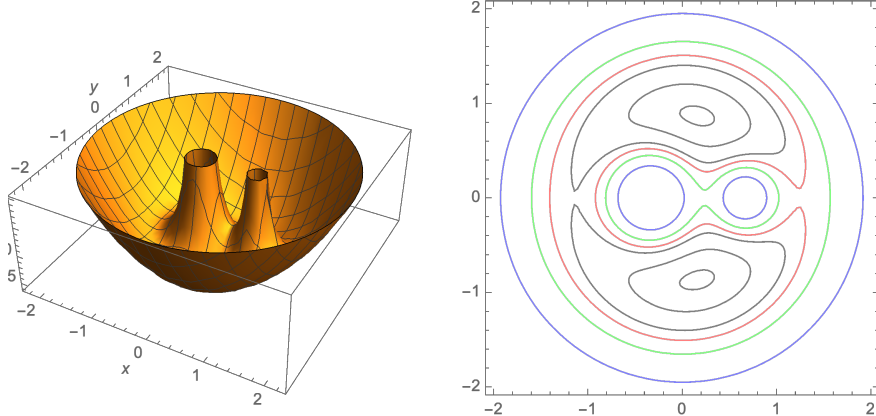


FIGURE 18. Graph of the planar potential $V(x, y)$ and the corresponding zero velocity curves. The primaries have masses $1 - \mu = \frac{2}{3}, \mu = \frac{1}{3}$. Zero velocity curves for $h = -2.4$ (blue), -1.95 (green), -1.77 (red), -1.66 (black), -1.5 (black), -1.4 (black) are shown.

Hill's regions are named for George W. Hill who used them in his study of the motion of the Moon [11]. The Hill's regions of the planar problem are easier to visualize. Figures 18 shows the graph of $V(x, y)$ and some of its level curves $\{V(x, y) = -h\}$. Note that $V(x, y) \rightarrow \infty$ as $|(x, y)| \rightarrow \infty$ and also as $(x, y) \rightarrow P_1, P_2$. It follows that every Hill's region $\mathcal{H}(h)$ contains all points sufficiently close to P_1, P_2, ∞ . For example, the three blue curves in the figure form $Z(h)$ for $h = -2.4$ and the corresponding Hill's region $\mathcal{H}(-2.4)$ consists of 2 disk-like regions near

P_1, P_2 and the region outside the largest blue curve. For $h = -1.4$, $Z(h)$ consists of the smallest, symmetrical pair of black circles and the Hill's region $\mathcal{H}(-1.4)$ is everything *outside* of these curves. Figure 19 shows one of the Hill's regions with the circle of admissible velocities shown at several points.

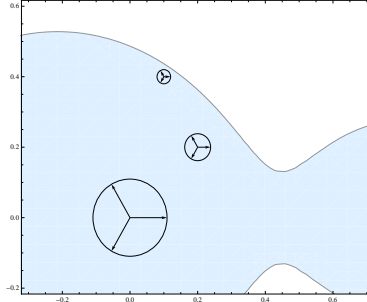


FIGURE 19. Circles of admissible velocities for points in a Hill's region. The circles shrink to points on the zero-velocity curve.

The following result shows how the spatial Hill's regions can be understood from the planar ones.

Proposition 6.1. *Let $h < 0$ and let $\mathcal{H}_2(h), \mathcal{H}_3(h)$ denote the planar and spatial Hill regions, respectively. Also, let $Z_2(h), Z_3(h)$ be the corresponding zero velocity curve and surface. Then*

- $Z_3(h) \cap \{z = 0\} = Z_2(h)$
- $Z_3(h) \cap \{z \geq 0\}$ is a continuous graph over $\mathcal{H}_2(h)$ of the form $z = g(x, y)$ with $g(x, y) = 0$ on $Z_2(h)$
- $Z_3(h) \cap \{z \leq 0\}$ is given by $z = -g(x, y)$
- $\mathcal{H}_3(h) = \{(x, y, z) : (x, y) \in \mathcal{H}_2, -g(x, y) \leq z \leq g(x, y)\}$

Proof. Fix any $(x_0, y_0) \in \mathbb{R}^2$ and consider the function $f(z) = V(x_0, y_0, z) + h$. The intersection of $\mathcal{H}_3(h)$ with the vertical line l through (x_0, y_0) is given by $f(z) \geq 0$. Since V is a function of z^2 , $f(-z) = f(z)$ and it suffices to consider $z \geq 0$. Note also that $f(z) \rightarrow h < 0$ as $|z| \rightarrow \infty$.

Now $f(0) = V(x_0, y_0, 0) + h$ and the derivative is

$$f'(z) = -z \left(\frac{1}{r_{13}^3} + \frac{1}{r_{23}^3} \right).$$

Thus $f'(z) < 0$ and $f(z)$ is strictly decreasing for $z > 0$. If $(x_0, y_0) \notin \mathcal{H}_2(h)$ then $f(0) < 0$ and the line l does not intersect $\mathcal{H}_3(h)$. If $(x_0, y_0) \in Z_2(h)$ then $f(0) = 0$ and the rest of the line l is not in $\mathcal{H}_3(h)$. If $(x_0, y_0) \in \mathcal{H}_2(h) \setminus Z_2(h)$, then $f(0) > 0$. It follows that there is a unique $z > 0$ with $f(z) = 0$. Call this point $z = g(x_0, y_0)$. The implicit function theorem shows that $g(x_0, y_0)$ is smooth on $\mathcal{H}_2(h) \setminus Z_2(h)$ and it clearly extends continuously to 0 on $Z_2(h)$. QED

For example, consider the the energy $h = -2.4$ where the planar Hill region consists of two disks around the primaries and the region outside the large blue curve, the corresponding spatial Hill region will consist of two solid balls around the primaries and an unbounded solid (see Figure 20).

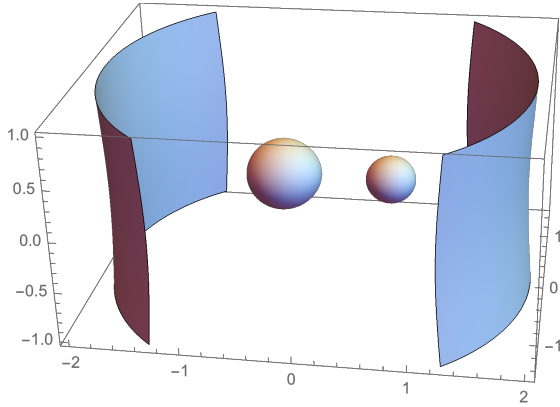


FIGURE 20. Zero-velocity surfaces corresponding to the curves with energy $h = -2.4$ in Figure 18.

The geometry of the Hill's regions allowed Hill to give a purely qualitative proof of a type of stability for the motion of the moon. Suppose the primary masses are the Sun and the Earth and the small mass is the Moon. Fitting the observed motion of the Moon to the CR3BP, Hill found that the energy level was such that the Hill's regions were similar to the case $\mathcal{H}(-2.4)$ in Figures 18 and 20. The Hill's region has three components, one of which is a bounded region around the Earth. Since the position of the Moon must remain in the Hill region, it must remain for all time in the component where it started. Thus, the moon can never "escape" from the Earth. A typical planar orbit is shown in Figure 21.

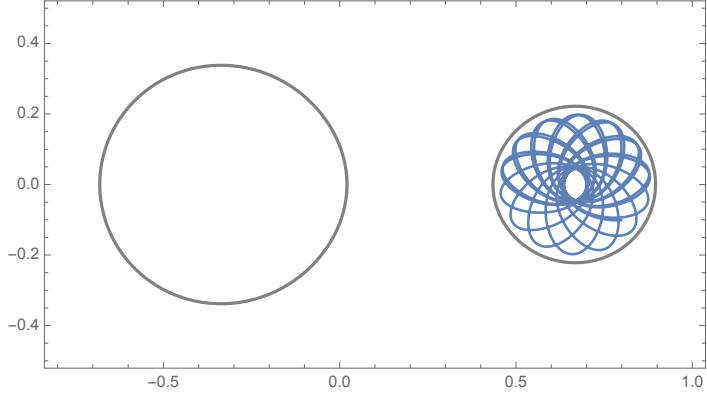


FIGURE 21. An orbit of the PCR3BP with $h = -2.4$ which is trapped near one of the primaries as in Hill's stability proof.

In studying the restricted three-body problem, a special role is played by the critical points of $V(x, y, z)$. In Figure 18 it is clear that for this value of μ , there are exactly five critical points for the planar potential $V(x, y, 0)$, three saddle points along the x axis and two minima with $y \neq 0$. It turns out that critical points are always planar and there are always exactly five.

Proposition 6.2. *For every $0 < \mu < 1$, $V(x, y, z)$ has exactly five critical points. There are two minima at $(\frac{1}{2} - \mu, \pm \frac{\sqrt{3}}{2}, 0)$ (the planar, equilateral triangle configurations) and three saddle points $(\xi_i, 0, 0)$ along the x -axis with $\xi_3 < -\mu < \xi_1 < 1 - \mu < \xi_2$.*

Definition 6.2. *The five critical points of V are called the Lagrange points. Assuming that the larger primary is the one with mass $1 - \mu$ and position $(-\mu, 0, 0)$, they are usually denoted L_1, \dots, L_5 where $L_i = (\xi_i, 0, 0)$, $i = 1, 2, 3$, $L_4 = (\frac{1}{2} - \mu, \frac{\sqrt{3}}{2}, 0)$ and $L_5 = (\frac{1}{2} - \mu, -\frac{\sqrt{3}}{2}, 0)$.*

The Lagrange points are easily located in the planar contour plot of Figure 18. At the equilateral points, V attains its minimum and the corresponding zero velocity curves reduce to points. At the collinear critical points where V has saddle points, the zero velocity curves have double points where they look locally like the letter X . It follows from the implicit function theorem that all of the noncritical level curves of V are smooth.

Proof of Proposition 6.2. The critical points are given by $V_x = V_y = V_z = 0$. Now $V_z = -z\gamma^2$ where

$$\gamma^2 = \frac{1 - \mu}{r_{13}^3} + \frac{\mu}{r_{23}^3} > 0.$$

It follows that all critical points have $z = 0$. Next,

$$\begin{aligned} V_x &= x(1 - \gamma^2) + (1 - \mu)\mu \left(\frac{1}{r_{23}^3} - \frac{1}{r_{13}^3} \right) \\ V_y &= y(1 - \gamma^2). \end{aligned}$$

The second equation gives two cases

$$y = 0 \quad \text{or} \quad F = 1 - \gamma^2 = 0.$$

Consider the case $F = 0$. The V_x equation then gives $r_{13} = r_{23}$. Then substitution into F gives $1 - \frac{1-\mu}{r_{13}^3} - \frac{\mu}{r_{13}^3} = 1 - \frac{1}{r_{13}^3} = 0$ so, in fact, $r_{13} = r_{23} = 1$. This gives the two equilateral triangle solutions.

On the other hand, if $y = z = 0$ the x equation simplifies to

$$(57) \quad V_x(x, 0, 0) = x - \frac{(1 - \mu)(x + \mu)}{|x + \mu|^3} - \frac{\mu(x + \mu - 1)}{|x + \mu - 1|^3} = 0.$$

There are several ways to see that this has exactly one solution in each of the intervals $(\infty, -\mu)$, $(-\mu, 1 - \mu)$, $(1 - \mu, \infty)$. Consider the middle interval where $-\mu < x < 1 - \mu$. It can be reparametrized by setting $x = -\mu + \frac{s}{1+s}$ where the new parameter, $s \in (0, \infty)$. Then equation (57) becomes

$$\frac{\mu s^5 + 3\mu s^4 + 3\mu s^3 - 3(1 - \mu)s^2 - 3(1 - \mu)s - (1 - \mu)}{s^2(1 + s)}.$$

Note that there is exactly one sign change in the coefficients of the numerator, so it follows from Descartes' rule of signs [1, 6] that there is exactly one positive root. A similar, purely algebraic approach works in each of the other two intervals (see Exercise 6.1). Although this proves existence of the collinear critical points, finding them involves solving the fifth-degree equation.

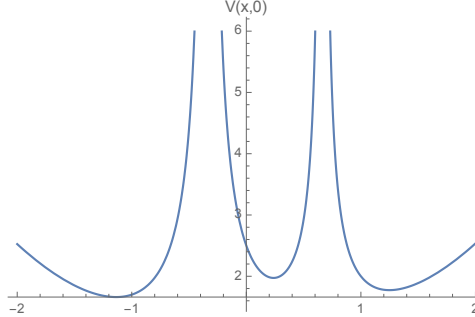


FIGURE 22. The collinear potential $V(x, 0)$ is convex in each of the intervals determined by the primaries.

A second approach uses some calculus. Consider the second derivatives of V

$$\begin{aligned} V_{xx} &= F + \frac{3(1-\mu)(x+\mu)^2}{r_{13}^5} + \frac{3\mu(x+\mu-1)^2}{r_{23}^5} \\ V_{xy} &= \frac{3(1-\mu)(x+\mu)y}{r_{13}^5} + \frac{3\mu(x+\mu-1)y}{r_{23}^5} \\ V_{yy} &= F + \frac{3(1-\mu)y^2}{r_{13}^5} + \frac{3\mu y^2}{r_{23}^5} \end{aligned}$$

For the collinear points, $y = z = 0$, these reduce to

$$V_{xx} = 1 + 2\gamma^2 \quad V_{xy} = 0 \quad V_{yy} = F = 1 - \gamma^2.$$

Since $V_{xx}(x, 0, 0) > 0$ the function $V(x, 0, 0)$ is strictly convex (see Figure 22). In addition, $V(x, 0, 0) \rightarrow \infty$ as $|x| \rightarrow \infty$ and as $x \rightarrow -\mu, 1-\mu$. It follows that $V(x, 0, 0)$ has exactly one critical point, a minimum, in each of the intervals $(-\infty, -\mu), (-\mu, 1-\mu), (1-\mu, \infty)$.

The second derivatives can be used to classify the five critical points. At the equilateral points $(\frac{1}{2} - \mu, \pm \frac{\sqrt{3}}{2}, 0)$, $F = 0$ and $r_{13} = 1$, so

$$V_{xx} = \frac{3}{4} \quad V_{xy} = \pm \frac{3\sqrt{3}(1-2\mu)}{4} \quad V_{yy} = \frac{9}{4}.$$

The diagonal entries of the matrix of second derivatives are positive and the determinant $\frac{27}{4}(1-\mu)\mu$ is also positive. So the equilateral points are minima of the planar potential $V(x, y, 0)$. When $z = 0$ the second derivatives involving z are $V_{xz} = V_{yz} = 0$ and $V_{zz} = -\gamma^2 < 0$. So as critical points of $V(x, y, z)$, the equilateral points have signature $(+, +, -)$.

At the collinear critical points $(\xi_i, 0, 0)$ it was shown above that $V_{xx} > 0$. Also $V_{xy} = 0$ and $V_{yy} = F = 1 - \gamma^2$. It turns out that $F(\xi_i, 0, 0) < 0$ and then it follows that the collinear points are saddles for the planar potential $V(x, y, 0)$. Since $V_{xz} = V_{yz} = 0$ and $V_{zz} < 0$, they have signature $(+, -, -)$ for $V(x, y, z)$. To see that $F < 0$, write the equation V_x equation as $V_x = xF + G = 0$ where $G = (1-\mu)\mu(1/r_{23}^3 - 1/r_{13}^3)$. In the interval $(-\infty, -\mu)$, $x < 0$ and $G < 0$. So it follows that at the critical point, $F < 0$. Similarly, in $(1-\mu, \infty)$ the claim follows from $x > 0$ and $G > 0$. Finally, Exercise 6.2 shows that $F < 0$ everywhere in the middle interval $(-\mu, 1-\mu)$. QED

Exercise 6.1. Use Descartes' rule of signs to show that (57) has exactly one root in each of the intervals $(1 - \mu, \infty), (-\infty, -\mu)$. For example, in the first of these intervals, set $x = 1 - \mu + s$ to reduce the problem to solving a polynomial equation for $s > 0$.

Exercise 6.2. This exercise shows one way to prove that the function $F = 1 - (1 - \mu)/r_{13}^3 - \mu/r_{23}^3$ satisfies $F(x, 0, 0) < 0$ for $-\mu < x < 1 - \mu$. Note that on the interval in question, $0 < r_{13} < 1$ and $r_{13} + r_{23} = 1$. The change of variables $r_{13} = s/(1 + s), r_{23} = 1/(1 + s)$ reduces the problem to showing that $F(s) < 0$ for $0 < s < \infty$. Show that

$$F(s) = -s^{-3} (\mu s^6 + 3\mu s^5 + 3\mu s^4 + 3(1 - \mu)s^2 + 3(1 - \mu)s + (1 - \mu))$$

to complete the proof.

Exercise 6.3. Let $L(q, v) = \frac{1}{2}|v|^2 - \frac{1}{|q|}$, $q \in \mathbb{R}^2 \setminus 0$, be the Lagrangian of the Kepler problem in \mathbb{R}^2 with mass $m = 1$. Introduce rotating coordinates Q where $q = R(t)Q$ and $R(t) = \begin{bmatrix} \cos t & -\sin t \\ \sin t & \cos t \end{bmatrix}$. Find the Lagrangian $L(Q, \dot{Q})$ of the *rotating Kepler problem*. Find the potential $V(Q)$, the zero velocity curves and the critical points.

6.2. Relative Equilibria. In addition to their geometrical significance as singular points of the zero velocity curves and surfaces, the Lagrange points also have a nice dynamical significance as *relative equilibrium points (RE)*, that is, they are equilibrium points in rotating coordinates. In nonrotating coordinates they give simple periodic orbits. Since it is not possible find the general solution of the n -body problem for $n \geq 3$, most of the results are either statements about the qualitative behavior of solutions (such as the confinement to Hill's regions) or existence theorems for special kinds of orbits. The existence of the five relative equilibria for the three-body problem is the simplest example of the latter.

Proposition 6.3. *The five points $(q, \dot{q}) = (L_i, 0)$ are equilibrium points of the CR3BP in rotating coordinates. In nonrotating coordinates they represent circular, periodic solutions with $q(t) = R(t)L_i$ where $R(t)$ is the matrix (52).*

Proof. The equilibria of (55) are given by $u = v = w = V_x = V_y = V_z = 0$. QED

To investigate the stability of these RE, consider the linearized differential equations. At any point (x, y, z) with $z = 0$, these decouple as follows

$$\begin{bmatrix} \dot{\delta x} \\ \dot{\delta y} \\ \dot{\delta u} \\ \dot{\delta v} \end{bmatrix} = \begin{bmatrix} 0 & 0 & 1 & 0 \\ 0 & 0 & 0 & 1 \\ V_{xx} & V_{xy} & 0 & 2 \\ V_{xy} & V_{yy} & -2 & 0 \end{bmatrix} \begin{bmatrix} \delta x \\ \delta y \\ \delta u \\ \delta v \end{bmatrix} \quad \begin{bmatrix} \dot{\delta z} \\ \dot{\delta w} \end{bmatrix} = \begin{bmatrix} 0 & 1 \\ V_{zz} & 0 \end{bmatrix} \begin{bmatrix} \delta z \\ \delta w \end{bmatrix}.$$

At all five Lagrange points, $V_{zz} = -\gamma^2$ and the 2×2 *vertical* block has imaginary eigenvalues

$$(58) \quad \pm i\gamma \quad \gamma = \sqrt{\frac{1 - \mu}{r_{13}^3} + \frac{\mu}{r_{23}^3}}.$$

The nature of the eigenvalues at the *planar* 4×4 block is different at the collinear points than at the equilateral ones.

At the collinear points, the characteristic polynomial can be written

$$z^2 + (4 - V_{xx} - V_{yy})z + V_{xx}V_{yy} = 0$$

where $z = \lambda^2$ represents the square of the eigenvalues. Since

$$V_{xx} = 1 + 2\gamma^2 > 0 \quad V_{yy} = F = 1 - \gamma^2 < 0$$

the two roots satisfy $z_- < 0 < z_+$ so two of the four eigenvalues are real and two are imaginary

$$(59) \quad \lambda = \pm\sqrt{z_+} \quad \lambda = \pm i\omega_1 \quad \omega_1 = \sqrt{|z_-|}.$$

Thus

Proposition 6.4. *The equilibrium points corresponding to the collinear Lagrange points L_1, L_2, L_3 are unstable. There are two imaginary pairs of eigenvalues and one pair of real eigenvalues of opposite sign.*

In spite of the instability, there is a four-dimensional invariant subspace for the linearized equations on which the linearized dynamics consists of stable oscillations. Some of the implications of this for the nonlinear flow will be considered later.

At the equilateral points, the characteristic polynomial of the 4×4 block is

$$z^2 + z + \frac{27}{4}\mu(1 - \mu) = 0$$

so

$$z = \lambda^2 = -\frac{1}{2} \left(1 \pm \sqrt{1 - 27\mu(1 - \mu)} \right).$$

Proposition 6.5. *The equilibrium points corresponding to the equilateral Lagrange points L_4, L_5 are unstable if $\mu(1 - \mu) > \frac{1}{27}$ with one pair of imaginary eigenvalues and four eigenvalues of the form $\pm a \pm ib$ with $a \neq 0, b \neq 0$. If $\mu(1 - \mu) < \frac{1}{27}$ they are linearly stable with three pairs of imaginary eigenvalues.*

Proof. If $\mu(1 - \mu) > \frac{1}{27}$, the eigenvalues satisfy $\lambda^2 = -\frac{1}{2} \pm ik$, $k \neq 0$. Since their squares are nonreal, the planar eigenvalues are neither real nor imaginary and must take the required form. If $\mu(1 - \mu) < \frac{1}{27}$, the values of λ^2 are real and negative so the λ are imaginary. QED

Assuming μ is the smaller of the two primary masses, the linear stability criterion is $\mu < \frac{1}{18}(9 - \sqrt{69}) \simeq 0.03852$. So unless one of the masses is much larger than the others, the triangular points will be unstable. But all of the primary pairs Sun-Jupiter, Sun-Earth and Earth-Moon satisfy the criterion. The neighborhoods of the Sun-Jupiter L_4 and L_5 points are, in fact, populated by groups of asteroids called the Trojans. They orbit around the Sun at the same rate as Jupiter, always maintaining an approximately equilateral configuration.

The presence of purely imaginary eigenvalues here is unusual from the point of view of general dynamical systems theory but is typical of equilibrium points in classical mechanics. Although the Lagrangian approach has been used here, it is easiest to understand this phenomenon from the Hamiltonian point of view. Since this can be arranged by a coordinate change (which would not change the eigenvalues), the results of this discussion also apply here.

Proposition 6.6. *Let $(q_0, p_0) \in R^{2m}$ be an equilibrium point of a Hamiltonian system and let $P(\lambda)$ be the characteristic polynomial of the linearized differential equation. Then $P(-\lambda) = P(\lambda)$. If λ is an eigenvalue, so are $-\lambda, \bar{\lambda}, -\bar{\lambda}$.*

Proof. Hamilton's equations are $\dot{q} = H_p, \dot{p} = -H_p$ where $q = (q_1, \dots, q_m), p = (p_1, \dots, p_m)$. Here we regard both of these as coordinate vectors in \mathbb{R}^m . The matrix of the linearized equations at (q_0, p_0) are

$$\begin{bmatrix} H_{pq} & H_{pp} \\ -H_{qq} & -H_{qp} \end{bmatrix} = -JS \quad J = \begin{bmatrix} 0 & -I_m \\ I_m & 0 \end{bmatrix} \quad S = \begin{bmatrix} H_{qq} & H_{qp} \\ H_{pq} & H_{pp} \end{bmatrix}.$$

where I_m is the $m \times m$ identity matrix. Let $P(\lambda) = \det(-JS - \lambda I_{2m})$. Since $S^T = S, J^2 = -I_{2m}, J^T = -J$ and $\det J = 1$,

$$\begin{aligned} P(-\lambda) &= \det(-JS + \lambda I_{2m}) = \det(-JS + \lambda I_{2m})^T = \det(SJ + \lambda I_{2m}) \\ &= \det(-S + \lambda J) = \det(-JS - \lambda I_{2m}) = P(\lambda) \end{aligned}$$

where the equations on the second line come from multiplication on the right and then the left by $\det J$. QED

Definition 6.3. A matrix of the form $A = JS$ where $S^T = S$ is called Hamiltonian.

The proof of the proposition applies to any Hamiltonian matrix. Write the characteristic polynomial as $P(\lambda) = f(z)$ where $z = \lambda^2$ and $f(z)$ is a polynomial of degree m . If $f(z)$ has a negative, real root then A has a pair of imaginary eigenvalues. If the root is simple then every Hamiltonian matrix sufficiently close to A will also have this property.

The next result, called the *Lyapunov center theorem* shows that a pair of imaginary eigenvalues for a system with an energy integral generally implies the existence of a family of periodic orbits near the equilibrium point.

Proposition 6.7. Let ξ_0 be an equilibrium point for a differential equation $\dot{\xi} = f(\xi), \xi \in \mathbb{R}^m$ and suppose

- i. $H(\xi)$ is an integral with $H(\xi_0) = H_0, DH(\xi_0) = 0, \det(D^2H(\xi_0)) \neq 0$
- ii. $Df(\xi_0)$ has an imaginary pair of eigenvalues $\pm i\omega$
- iii. the other eigenvalues are not integer multiples of $\pm i\omega: \lambda \neq \pm ik\omega$ for $k \in \mathbb{Z}$
- iv. $D^2H(\xi_0)$ is either positive or negative definite on the eigenspace of $\pm i\omega$

Then there is a family of periodic solutions γ_ϵ with $H(\gamma_\epsilon) = \pm\epsilon^2, 0 < \epsilon < \epsilon_0$ where the sign depends of the definiteness in hypotheses (iv). Moreover, $\gamma_\epsilon \rightarrow 0$ as $\epsilon \rightarrow 0$ and the family forms a C^1 surface through 0 and tangent to the eigenspace of $\pm i\omega$. The periods $T(\epsilon)$ converge to $2\pi/\omega$ as $\epsilon \rightarrow 0$.

Example 6.1. Consider $\xi_0 = (L_1, 0)$ for the collinear RE L_1 of the CR3BP and let H be the energy function (56). Then

$$DH(\xi_0) = (-V_x, -V_y, -V_z, u, v, w) = 0 \quad D^2H(\xi_0) = \begin{bmatrix} -D^2V(L_1) & 0 \\ 0 & 2I_m \end{bmatrix}$$

It was shown above that $D^2V(\xi_0) = \text{diag}(V_{xx}, V_{yy}, V_{zz})$ with $V_{xx} > 0, V_{yy} < 0$ and $V_{zz} < 0$ so first hypothesis of the theorem is satisfied. Now there are two pairs of imaginary eigenvalues at ξ_0 , the vertical pair $\pm i\gamma$ from (58) and a planar pair $\pm i\omega_1$ from (59).

For the planar pair $\pm i\omega_1$, the question of an integer resonance with ω_z can be avoided by restricting attention to the PCR3BP. The other planar eigenvalues are real. It will be shown later on that $D^2H(\xi_0) > 0$ on this eigenspace as well, so the theorem can be applied to give a Lyapunov family of planar periodic orbits.

Next consider the pair $\pm i\omega_z$. The eigenspace is the (z, w) plane. The restriction of $D^2H(\xi_0)$ has matrix $\text{diag}(-V_{zz}, 2)$ which is positive definite. Finally, it is possible

to check, with some effort, that $\gamma < |\omega_1| < \sqrt{2}\gamma$ (see Exercise 6.7) so it is impossible for ω_1 to be an integer multiple of γ . So the Lyapunov center theorem applies to prove existence of a family of periodic orbits with energies slightly bigger than $h_1 = H(L_1, 0)$, emanating from ξ_0 and tangent to the (z, w) plane.

Example 6.2. Now consider $\xi_0 = (L_4, 0)$ for the equilateral RE L_4 for $\mu(1 - \mu) < \frac{1}{27}$. This time there are three imaginary pairs $\pm i\omega_z, \pm i\omega_1, \pm i\omega_2$ where

$$\omega_z = 1 \quad \omega_1^2 = \frac{1}{2} \left(1 + \sqrt{1 - 27\mu(1 - \mu)} \right) \quad \omega_2^2 = \frac{1}{2} \left(1 - \sqrt{1 - 27\mu(1 - \mu)} \right).$$

Note that $\omega_z > \omega_1 > \omega_2$. The existence of a vertical Lyapunov family follows as before. Restricting to the planar problem, it turns out that $D^2H(\xi_0)$ is definite on the eigenspaces of the planar pairs, positive for $\pm i\omega_1$ and negative for $\pm i\omega_2$. Existence of a Lyapunov family tangent to the $\pm i\omega_1$ eigenspace follows. To get the third family, it is necessary to avoid integer resonances $\omega_1 = k\omega_2$. In fact there is a sequence of bad masses $\mu_1 > \mu_2 > \mu_3 > \dots, \mu_1 = \frac{1}{18}(9 - \sqrt{69})$, such that $\omega_1 = k\omega_2$ at $\mu = \mu_k$ (see Exercise 6.5). Assuming $\mu \neq \mu_k$, the existence of the third family is assured. See Figure 23.

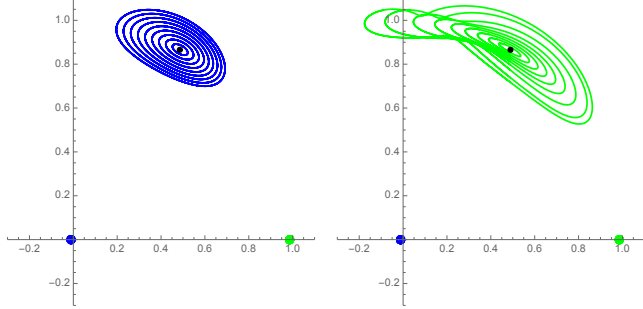


FIGURE 23. Two families of periodic orbits near L_4 for $\mu = \frac{1}{82}$. The blue family has energies above that of L_4 while the green one has energies below. Each energy level sufficiently near that of L_4 contains one of these orbits.

It should be emphasized that these periodic solutions are very special. Even for the linearized system, most solutions are not periodic. For example, in the case of L_4 with μ small, most solutions of the linearized system will be linear combinations of the two periodic motions and are therefore quasiperiodic, rather than periodic. Figure 24 shows one solution of the full nonlinear equations starting near L_4 . For the linearized equations, such a solution would move on an invariant two-torus in phase space. Using KAM theory, one can show that, in fact, there are many invariant tori near L_4 in the PCR3BP. Since the energy manifolds are three-dimensional, these tori separate the energy manifold and prevent orbits like the one in the figure from drifting away from the equilibrium point. In other words, L_4 really is stable even for the full nonlinear PCR3BP. However, KAM theory will not be discussed here. For more information, see [22, 15].

Proof of Proposition 6.7. The proof introduces a useful trick for studying the local dynamics near an equilibrium, namely, blowing up the coordinates. Assume $\xi_0 = 0$

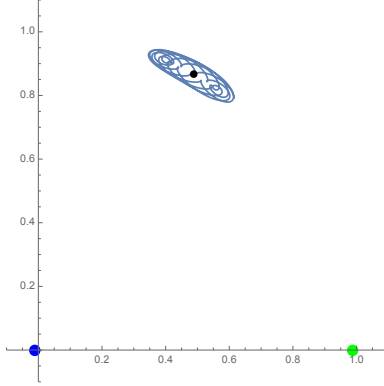


FIGURE 24. A typical nonperiodic solution near L_4 with $\mu = \frac{1}{82}$.

and consider the lowest order terms in the Taylor series expansions of the differential equation and of the integral. Of course, $f(0) = 0$ and one may assume that the matrix $Df(0)$ is in block diagonal form

$$Df(0) = \begin{bmatrix} A & 0 \\ 0 & B \end{bmatrix} \quad A = \begin{bmatrix} 0 & -\omega \\ \omega & 0 \end{bmatrix}, \det B \neq 0.$$

Writing $\xi = (x, y)$ with $x \in \mathbb{R}^2, y \in \mathbb{R}^{m-2}$, the differential equation will be

$$\begin{aligned} \dot{x} &= \begin{bmatrix} 0 & -\omega \\ \omega & 0 \end{bmatrix} x + g_1(x, y) \\ \dot{y} &= By + g_2(x, y) \end{aligned}$$

with $g_i = O(|(x, y)|^2)$. Furthermore, the integral $H(x, y)$ will be of the form

$$H(x, y) = (x, y) \cdot S \cdot (x, y) + h(x, y)$$

for some nondegenerate symmetric matrix S , where $h = O(|(x, y)|^3)$. Now define blown-up variables X, Y with $x = \epsilon X, y = \epsilon Y, \epsilon > 0$. Then the differential equations for X, Y are of the form

$$(60) \quad \begin{aligned} \dot{X} &= \begin{bmatrix} 0 & -\omega \\ \omega & 0 \end{bmatrix} X + \epsilon G_1(X, Y, \epsilon) \\ \dot{Y} &= BY + \epsilon G_2(X, Y, \epsilon) \end{aligned}$$

where $g_i(\epsilon X, \epsilon Y) = \epsilon^2 G_i(X, Y, \epsilon)$ (one factor of ϵ has been cancelled out). These equations have an integral

$$K(X, Y, \epsilon) = \epsilon^{-2} H(\epsilon X, \epsilon Y) = (X, Y) \cdot S \cdot (X, Y) + \epsilon k(X, Y, \epsilon).$$

This trick produces a family of equations such that the behavior of (X, Y) in a ball of radius r is a blown-up image of the behavior of (x, y) in a ball of radius ϵr . The advantage of this approach is that the new equations have a nontrivial limit as $\epsilon \rightarrow 0$. By studying this limit problem, one can get information about the original problem for $\epsilon > 0$ sufficiently small.

It will be shown that there is a family of periodic orbits Γ_ϵ with $K(X, Y, \epsilon) = 1$ which translates to a family in the integral levels $H(x, y) = \epsilon^2$. For $\epsilon = 0$, (60) is

linear with matrix $\begin{bmatrix} A & 0 \\ 0 & B \end{bmatrix}$ and the integral $K(X, Y, 0)$ is quadratic with matrix S .

The fact that $K(X, Y, 0)$ is an integral implies that S must be of the form

$$(61) \quad S = \begin{bmatrix} S_1 & 0 \\ 0 & S_2 \end{bmatrix} \quad S_1 = \begin{bmatrix} a & 0 \\ 0 & a \end{bmatrix}, \det S_2 \neq 0$$

with $a > 0$ (see Exercise 6.6). There is a periodic solution of this linear equation $X(t) = a^{-\frac{1}{2}}(\cos \omega t, \sin \omega t)$, $Y(0) = 0$ with $K(X, Y, 0) = 1$. Using Poincaré continuation, this will be extended to the required family Γ_ϵ .

The integral can be used to eliminate one of the m variables. Let R, θ be polar coordinates in the (X, Y) plane. Then the equation

$$K(R, \theta, Y, \epsilon) = aR^2 + Y \cdot S_2 \cdot Y + \epsilon k(R, \theta, Y, \epsilon) = 1$$

can be solved as $R = a^{-\frac{1}{2}} + \epsilon R_1(\theta, Y, \epsilon)$. This gives a family of differential equations

$$\begin{aligned} \dot{\theta} &= \omega + \epsilon G_3(\theta, Y, \epsilon) \\ \dot{Y} &= BY + \epsilon G_4(\theta, Y, \epsilon). \end{aligned}$$

The periodic orbit for $\epsilon = 0$ is now given by $Y = 0$ with θ arbitrary. Consider the Poincaré map $\Phi(Y, \epsilon)$ of the section $\theta = 0 \bmod 2\pi$. The fixed point $Y = 0$ continues to a family of fixed points $Y(\epsilon)$ provided $\mu = 1$ is not eigenvalues of $D\Phi(0, 0)$. Because the equations are linear when $\epsilon = 0$, $D\Phi(0, 0)$ is the matrix exponential $\exp(\frac{2\pi}{\omega}B)$ and the eigenvalues are $\mu = \exp(\frac{2\pi\lambda}{\omega})$ where λ is an eigenvalue of B . By hypothesis, $\lambda \neq i\omega k$ for $k \in \mathbb{Z}$ and it follows that $\mu \neq 1$.

Let $Y(\epsilon)$ denote the smooth family of fixed points of $\Phi(Y, \epsilon)$ with $Y(0) = 0$. Then there is a family of fixed points $y(\epsilon) = \epsilon Y(\epsilon)$ for the original equations with $\theta = 0 \bmod 2\phi$ and $r = \epsilon R(0, Y(\epsilon), \epsilon)$. Note that $y(\epsilon)/r(\epsilon) = Y(\epsilon)/R(\epsilon) \rightarrow 0$ as $\epsilon \rightarrow 0$. It follows that the family of fixed points forms a C^1 curve through the origin in the (r, y) space, tangent to r axis. Then the family $\gamma_\epsilon = \epsilon \Gamma_\epsilon$ of periodic orbits will form a smooth surface tangent to the (x, y) plane. QED

Exercise 6.4. What are the relative equilibria of the rotating Kepler problem from Exercise 6.3 ? Find the eigenvalues. Does the Lyapunov center theorem apply here?

Exercise 6.5. Verify the claim about the sequence of bad mass ratios $\mu_1 > \mu_2 > \mu_3 > \dots$ in Example 6.2.

Exercise 6.6. Show that if the nondegenerate quadratic form $(x, y) \cdot S \cdot (x, y)$ is an integral for a linear differential equation with matrix $\begin{bmatrix} A & 0 \\ 0 & B \end{bmatrix}$, $A = \begin{bmatrix} 0 & -\omega \\ \omega & 0 \end{bmatrix}$, $\omega \neq 0$, then S is of the form (61).

Exercise 6.7. At the collinear Lagrange points, the squares of the eigenvalues, $z = \lambda^2$ satisfy

$$z^2 + (4 - V_{xx} - V_{yy})z + V_{xx}V_{yy} = z^2 + (2 - \gamma^2)z + (1 + 2\gamma^2)(1 - \gamma^2) = 0$$

and recall that $1 - \gamma^2 < 0$. Show that the negative root z_- of this equation satisfies $-2\gamma^2 < z_- < -\gamma^2$. Conclude that for the imaginary eigenvalues $\pm i\omega_1$ satisfy $\gamma < |\omega_1| < \sqrt{2}\gamma$. In particular, there can be no integer resonance with $\pm i\gamma$.

6.3. Levi-Civita regularization, complex notation. Regularization of the Kepler problem in \mathbb{R}^d was discussed in Section 4.3. There are other, simpler ways to regularize binary collisions which work in \mathbb{R}^2 or \mathbb{R}^3 and which extend more readily to the three-body problem.

Consider the Kepler problem in \mathbb{R}^2

$$\dot{q} = rv \quad \dot{v} = -\frac{mq}{r^q} \quad r = |q|.$$

Viewing $q = (q_1, q_2)$ as the complex number $q = q_1 + i q_2$, define a new variable $z = x + i y$ by the complex squaring map $q = z^2$, that is

$$q_1 + i q_2 = (x + i y)^2 \quad \text{or} \quad q_1 = x^2 - y^2 \quad q_2 = 2xy.$$

Also define a new timescale such that $' = r'$. Continuing with complex notation,

$$q' = 2z z' = rv = |z|^2 v = z \bar{z} v$$

where $\bar{z} = x - i y$ denotes the complex conjugate. Next define a new, complex velocity variable $w = \frac{1}{2} \bar{z} v$ so that $z' = w$. Now calculate

$$2w' = \bar{z}' v + \bar{z} v' = \bar{w} v + \bar{z} \left(-\frac{mz^2}{|z|^4} \right) = \frac{1}{2} z |v|^2 - \frac{mz}{r} = hz$$

where

$$h = \frac{1}{2} |v|^2 - \frac{m}{r}.$$

is the energy. Note that this can be written

$$\frac{1}{2} |w|^2 - \frac{1}{4} (m + h |z|^2) = 0.$$

Since the new differential equations $z' = w$, $w' = \frac{1}{2} h z$ are nonsingular, this provides a regularization of the collision. The idea of using the squaring map is attributed to Tullio Levi-Civita.

A variation on the squaring map near P_1 or P_2 can be used to regularize one of the two binary collisions in the PCR3BP. For example, if the Hill's region is as in Figure 21, solutions are trapped near one or the other of the primaries, say P_2 . To regularize the singularity there replace $q = x + i y$ and $p = u + i v$ in the PCR3BP with $z = \xi + i \eta$ and $w = \alpha + i \beta$ where $q = z^2 + 1 - \mu$ and $w = \frac{1}{2} \bar{z} p$. Also introduce a new timescale so that $' = |z|^2$. Then $q' = 2zz' = |z|^2 p$ so $z' = w$ as for the Kepler problem above. The differential equation for the PCR3BP gives $\dot{p} = (V_x + i V_y) + 2i p$ and $p' = |z|^2 (V_x + i V_y) + 4izw$.

$$\begin{aligned} (62) \quad w' &= \frac{1}{2} \bar{z}' p + \frac{1}{2} \bar{z} p' = \frac{1}{4} z |p|^2 + 2i |z|^2 w + \frac{1}{2} \bar{z} |z|^2 (V_x + i V_y) \\ &= 2i |z|^2 w + \frac{z}{2} (h + V) + \frac{1}{2} \bar{z} |z|^2 (V_x + i V_y) \end{aligned}$$

where $h = \frac{1}{2} |p|^2 - V$.

To facilitate the rest of the computation it's useful to express the partial derivatives of V in terms of the complex variables q, \bar{q}, z, \bar{z} .

Lemma 6.1. *Let $V(x, y)$ be a real analytic function and let $q = x + i y$ and $\bar{q} = x - i y$ so that $x = \frac{1}{2}(q + \bar{q})$ and $y = \frac{1}{2i}(q - \bar{q})$. View x, y, q, \bar{q} as four complex variables and consider the function $F(q, \bar{q}) = V(\frac{1}{2}(q + \bar{q}), \frac{1}{2i}(q - \bar{q}))$. Then*

$$V_x - i V_y = 2F_q \quad V_x + i V_y = 2F_{\bar{q}}.$$

If $q = z^2$ where $z = \xi + i\eta$ and $G(z, \bar{z}) = F(z^2, \bar{z}^2)$ then

$$G_\xi + iG_\eta = 2\bar{z}(V_x + iV_y).$$

Proof. These follows immediately from the chain rule. For example

$$F_{\bar{q}} = V_x x_{\bar{q}} + V_y y_{\bar{q}} = \frac{1}{2}V_x - \frac{1}{2i}V_y = \frac{1}{2}(V_x + iV_y).$$

Also

$$G_\xi + iG_\eta = 2G_{\bar{z}} = 2(F(z^2, \bar{z}^2))_{\bar{z}} = 2F_{\bar{q}} 2\bar{z} = 2\bar{z}(V_x + iV_y).$$

QED

The strange part about these equations lies in thinking of q, \bar{q} as independent complex variables and the equations $q = x + iy, \bar{q} = x - iy$ as a change of variables.

Abusing the notation a bit by writing $G(z, \bar{z})$ as $V(z, \bar{z})$, one can write $\bar{z}(V_x + iV_y) = V_{\bar{z}}$ and the regularized equations (62) become

$$z' = w \quad w' = 2i|z|^2w + \frac{z}{2}(h + V) + \frac{|z|^2}{2}V_{\bar{z}}.$$

Define a *regularized potential*

$$\begin{aligned} (63) \quad W &= \frac{|z|^2}{4}(V + h) = \frac{|z|^2}{4} \left(\frac{1}{2}|z^2 + 1 - \mu|^2 + \frac{1 - \mu}{|z^2 + 1|} + \frac{\mu}{|z|^2} + h \right) \\ &= \frac{1}{8}|z|^2|z^2 + 1 - \mu|^2 + \frac{(1 - \mu)|z|^2}{4|z^2 + 1|} + \frac{1}{4}(\mu + h|z|^2). \end{aligned}$$

This can be viewed as $W(\xi, \eta)$ or as $W(z, \bar{z})$. Note that W is nonsingular near the collision at $z = 0$. Also, the energy equation can be written

$$\frac{1}{2}|w|^2 - W = 0.$$

Using Lemma 6.1 and the fact that $|z|^2 = z\bar{z}$ gives

$$W_\xi + iW_\eta = 2W_{\bar{z}} = \frac{\partial}{\partial \bar{z}} \frac{|z|^2}{2}(V(z, \bar{z}) + h) = \frac{z}{2}(V(z, \bar{z}) + h) + \frac{|z|^2}{2}V_{\bar{z}}.$$

Then the regularized differential equations are

$$z' = w \quad w' = 2i|z|^2w + W_\xi + iW_\eta$$

or

$$(64) \quad \begin{aligned} \xi' &= \alpha & \alpha' &= W_\xi + 2(\xi^2 + \eta^2)\beta \\ \eta' &= \beta & \beta' &= W_\eta - 2(\xi^2 + \eta^2)\alpha. \end{aligned}$$

The Hill's regions for the regularized problem are given by $W(\xi, \eta) \geq 0$. Figure 25 shows the $\mathcal{H}(-2.4)$ for the mass ratio $\mu = \frac{1}{3}$ as in Figure 21 together with a typical orbit. The squaring map $q = z^2 + 1 - \mu$ takes the central disk to the disk around P_2 in Figure 21 and takes the two disks containing $z = \pm i$ to the disk around P_1 .

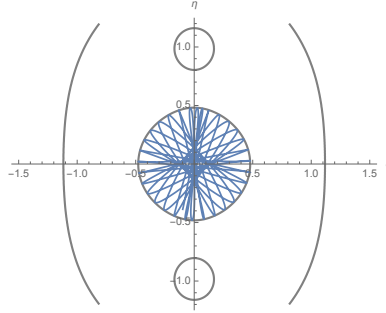


FIGURE 25. Hill's region for the regularized PCR3BP with $\mu = 1/3$ and $h = -2.4$. The Hill's region consist of the inside of the three small curves and the outside of the large one. The origin $z = 0$ represents the primary mass P_2 while P_1 is represented twice, at $z = \pm i$. The regularized orbit shown here is a collision orbit with initial position $z = 0$.

6.4. Conley's isolating block and the retrograde periodic orbit around P_2 . A nice application of the regularized equations is Conley's proof of the existence of a simple, symmetric retrograde periodic solution around P_2 [7]. The presentation here differs slightly from Conley's paper. Fix an energy so that the Hill's region of the regularized problem is as in Figure 25. Recall that in the nonrotating coordinates, the primary masses are moving in a counter-clockwise circular orbit. The periodic orbit to be constructed will move once around the origin $z = 0$ in the clockwise sense (hence retrograde) before closing up (see Figure 26).

The proof is based on a so-called *shooting* argument. Consider initial conditions of the form $(\xi, \eta, \alpha, \beta) = (0, \eta_0, \alpha_0, 0)$ with $\eta_0 > 0$ and $\alpha_0 > 0$. In other words, the solution will start on the positive η axis with initial velocity vector orthogonal to the axis and pointing to the right. The value of α_0 is uniquely determined by η_0 due to the energy equation. The initial $\eta_0 \in [0, k]$ where k represents the point in the zero-velocity curve. It will be shown that for some η_0 in this interval the corresponding solution $(\xi(t), \eta(t))$ moves through the first quadrant and meets the positive ξ axis orthogonally, say at time $t = t_1$ (red curve in Figure 26). The rest of the orbit can be found by reflecting through the coordinate axes to produce an orbit consisting for 4 congruent orbit segments with period $T = 4t_1$. Details of this symmetry argument are in Exercise 6.8. The term "shooting" refers to varying an initial condition in an attempt to find a solution with a desired final state

The proof involves constructing an *isolating block* in \mathcal{M}_0 , the component of the energy manifold $\mathcal{M}(h)$ which projects to the disk containing $z = 0$. First consider the topological structure of \mathcal{M}_0 .

Proposition 6.8. \mathcal{M}_0 is homeomorphic to the three-sphere \mathbb{S}^3 .

Proof. Let \mathcal{H}_0 be the component of the Hill's region containing $z = 0$ (shaded in Figure 26). For energy levels below that of the L_1 Lagrange point, it can be shown that \mathcal{H}_0 is diffeomorphic to the two-dimensional unit disk, $D = \{(x_1, x_2) : x_1^2 + x_2^2 = 1\}$. Let $\mathbb{S}^3 = \{(x_1, x_2, x_3, x_4) : x_1^2 + x_2^2 + x_3^2 + x_4^2 = 1\}$ and let $\pi(x_1, x_2, x_3, x_4) = (x_1, x_2)$ be the projection D . For each point (x_1, x_2) in the interior of D , the preimage $\pi^{-1}(x_1, x_2)$ is a circle with radii of these circles shrinking to zero at the

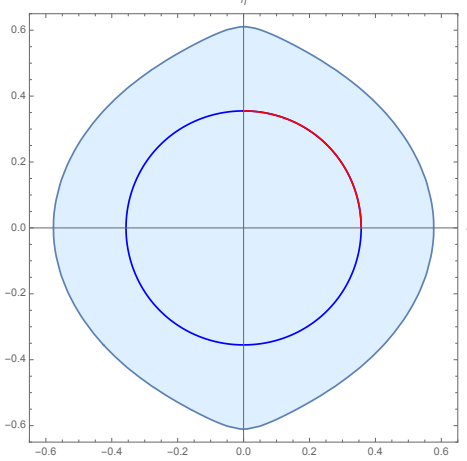


FIGURE 26. Conley's retrograde periodic orbit. The first quarter of the orbit (red) connects the axes orthogonally. The rest is obtained by symmetry.

boundary. A similar description applies to the projection $\pi(\xi, \eta, \alpha, \beta)$ mapping \mathcal{M}_0 to \mathcal{C}_0 , namely, the preimage of $(\xi, \eta) \in \mathcal{C}_0$ is given by $\alpha^2 + \beta^2 = 2W(\xi, \eta)$. From this it is possible to construct the required homeomorphism by mapping the circle above each (ξ, η) to the circle above the corresponding (x_1, x_2) . QED

The isolating block will be the following subset of \mathcal{M}_0

$$(65) \quad \mathcal{B} = \{(\xi, \eta, \alpha, \beta) \in \mathcal{M}_0 : \xi \geq 0, \eta \geq 0, \alpha \geq 0, \beta \leq 0\}.$$

Thus \mathcal{B} consists of points (ξ, η) in the first quadrant of the Hill's region \mathcal{C}_0 whose velocity vectors lie in the fourth quadrant (that is, they point southeast).

Definition 6.4. Let $\phi_t(p)$ be a flow on a metric space \mathcal{M} and let $\mathcal{B} \subset \mathcal{M}$ be a compact subset. \mathcal{B} is an isolating block if every boundary point $p \in \partial\mathcal{B}$ falls into one of the following three categories. For some $\delta > 0$, either

- $\phi_{(0,\delta)} \subset \text{int } \mathcal{B}$ and $\phi_{(-\delta,0)} \subset \text{ext } \mathcal{B}$
- $\phi_{(0,\delta)} \subset \text{ext } \mathcal{B}$ and $\phi_{(-\delta,0)} \subset \text{int } \mathcal{B}$
- $\phi_{(0,\delta)} \subset \text{ext } \mathcal{B}$ and $\phi_{(-\delta,0)} \subset \text{ext } \mathcal{B}$

Here $\text{int } \mathcal{B}, \text{ext } \mathcal{B}$ denote the interior and exterior of \mathcal{B} (both of which are open sets) and for any interval $I \subset \mathbb{R}$, $\phi_I(p)$ denotes the orbit segment $\{\phi_t(p) : t \in I\}$.

Thus all of the boundary points are either passing from inside to outside or from outside to inside or are “bouncing off”. There are no orbits which are “internally tangent” to the boundary.

The force of this definition is reflected in

Proposition 6.9. Let \mathcal{B} be an isolating block. For $p \in \mathcal{B}$ define the exit time as

$$\tau(p) = \sup\{t : \phi_{[0,t]}(p) \subset \mathcal{B}\}.$$

Then τ is a continuous function on $\{p : \tau(p) < \infty\}$. The exit point $\phi_{\tau(p)}(p)$ is also continuous.

Proof. Upper semicontinuity holds for any compact set \mathcal{B} , isolating block or not. To see this, let $p \in \mathcal{B}$ have $\tau(p) < \infty$ and let $\epsilon > 0$ be given. By definition of $\tau(p)$, there is a time $t_0 \in (\tau(p), \tau(p) + \epsilon)$ such that $\phi_{t_0}(p) \in \text{ext } \mathcal{B}$. By continuity of the flow, there is some neighborhood \mathcal{U} of p such that $\phi_{t_0}(q) \in \text{ext } \mathcal{B}$ for all $q \in \mathcal{U}$. So for all $q \in \mathcal{U}$, $\tau(q) \leq t_0 < \tau(p) + \epsilon$.

To prove lower semicontinuity, let $p \in \mathcal{B}$ have $\tau(p) < \infty$ and let $\epsilon > 0$ be given. If $\tau(p) = 0$ then $\tau(q) > \tau(p) - \epsilon = -\epsilon$ holds automatically. So suppose $\tau(p) > 0$. Since \mathcal{B} is an isolating block, none of the points on the orbit segment $\phi_{[0, \tau(p)]}(p)$ can be boundary points. In particular, $\phi_{[0, \tau(p)-\epsilon]}(p) \subset \text{int } \mathcal{B}$. By continuity of the flow, the same will be true for all q in some neighborhood \mathcal{U} of p . For all these points $\tau(q) > \tau(p) - \epsilon$ as required. QED

Proposition 6.10. *The subset \mathcal{B} is an isolating block for the regularized flow on \mathcal{M}_0 .*

Proof. The boundary of \mathcal{B} consists of points where one or more of the inequalities is an equality. It must be shown that all of these points fall into one of the three categories of Definition 6.4. Points in these categories will be called entrance points, exit points and bounce points.

\mathcal{B} is a three-dimensional subset of the three-dimensional energy manifold. The four inequalities cut out a region of the three-sphere \mathcal{M}_0 homeomorphic to a solid tetrahedron (see Figure 27). In this figure, the α coordinate has been projected out. It is given uniquely by $\alpha = \sqrt{2W(\xi, \eta) - \beta^2}$. The boundary $\partial\mathcal{B}$ consists of four faces defined by $\xi = 0, \eta = 0, \alpha = 0, \beta = 0$. The face with $\alpha = 0$ appears as the bottom, curved surface in the projection. If the faces are viewed as open disks, rather than closed ones, then the boundary also contains six open arcs defined by setting two of the variables to zero and four corner points defined by the vanishing of three of the variables. Each of these will be considered in turn. It may be helpful to refer to Figure 27 throughout the proof.

First consider the open face $F_1 = \{\xi = 0, \eta > 0, \alpha > 0, \beta < 0\}$. Since $\xi' = \alpha > 0$, it follows that for some $\delta > 0$, $\xi(t) < 0$ for $t \in (-\delta, 0)$ and $\xi(t) > 0$ for $t \in (0, \delta)$. If δ is sufficiently small, the inequalities about η, α, β will continue to hold. Hence F_1 consists of entrance points. A similar argument shows that $F_2 = \{\xi > 0, \eta = 0, \alpha > 0, \beta < 0\}$ consists of exit points.

To handle the open faces $F_3 = \{\xi > 0, \eta > 0, \alpha = 0, \beta < 0\}$ and $F_4 = \{\xi > 0, \eta > 0, \alpha > 0, \beta = 0\}$, a lemma is needed.

Lemma 6.2. *For $\xi \geq 0, \eta \geq 0$ the regularized potential satisfies $W_\xi \leq 0$ with equality only when $\xi = 0$ and $W_\eta \leq 0$ with equality only when $\eta = 0$.*

In other words, for (ξ, η) in the first quadrant, the gradient of W is in the third quadrant (see Figure 28). Assuming this, then $\beta' = W_\eta - 2(\xi^2 + \eta^2)\alpha < 0$ in F_4 . So β becomes negative in forward time and positive in backward time. Therefore F_4 consists of entrance points. A similar analysis shows that F_3 consists of exit points (see Exercise 6.9).

Turning to the six open arcs, consider $A_1 = \{\xi > 0, \eta > 0, \alpha = \beta = 0\}$, that is, the part of the zero-velocity curve in \mathcal{B} . Along the curve $\alpha' = W_\xi \leq 0$ with equality only at the endpoint with $\xi = 0$ and $\beta' = W_\eta \leq 0$ with equality only at the endpoint with $\eta = 0$. Since these endpoints are not being considered, it follows that A_1 consists of bounce points. Namely, in forward time, α becomes negative while in backward time β becomes positive.

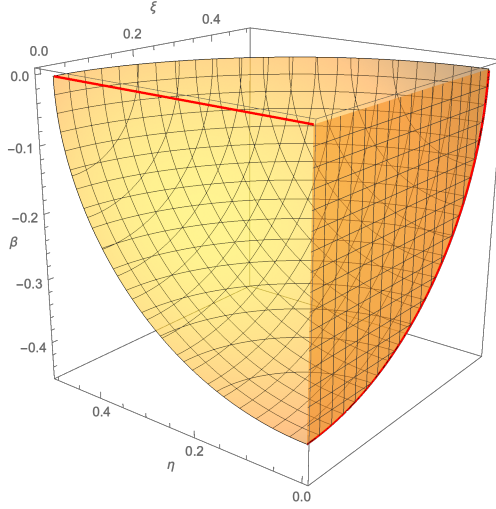


FIGURE 27. Projection of the isolating block \mathcal{B} to (ξ, η, β) space. Points which exit immediately in forward time are shaded.

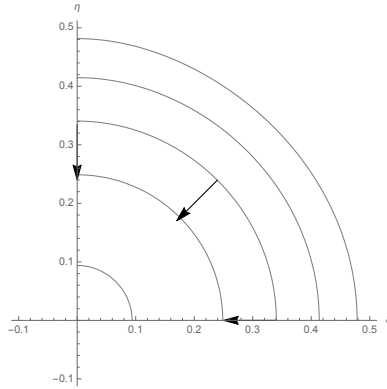


FIGURE 28. Projection \mathcal{Q} of the isolating block \mathcal{B} to (ξ, η) space. The projection is just the part of the second quadrant which lies in \mathcal{C}_0 . Some level curves of the regularized potential $W(\xi, \eta)$ are shown along with some of the gradient vectors (W_ξ, W_η) .

Next, consider $A_2 = \{\xi = 0, \eta = 0, \alpha > 0, \beta < 0\}$, the vertical, open segment above the origin in Figure 27. Since $\xi' = \alpha > 0$, these orbits leave \mathcal{B} in forward time and since $\eta' = \beta < 0$, they also leave in backward time. Thus, A_2 consists of bounce points.

Next consider the open arc $A_3 = \{\xi > 0, \eta = 0, \alpha = 0, \beta < 0\}$, the red curved arc in the figure. On this arc, $\eta' = \beta < 0$ so the orbits leave in forward time. Also $\alpha' = W_\xi + 2(\xi^2 + \eta^2)\beta < 0$. So in backward time, α becomes positive and η becomes positive which means the orbit enters the interior of \mathcal{B} . Hence A_3 consists of exit points. In $A_4 = \{\xi = 0, \eta > 0, \alpha > 0, \beta = 0\}$, the red segment at the top of the figure, the situation is reversed. These are entrance points (see Exercise 6.9).

This leaves $A_5 = \{\xi = 0, \eta > 0, \alpha = 0, \beta < 0\}$ and $A_6 = \{\xi > 0, \eta = 0, \alpha = 0, \beta < 0\}$. In A_5 , $\xi' = \alpha = 0$ and $\xi'' = \alpha' = W_\xi + 2(\xi^2 + \eta^2)\beta = 2\eta^2\beta < 0$ so ξ becomes negative in both forward and backward time. These are bounce points. Similarly, in A_6 , $\eta' = \beta = 0$ and $\eta'' = \beta' = -2\xi^2\alpha < 0$ so β becomes negative in both time directions. Once again, these are bounce points.

It remains to analyze the four corner points of \mathcal{B} . First consider the endpoints of the zero velocity curve. At the endpoint of the form $(\xi, \eta, \alpha, \beta) = (\xi, 0, 0, 0)$ the derivatives are $(\xi', \eta', \alpha', \beta') = (0, 0, W_\xi, 0)$ with $W_\xi < 0$. The orbit leaves \mathcal{B} in forward time since α becomes negative. In backward time, it will be shown that η becomes negative. The first two derivatives are $\eta' = \beta = 0$ and $\eta'' = \beta' = W_\eta - 2(\xi^2 + \eta^2)\alpha = 0$. The third derivative, however, is

$$\eta''' = W_{\eta\xi}\alpha + W_{\eta\eta}\beta - 4(\xi\alpha + \eta\beta)\alpha - 2(\xi^2 + \eta^2)\alpha' = -2\xi^2W_\xi > 0$$

and it follows that η becomes negative in backward time. So this endpoint is a bounce point. A similar analysis applies at the other endpoint, of the form $(\xi, \eta, \alpha, \beta) = (0, \eta, 0, 0)$ (see Exercise 6.9).

The remaining corners are the endpoints of the vertical segment over the origin in Figure 27, which are of the form $(0, 0, \alpha, 0)$ and $(0, 0, 0, \beta)$ with $\alpha > 0, \beta > 0$. The regularized potential satisfies $W_\xi = W_\eta = 0$. At the first point, $\alpha > 0$ so ξ becomes positive in forward time and the orbit leaves \mathcal{B} . It will be shown that the orbit also leaves \mathcal{B} in backward time with η becoming negative. The derivatives of η are $\eta' = \eta'' = 0$ and

$$\eta''' = W_{\eta\xi}\alpha + W_{\eta\eta}\beta - 4(\xi\alpha + \eta\beta)\alpha - 2(\xi^2 + \eta^2)\alpha' = W_{\eta\xi}\alpha.$$

At the origin, it turns out that $W_{\eta\xi} = 0$ so also $\eta''' = 0$. However

$$\eta''' = -4\alpha^3 < 0$$

so η becomes negative in backward time as required. The case $\beta < 0, \alpha = 0$ is similar (see Exercise 6.9).

This completes the proof. QED

The last ingredient in Conley's proof is

Proposition 6.11. *Every orbit starting in \mathcal{B} eventually leaves \mathcal{B} in forward time. Hence the exit time and exit point are continuous functions on all of \mathcal{B} .*

Proof. Since $\alpha \geq 0$ and $\beta \leq 0$ in \mathcal{B} , the coordinates $\xi(t), \eta(t)$ are monotone along orbits in \mathcal{B} . Suppose, for the sake of contradiction, that some orbit remains in \mathcal{B} for all $t \geq 0$. Then the limits $\bar{\xi} = \lim_{t \rightarrow \infty} \xi(t)$ and $\bar{\eta} = \lim_{t \rightarrow \infty} \eta(t)$ exist. It follows that the orbit has a nonempty ω limit set contained in the compact set $S = \{(\xi, \eta, \alpha, \beta) : \xi = \bar{\xi}, \eta = \bar{\eta}\}$ (a vertical line segment in Figure 27). At any point in this limit set, the vectorfield would have to be tangent to S . In particular, $x' = \alpha = 0, y' = \beta = 0$. So the only possible limit point is $(\bar{\xi}, \bar{\eta}, 0, 0)$ on the zero velocity curve, which would have to be an equilibrium point. However, at this point, $\alpha' = W_\xi \leq 0$ and $\beta' = W_\eta \leq 0$ and they are never both 0, a contradiction. QED

Now for the shooting argument. Consider the set of initial conditions in \mathcal{M}_0 starting on the positive η axis and moving into the first quadrant with velocities orthogonal to the axis. This is just the closed arc $\overline{A_4} = \{\xi = 0, \eta \geq 0, \alpha \geq 0, \beta = 0\}$, that is, the arc A_4 together with its endpoints. Recall that the open arc A_4 consists of entrance points. Let \mathcal{E} denote the exit set of \mathcal{B} consisting of all the points on

the boundary which move into $\text{ext } \mathcal{B}$ in forward time. This is the union of the exit points and the bounce points above. In Figure 27, the exit set consists of the closures of the shaded faces.

Because \mathcal{B} is an isolating block, there is a continuous Poincaré map $\Phi : \overline{A_4} \rightarrow \mathcal{E}$ assigning to each initial point its exit point. Note that the endpoints p, q of $\overline{A_4}$ are already in the exit set, that is, Φ maps these points to themselves. On the other hand, the open arc A_4 consists of entrance points and these will enter the interior and flow to the exit set. The image $\Phi(\overline{A_4})$ will be a continuous arc in \mathcal{E} connecting p to q .

Define a target set $\mathcal{T} = \overline{A_3} = \{(\xi, 0, 0, \beta)\}$, the closure of the red curve along the bottom in the figure. These are points which are leaving \mathcal{B} along the positive ξ axis with velocities $(0, \beta)$ orthogonal to the axis. Since \mathcal{T} separates p, q in the exit set, continuity of Φ shows that there must be at least one initial point $(0, \eta, \alpha, 0) \in A_4$ such that $\Phi(0, \eta, \alpha, 0) = (\xi, 0, 0, \beta) \in A_3$, as required.

Exercise 6.8. Let $R_1(\xi, \eta, \alpha, \beta) = (-\xi, \eta, -\alpha, \beta)$ be reflection through the η axis and $R_2(\xi, \eta, \alpha, \beta) = (\xi, -\eta, \alpha, -\beta)$ be reflection through the ξ axis. This exercise shows that these are symmetries of the regularized PCR3BP and shows how to use these to construct the a symmetric periodic orbit.

- i. Note that $W(\xi, \eta)$ can be written as a function of $F(\xi^2, \eta^2)$. Use this to show that

$$\begin{aligned} W_\xi(R_1(\xi, \eta)) &= -W_\xi(\xi, \eta) & W_\eta(R_1(\xi, \eta)) &= W_\eta(\xi, \eta) \\ W_\xi(R_2(\xi, \eta)) &= W_\xi(\xi, \eta) & W_\eta(R_2(\xi, \eta)) &= -W_\eta(\xi, \eta). \end{aligned}$$

- ii. Show that if $(\xi(t), \eta(t))$ is a solution, so are $R_i(\xi(-t), \eta(-t))$, $i = 1, 2$. In other words, reflection together with time reversal takes solutions to solutions.
- iii. Let $(\xi(t), \eta(t))$, $0 \leq t \leq t_1$, be the solution produced by Conley's isolating block argument. Show that the following is a periodic solution with period $T = 4t_1$:

$$\begin{aligned} (\xi(t), \eta(t)) && 0 \leq t \leq t_1 \\ (\xi(2t_1 - t), -\eta(2t_1 - t)) && t_1 \leq t \leq 2t_1 \\ (-\xi(t - 2t_1), -\eta(t - 2t_1)) && 2t_1 \leq t \leq 3t_1 \\ (-\xi(4t_1 - t), \eta(4t_1 - t)) && 3t_1 \leq t \leq 4t_1. \end{aligned}$$

Hint: Time translation is no problem. One needs to show that these are all solutions and that they match up at the endpoints in $(\xi, \eta, \alpha, \beta)$ space.

Exercise 6.9. Verify the isolating block conditions on the open face F_3 , the open arc A_4 and the corner points where $\xi = \alpha = \beta = 0$ and where $\xi = \eta = \alpha = 0$. More precisely, show that F_3 consists of exit points, A_4 consists of entrance points and the corner points are bounce points.

6.5. Dynamics near L_1 . Recall that L_1 is the collinear Lagrange point in the interval $(-\mu, 1 - \mu)$ between the primaries. Let h_1 be the energy of L_1 . For $h < h_1$, the Hill's region $\mathcal{H}(h)$ contains two bounded components, one around each primary, as well as an unbounded component. As h increases, the bounded components meet at the saddle point L_1 and then a small tunnel or neck opens up, and the primaries now lie in the same bounded component of the $\mathcal{H}(h)$ (see Figure). Thus h_1 represents an “energy barrier” below which it is impossible to move between the

primaries. Consequently, L_1 and the other collinear Lagrange points have played a role in designing space missions [?].

In the PCR3BP, the equilibrium point at L_1 has a pair of imaginary eigenvalues $\pm i\omega_1$ and the Lyapunov center theorem shows that there is a family of periodic orbits nearby, one in each of the energy manifolds with $h > h_1$ and $h - h_1$ sufficiently small. In the 3D CR3BP there is another pair of imaginary eigenvalues $\pm i\gamma$ and another family of approximately vertical periodic orbits.

Even though L_1 is unstable, the center manifold theorem can be used to prove existence of orbits which stay near L_1 for all time. Namely, it can be shown by straightforward computations involving the eigenvectors that the Hessian of the energy function D^2H is positive definite on the center subspace (the 4D space spanned by the combined eigenspaces of $\pm i\omega_1, \pm i\gamma$). Assuming this, one can show that each energy manifold $h > h_1$, $h - h_1$ sufficiently small, contains a compact, invariant manifold diffeomorphic to the three-sphere \mathbb{S}^3 . To see this, note that D^2H determines a positive definite quadratic form on the 4D center subspace. The level sets will be 3D ellipsoids. Using a blowup argument as in the proof of the Lyapunov center theorem with $h = h_1 + \epsilon^2$ it follows that for ϵ sufficiently small, the equation $H = h_1 + \epsilon^2$ determines a submanifold of the center manifold diffeomorphic to the 3D ellipsoid. This invariant three-sphere near L_1 will contain the two Lyapunov periodic orbits and many others as well.

For the PCR3BP the center manifolds is 2D and the intersection with the energy manifold is diffeomorphic to \mathbb{S}^1 , that is, to a circle. This circle must be a periodic orbit (see Exercise 6.10). This provides an alternative proof of the Lyapunov center theorem in this case.

Both the Lyapunov center theorem and the center manifold theorem apply only in a “sufficiently small” neighborhood of the equilibrium point, where the smallness is difficult to quantify. There is an interesting approach to the problem due to Conley using an isolating block which proves existence of orbits remaining for all time near L_1 and which can be applied with some effort to specific energies with $h > h_1$. In addition to its attractive geometric and topological content, it is a prototype for development of the theory of isolating blocks and the Conley index.

Fix an energy level $h > h_1$ such that there is a tunnel between the primaries in the Hill's region $\mathcal{H}(h)$. Cut off the tunnel on each side by vertical walls of the form $x = a, x = b$ where $a < \xi_1 < b$ and ξ_1 is the x coordinate of the L_1 (see Figure 29). The isolating block will be

$$\mathcal{B}(h) = \{(x, y, z, u, v, w); H = h, a \leq x \leq b\}.$$

In other words, \mathcal{B} is the preimage of the cut-off tunnel under the projection $\pi : \mathcal{M}(h) \rightarrow \mathcal{C}(h)$ from the energy manifold to the Hill's region. The walls of the block will be denoted by $W_{a,b} = \{(x, y, z, u, v, w); H = h, x = a, b\}$. For the planar case just ignore z, w (see Figure 30).

Proposition 6.12. *Suppose a, b, h are such that the walls $W_{a,b}$ are convex to the flow. That is, if $(x, y, z, u, v, w) = (a, y, z, 0, v, w) \in \mathcal{B}$ is tangent to W_a then $\ddot{x} < 0$ and if $(x, y, z, u, v, w) = (b, y, z, 0, v, w) \in \mathcal{B}$ is tangent to W_b then $\ddot{x} > 0$. Then \mathcal{B} is an isolating block. Moreover, there is a nonempty invariant set S in the interior of \mathcal{B} .*

Proof. \mathcal{B} is a subset of the manifold $\mathcal{M}(h)$ in phase space. The boundary $\partial\mathcal{B}$ is just $W_a \cup W_b$. According to Definition 6.4, it must be shown that each boundary

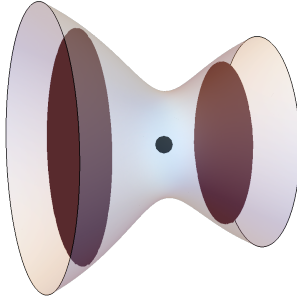


FIGURE 29. Projection of the 3D isolating block \mathcal{B} to (x, y, z) space for $\mu = \frac{1}{3}$, $h = -1.9$, $a = 0$, $b = 0.4$.

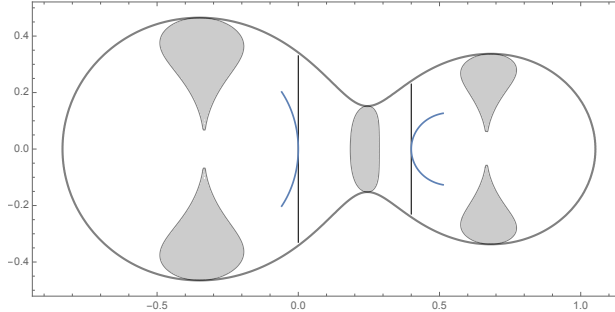


FIGURE 30. Projection of the planar isolating block \mathcal{B} to (x, y) space. Orbits tangent to the walls bounce off. Here $\mu = \frac{1}{3}$, $h = -1.9$, $a = 0$, $b = 0.4$.

point is either entering, exiting or bouncing off. Clearly, points with $x = a$ and $u = \dot{x} > 0$ are entering while those with $u < 0$ are exiting. It remains to check the points with $u = 0$ and the hypothesis that $\ddot{x} < 0$ implies that the solution exits in both time directions, so these orbits bounce off, as required. A similar discussion applies when $x = b$.

To see that there must be solutions which remain in \mathcal{B} for all time, a bit of topology is needed. First note that \mathcal{B} is a connected set. On the other hand, note that there are points in each of the two walls which are exiting in forward time, either by moving from inside to out or by bouncing off. Let \mathcal{E} be the exit set of \mathcal{B} , that is, the closed set of points leaving \mathcal{B} in forward time. \mathcal{E} is a union $\mathcal{E} = \mathcal{E}_a \cup \mathcal{E}_b$ of two nonempty, compact sets. Let S_+ be the set of all initial conditions in \mathcal{B} whose orbits remain in \mathcal{B} for all $t \geq 0$. If it were the case that $S_+ = \emptyset$ then there would be a continuous surjective map $\mathcal{B} \rightarrow \mathcal{E}_a \cup \mathcal{E}_b$, which is impossible since \mathcal{B} is connected. Therefore $S_+ \neq \emptyset$ and, in fact, it must be large enough to separate \mathcal{E}_a from \mathcal{E}_b in \mathcal{B} .

By definition S_+ is a positively invariant set. To find a set which is invariant in both forward and backward time, just take the omega limit set

$$S = \omega(S_+) = \cap_{t \geq 0} \overline{\phi_t(S_+)}$$

where the bar denotes the closure of a set. This will be nonempty, compact and invariant. Moreover, since \mathcal{B} is an isolating block, S does not intersect the boundary, so must lie in the interior of \mathcal{B} . QED

How can one check the hypotheses of Proposition 6.12 for particular a, b, h ?

Proposition 6.13. *Let $a < \xi_1 < b$ and let $F(x, y, z) = V_x(x, y, z)^2 - 8(V + h)$. If $F > 0$ on the walls W_a, W_b , then \mathcal{B} is an isolating block.*

Proof. The differential equation gives $\ddot{x} = \dot{u} = V_x(x, y, z) + 2v$ and if $u = 0$, the energy equation gives $v^2 = 2(V(x, y, z) + h)$. The hypothesis on F gives $|V_x| > |2v|$ for all points tangent to one of the walls of \mathcal{B} . In particular, V_x cannot change sign on the walls. Now the convexity of $V(x, 0, 0)$ implies that $V_x(a, 0, 0) < 0$ and $V_x(b, 0, 0) > 0$. Hence $V_x < 0$ on W_a and $V_x > 0$ on W_b . Then $|V_x| > |2v|$ gives $\ddot{x} < 0$ on W_a and $\ddot{x} > 0$ on W_b , as claimed. QED

The hypothesis $F > 0$ of Proposition 6.13 can be checked when $h > h_1$ and $|h - h_1|$ is sufficiently small. To see this, blow up a neighborhood of L_1 by setting $h = h_1 + \epsilon^2$, $x = \xi_1 + \epsilon \xi$, $y = \epsilon \eta$ and $z = \epsilon \zeta$ where $\epsilon > 0$ is small. Then using the Taylor series of V from Section 6.2

$$V = V_0 + \frac{\epsilon^2}{2}(\alpha \xi^2 - \beta \eta^2 - \gamma^2 \zeta^2) + O(\epsilon^3) \quad V_x = \epsilon \alpha \xi + O(\epsilon^2)$$

where $V_0 = V(L_1) = -h_1$, $\alpha = V_{xx}(L_1) > 0$, $\beta = -V_{yy}(L_1) < 0$, $\gamma^2 = -V_{zz}(L_1)$. After canceling a factor of ϵ^2 , the inequality $F > 0$ at the worst-case point where $\eta = \zeta = 0$ becomes $\alpha(\alpha - 4)\xi^2 > 8$. It turns out that the second derivative $\alpha = V_{xx}(L_1)$ satisfies $\alpha > 4$ for all values of μ (see Exercise 6.12). Choose any $\xi > 0$ with $\alpha(\alpha - 4)\xi^2 > 8$ and let $a = \xi_1 - \epsilon \xi$ and $b = \xi_1 + \epsilon \xi$ to get an isolating block for ϵ sufficiently small.

One can also check $F > 0$ numerically or otherwise for larger energies. For example, the nonshaded part of Figure 30 shows the region around L_1 such that $F > 0$ for $\mu = \frac{1}{3}$ and $h = -1.9$. By choosing the walls as in the figure, one can satisfy the isolating block condition in the planar case.

Finally, consider the problem of computing the Lyapunov family of periodic orbits near L_1 in the PCR3BP by shooting. It suffices to look for periodic orbits which are symmetric under reflection through the x axis (see Exercise 6.11). In particular, such an orbit must meet the x axis orthogonally and top and bottom halves are symmetric. Suppose an isolating block like that in Figure 30 has been found and consider initial conditions of the form $(x, y, u, v) = (a, 0, 0, v)$ with $a \leq x \leq \xi_1$ and $v > 0$. Shooting can be used to find such an orbit which returns orthogonally to the x axis. Figure 31 shows the result.

Exercise 6.10. Let S be an invariant set for a flow which is diffeomorphic to \mathbb{S}^1 . Show that if S contains no equilibrium points, then it must consist of a single periodic orbit.

Exercise 6.11. Show that if $(x(t), y(t))$ is a solution of the PCR3BP, then so is $(x(-t), -y(-t))$. That is, reflection through the x axis combined with time reversal

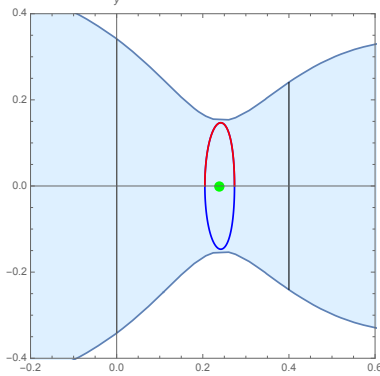


FIGURE 31. A symmetric periodic orbit near L_1 inside the projection of the isolating block of Figure 30.

is a symmetry of the problem. Show that if $(x(t), y(t))$, $0 \leq t \leq t_1$ is an orbit segment with $y(t) \geq 0$ which meet the x axis orthogonally when $t = 0, t_1$, then extending the orbit via $(x(t_1 - t), -y(t_1 - t))$ gives a symmetric periodic orbit of period $2t_1$.

Exercise 6.12. Recall from Section 6.2 that $V_{xx}(L_1) = 1 + 2\gamma^2$ where $\gamma^2 = (1 - \mu)/r_{13}^3 + \mu/r_{23}^3$. It was shown in Exercise 6.2 that $\gamma^2 > 1$ on the whole interval $(-\mu, 1 - \mu)$ but in order to get $\alpha = 1 + 2\gamma^2 > 4$, the stronger inequality $\gamma^2 > \frac{3}{2}$ is needed. Here is an algebraic approach to proving this at the point L_1 itself. As in Exercise 6.2 one can set $r_{13} = \frac{s}{1+s}$ and $r_{23} = \frac{1}{1+s}$. Also $x = \mu + r_{13}$. Making all these substitutions makes the potential $V(x, 0)$ into a rational function $V(s)$. The location of L_1 is given by setting $V'(s) = 0$ which amounts to solving a fifth degree polynomial equation $P(s) = 0$. Similarly, the difference $\gamma^2 - \frac{3}{2}$ can be expressed as a rational function with a positive denominator and a numerator $Q(s)$, of degree 6. The value of $Q(s)$ at the root of $P(s)$ should be positive. To prove this, first calculate the *resultant* of the two polynomials to obtain a polynomial in μ which is never 0. So $P(s), Q(s)$ have no common roots. Finally check that for the special case $\mu = \frac{1}{2}$, the root of $P(s)$ is $s = 1$ and $Q(1) > 0$.

7. BLOWING UP THE TOTAL COLLISION – MCGEHEE COORDINATES

Consider the n -body problem in \mathbb{R}^d . Let $q = (q_1, q_2, \dots, q_n) \in \mathbb{R}^{dn}$ be the configuration vector and $v = (v_1, v_2, \dots, v_n) \in \mathbb{R}^{dn}$ the velocity vector. The Lagrangian is

$$L(q, v) = \frac{1}{2}v^T M v - U(q)$$

where $U(q)$ is the Newtonian potential and $M = \text{diag}(m_1, \dots, m_1, m_2, \dots, m_2, \dots)$ is the $dn \times dn$ mass matrix. As in Section 3.1, one may assume that the total momentum is zero and the center of mass is at the origin:

$$\begin{aligned} m_1 q_1 + \dots + m_n q_n &= 0 \\ m_1 v_1 + \dots + m_n v_n &= 0. \end{aligned}$$

The translation reduced phase space is $(X \setminus \Delta) \times X$ where $X \subset \mathbb{R}^{dn}$ is the subspace of dimension $d(n-1)$ given by either one of these equations and Δ is the collision set.

One type of collision is when all n bodies arrive at the same position at the same time. The center of mass condition implies that this can only happen at the origin. By introducing a version of polar coordinates in the subspace X , the singularity can be blown up. The first step is to introduce a natural radial variable based on the *mass norm*. First introduce a *mass inner product* or *mass metric* in \mathbb{R}^{dn} via

$$\langle\langle v, w \rangle\rangle = V^T M W = \sum m_i v_i \cdot w_i$$

where $v = (v_1, v_2, \dots, v_n), w = (w_1, w_2, \dots, w_n)$ are arbitrary vectors in \mathbb{R}^{dn} . The corresponding norm is given by

$$\|v\|^2 = \langle\langle v, v \rangle\rangle = \sum m_i |v_i|^2.$$

Thus $\|v\|$ is a mass-weighted measure of the distance to the origin. Using the mass norm, the energy equation can be written

$$(66) \quad \frac{1}{2} \|v\|^2 - U(q) = h.$$

For configuration vectors $q \in X$, $r = \|q\|$ can be viewed as a measure of the size of the configuration. In particular $r = 0$ represents total collision of all of the bodies. The square of the norm $\mathcal{I} = \|q\|^2$ is the *moment of inertia* of the configuration with respect to the origin. Given any configuration with $r > 0$, defined a *normalized configuration* $s = q/r$. Then $s = (s_1, s_2, \dots, s_n) \in X$ represents a configuration of n -bodies with the same shape as q but with size

$$(67) \quad \|s\|^2 = s^T M s = 1.$$

Let $\mathcal{E} \subset X$ denote the ellipsoid where (67) holds. Replacing $q \in X$ by $(r, s) \in \mathbb{R}^+ \times \mathcal{E}$ is a variation on polar or spherical coordinates.

There is a useful alternative formula for the mass norm for configurations in X .

Proposition 7.1. *If $q = (q_1, \dots, q_n) \in \mathbb{R}^{dn}$ satisfies $m_1 q_1 + \dots + m_n q_n = 0$ then*

$$(68) \quad \|q\|^2 = \frac{1}{m} \sum m_i m_j r_{ij}^2 \quad r_{ij} = |q_i - q_j|$$

where the sum is over all pairs $1 \leq i < j \leq n$.

Before discussing the rest of McGehee's coordinate system, some classical results involving the size of the configuration will be given. The following result is called the *Lagrange-Jacobi identity*.

Proposition 7.2. *The moment of inertia $\mathcal{I} = \|q\|^2$ satisfies*

$$\ddot{\mathcal{I}} = 2U(q) + 4h$$

where h is the total energy.

Proof. Since $\mathcal{I} = q^T M q$, $\dot{\mathcal{I}} = 2q^T M v$ and

$$\ddot{\mathcal{I}} = 2v^2 M v + 2q^T \nabla U(q).$$

Since $U(q)$ is a homogenous function of degree -1 , $q^T \nabla U(q) = -U(q)$. Using this and (66) gives

$$\ddot{\mathcal{I}} = 4(h + U(q)) - 2U(q) = 4h + 2U(q).$$

QED

Using this, it is easy to get an important qualitative result about the n -body problem. Recall that for the two-body problem and the Kepler problem, all of the bounded solutions (the ellipses) have negative energy. The same is true for the n -body problem.

Proposition 7.3. *Let $q(t)$ be a solution of the n -body problem which exists for all $t \in \mathbb{R}$. If $q(t)$ has energy $h \geq 0$ then $r(t) = \|q(t)\| \rightarrow \infty$ as $t \rightarrow \pm\infty$.*

Proof. Consider $\mathcal{I}(t) = r(t)^2$. The Lagrange-Jacobi identity shows that $\ddot{\mathcal{I}} = 4h + 2U(q) \geq 2U(q) > 0$. In other words, $\mathcal{I}(t)$ is a convex function. Consider the derivative $\dot{\mathcal{I}}(t)$ which will be a strictly increasing function. If $\dot{\mathcal{I}}(t_0) > 0$ for some t_0 then since $\dot{\mathcal{I}}(t) \geq \dot{\mathcal{I}}(t_0)$ for all $t \geq t_0$. Then $\mathcal{I}(t) \geq \mathcal{I}(t_0) + \dot{\mathcal{I}}(t_0)(t - t_0) \rightarrow \infty$ as $t \rightarrow \infty$. Similarly if $\dot{\mathcal{I}}(t_0) < 0$ for some t_0 then $\mathcal{I}(t) \rightarrow \infty$ as $t \rightarrow -\infty$. If $\dot{\mathcal{I}}(t_0) = 0$ for some t_0 then $\dot{\mathcal{I}}(t)$ will take both positive and negative values for t near t_0 and so $\mathcal{I}(t) \rightarrow \infty$ as $t \rightarrow \pm\infty$.

It only remains to show that it is impossible for $\dot{\mathcal{I}}(t)$ to always have the same sign. Suppose, for example, that $\dot{\mathcal{I}}(t) < 0$ for all t . Then $\mathcal{I}(t)$ is monotonically decreasing and so for any t_0 , $\mathcal{I}(t) \leq \mathcal{I}(t_0)$ for $t \geq t_0$. Recall that $r = \sqrt{\mathcal{I}}$ and let $s = q/r$ be the normalized configuration. Note that since the potential $U(q)$ is homogeneous of degree -1 , $U(q) = U(rs) = r^{-1}U(s)$. Now $U(s)$ is a positive function on the ellipsoid \mathcal{E} where $s^T M s = 1$ and it follows that it has a positive lower bound $U(s) \geq K_1 > 0$. Then $U(q(t)) \geq K_1 r(t)^{-1} \geq K_1 \mathcal{I}(t_0)^{-\frac{1}{2}} = K_2$ for all $t \geq t_0$. This gives $\ddot{\mathcal{I}} \geq 2U(q) \geq 2K_2$. This estimate implies that $\dot{\mathcal{I}}(t)$ becomes positive after a finite time, a contradiction. QED

McGehee's idea was to combine the coordinate change $q = rs$ with an appropriate change of velocity variables and timescale [13, 14]. Define a new velocity variable z by $z = \sqrt{r}v$ and a new timescale such that $' = r^{\frac{3}{2}}$. In other words the new time variable τ is related to the old time variable t by

$$\frac{dt}{d\tau} = r(\tau)^{\frac{3}{2}}, \quad \frac{d\tau}{dt} = r(\tau)^{-\frac{3}{2}}.$$

Then a short computation (Exercise 7.2) gives the differential equations

$$(69) \quad \begin{aligned} r' &= \nu r \\ s' &= z - \nu s \\ z' &= M^{-1} \nabla U(s) + \frac{1}{2} \nu z \end{aligned}$$

where $\nu = \langle\langle s, z \rangle\rangle$. For example, since $r^2 = \langle\langle q, q \rangle\rangle$ and $q' = r^{\frac{3}{2}}v = zr$, one computes

$$2rr' = 2\langle\langle q, q' \rangle\rangle = 2r^2 \langle\langle s, z \rangle\rangle = 2vr^2.$$

Using the homogeneity of the potential, the energy equation becomes

$$\frac{1}{2} \|z\|^2 - U(s) = rh.$$

Note that $\{r = 0\}$ is now an invariant *total collision manifold* for the rescaled equations.

The variable $\nu = \langle\langle s, z \rangle\rangle$ is a scaled radial velocity, as the first equation in (69) shows. Because of the second equation, the vector $w = z - \nu s$ is tangent to the

ellipsoid \mathcal{E} and can be viewed as a tangential velocity. It is easy to check that $\langle\langle s, w \rangle\rangle = 0$. Then $z = \nu s + w$ decomposes z as a radial and tangential part. Another calculation gives

$$(70) \quad \begin{aligned} r' &= \nu r \\ s' &= w \\ \nu' &= \frac{1}{2}\nu^2 + \|w\|^2 - U(s) \\ w' &= M^{-1}\nabla U(s) + U(s)s - \frac{1}{2}\nu w - \|w\|^2 s = \tilde{\nabla}U(s) - \frac{1}{2}\nu w - \|w\|^2 s \end{aligned}$$

where

$$(71) \quad \tilde{\nabla}U(s) = M^{-1}\nabla U(s) + U(s)s.$$

Finally, since $z = \nu s + w$ is a decomposition into vectors which are orthogonal with respect to the mass metric, the energy equation becomes

$$(72) \quad \frac{1}{2}(\nu^2 + \|w\|^2) - U(s) = rh.$$

The vector $\tilde{\nabla}U(s)$ is the tangential gradient of the potential. More precisely, it is the gradient vector of the restriction of $U(s)$ to the ellipsoid \mathcal{E} with respect to the mass metric. The meaning of this statement is as follows. First of all $\tilde{\nabla}U(s)$ is tangent to the ellipsoid since

$$\begin{aligned} \langle\langle s, \tilde{\nabla}U(s) \rangle\rangle &= s^T M(M^{-1}\nabla U(s) + U(s)s) \\ &= s^T \nabla U(s) + U(s)s^T M s = -U(s) + U(s) = 0. \end{aligned}$$

Second, if w is a vector tangent to the ellipsoid, that is $\langle\langle s, w \rangle\rangle = 0$, then

$$\langle\langle \tilde{\nabla}U(s), w \rangle\rangle = (M^{-1}\nabla U(s) + U(s)s)^T M w = \nabla U(s)^T w = dU(s)w.$$

Before turning to the discussion of total collision, an important property of the radial velocity ν will be given. Using the energy equation, the differential equation for ν' can be written

$$(73) \quad \nu' = \frac{1}{2}\nu^2 + \|w\|^2 - U(s) = \frac{1}{2}\|w\|^2 + rh.$$

If $h \geq 0$ or else if $r = 0$ (the collision manifold), $\nu' = \frac{1}{2}\|w\|^2 \geq 0$. So $\nu(t)$ is a nondecreasing Lyapunov function. This fact is closely related to the Lagrange-Jacobi identity and the connections are explored in Exercise 7.3.

Exercise 7.1. Prove Proposition 7.1.

Exercise 7.2. Derive equations (69) and (70). The homogeneity of $U(q)$ will be needed to express $\nabla U(q)$ in terms of $\nabla U(s)$.

Exercise 7.3. Note that $\dot{\mathcal{I}}(t)$ and $\nu(\tau)$ are both connected with the rate of change of the size of the configuration. Their derivatives $\ddot{\mathcal{I}}(t)$ from the Lagrange-Jacobi equation from Proposition 7.2 and $\nu'(\tau)$ from (73) are also closely connected. To explore this, use the fact that $\mathcal{I} = r^2$ and the change of timescale to derive (73) from the Lagrange-Jacobi equation.

7.1. Total Collision. In this section, solutions of the n -body problem which experience a total collision will be discussed using McGehee coordinates. But first some simple examples of such orbits will be given.

Example 7.1. The collinear Kepler problem. Consider the Kepler problem in \mathbb{R}^1 . If the center of attraction at the origin has mass λ and if $r(t) > 0$ is the position of the moving body, then the differential equation is

$$(74) \quad \ddot{r}(t) = -\frac{\lambda}{r(t)^2}$$

and the energy equation is $\frac{1}{2}\dot{r}^2 - \frac{\lambda}{r} = h$. Since the motion is confined to a line, collisions are inevitable. For example, if the initial velocity is $\dot{r} = 0$, it's clear that there will be collisions with the origin in both forward and backward time. Such a solution has negative energy $h < 0$. For solutions with $h \geq 0$. There will be a collision in one time direction while $r(t) \rightarrow \infty$ in the other.

Since the Kepler problem models the translation reduced two-body problem, there will be corresponding solutions of the two-body problem which begin and/or end in total collision. See Exercise 1.5 for an example with $h = 0$.

For the two-body problem in \mathbb{R}^d , one can find such solutions moving along any given line through the origin. Clearly these will have angular momentum zero.

Based on this simple example, one can construct analogous solutions of the n -body problem, the so-called *homothetic solutions*. Starting from some initial configuration, these solutions simply collapse to the origin with each body moving along a straight line. However, this is only possible if the initial configuration is carefully chosen.

Proposition 7.4. *Let $q_0 \in \mathbb{R}^{dn}$ be a configuration of n bodies in \mathbb{R}^d . Then $q(t) = r(t)q_0$, $r(t) > 0$ is a solution of the n -body problem if and only if q_0 satisfies the equation*

$$(75) \quad \nabla U(q_0) + \lambda M q_0 = 0$$

where M is the mass matrix and λ is a constant, and $r(t)$ is a solution of the collinear Kepler problem (74).

Proof. Let $q(t) = r(t)q_0$. Then $q(t)$ solves Newton's equation if and only if

$$M\ddot{r}(t)q_0 = \nabla U(r(t)q_0) = r(t)^{-2}\nabla U(q_0).$$

Writing this as $r(t)^2\ddot{r}(t)Mq_0 = \nabla U(q_0)$, the right-hand side is a constant vector so the left-hand side must also be constant. Writing $r(t)^2\ddot{r}(t) = -\lambda$ for some λ gives both equations (74) and (75). QED

Definition 7.1. A configuration $q_0 = (q_1, \dots, q_n) \in \mathbb{R}^{dn}$ is a central configuration or CC if (75) holds for some λ .

For example, it will be shown later that for every choice of masses, the equilateral triangle configurations are central configurations of the planar three-body problem. This gives rise to homothetic solutions as in Figure 32. The bodies move along straight lines, always maintaining an equilateral shape until they collide at the center of mass.

It can be shown that if q is a CC then the center of mass is automatically at the origin and $\lambda = U(q)/\|q\|^2 > 0$. Moreover if q is a CC then so are all of the

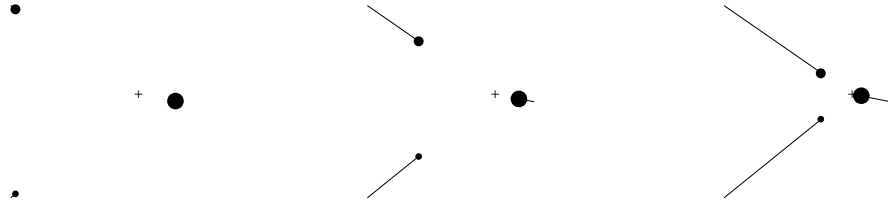


FIGURE 32. A homothetic solution of the planar three-body problem based on Lagrange's equilateral central configuration.

configurations obtained from q by scaling and rotation, that is, $\tilde{q} = kRq$ where $k > 0$ and $R \in \mathbf{SO}(d)$ (acting on each q_i as usual). See Exercise 7.4.

One might ask what the homothetic solutions look like in McGehee's blown-up coordinates. For such a solution, the normalized configuration $s(\tau) = q(\tau)/\|q(\tau)\| = s_0$ is constant. Only the size $r(\tau)$ varies. From the ODE (70), one finds $s(\tau) = s_0$, $w(\tau) = s'(\tau) = 0$. The size variables satisfy

$$r' = \nu r \quad \nu' = \frac{1}{2}\nu^2 - U(s_0)$$

while the fact that $w' = 0$ gives

$$\tilde{\nabla}U(s_0) = M^{-1}\nabla U(s_0) + U(s_0)s_0 = 0.$$

In addition, the energy equation gives

$$\frac{1}{2}\nu^2 - U(s_0) = rh.$$

The equation $\tilde{\nabla}U(s_0) = 0$ is equivalent to the CC equation (75) with $\lambda = U(s_0)$, which is the right value for normalized configurations $\|s_0\| = 1$. Figure 33 shows the behavior of the size variables (r, ν) for various energies. Note that the homothetic orbits converge to restpoints p_{\pm} with $(r, s, \nu, w) = (0, s_0, \pm\sqrt{U(s_0)}, 0)$ as $\tau \rightarrow \pm\infty$.

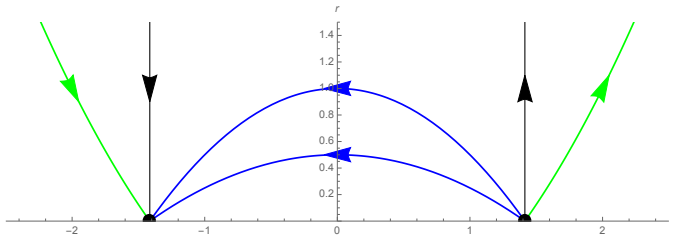


FIGURE 33. Phase portrait of size variables for homothetic orbits, showing convergence to restpoints on the collision manifold $r = 0$. For $h < 0$ (blue), the homothetic orbits connect two restpoints. The other curves are for $h > 0$ (blue) and $h = 0$ (black).

The homothetic orbits are the simplest examples of total collision solutions, but it turns out that there are many others. The rest of this section is devoted to understanding all of them. It will turn out that the behavior in Figure 33 is typical: collision solutions converge to restpoints on the collision manifold.

For equations (70) in McGehee coordinates (r, s, ν, w) , the total collision $\{r = 0\}$ is blown-up into an invariant manifold

$$\mathcal{M}_0 = \{r = 0, s \in X, w \in X, \|s\| = 1, \langle s, w \rangle = 0, \frac{1}{2}(\nu^2 + \|w\|^2) - U(s) = 0\}.$$

Since the subspace X has dimension $d(n-1)$, the dimension of \mathcal{M}_0 is $2d(n-1) - 2$. The energy manifold, $\mathcal{M}(h)$, given by the same equations but with $r \geq 0$ has dimension $2d(n-1) - 1$.

Solutions $q(t)$ of the n -body problem which experience a total collision in finite time, now appear as solutions converging asymptotically to the collision manifold. The following result makes this more precise for collisions which occur in forward time. Reversing time, one can find the analogous result for collisions in the past.

Proposition 7.5. *Suppose $q(t)$ is a solution of the n -body problem for $t \in [0, t_0)$ which experiences a total collision at $t = t_0$ and let $\gamma(\tau) = (r(\tau), s(\tau), \nu(\tau), w(\tau))$ be the corresponding solution in McGehee coordinates. Then*

- i. $\gamma(\tau)$ exists for $\tau \in [0, \infty)$
- ii. $\nu(\tau)$ converges to a limit $-\nu_0 < 0$ and $r(\tau) \rightarrow 0$ exponentially
- iii. the omega limit set $\omega(\gamma)$ is a nonempty compact subset of the set of restpoints in \mathcal{M}_0
- iv. the angular momentum is zero

Proof. The key point of the proof is to use the fact that $\nu(\tau)$ is a Lyapunov function. From (73) and the energy equation one can derive yet another formula

$$\nu' = U(s) - \frac{1}{2}\nu^2 + 2rh.$$

Recall that there is a positive lower bound $U(s) \geq K > 0$. It follows that there exist positive constants ν_1, r_0, k such that

$$\nu' \geq k > 0 \quad \text{when } r \leq r_0, -\nu_1 \leq \nu \leq \nu_1.$$

Suppose $\gamma(\tau)$ exists on some interval $[0, b)$ (later it will be shown that $b = \infty$). Since $r(\tau) \rightarrow 0$ as $\tau \rightarrow b$, there will be some time τ_0 such that $r(\tau) \leq r_0$ for $\tau \geq \tau_0$. It follows that $\nu(\tau) \leq -\nu_1$ for $\tau \geq \tau_0$. Otherwise, $\nu(\tau)$ would enter the region $r \leq r_0, -\nu_1 \leq \nu \leq \nu_1$ where the lower bound $\nu' \geq k$ holds. $\nu(\tau)$ would have to increase beyond $+\nu_1$ and could then never decrease below this bound again. But $\nu' \geq \nu_1 r > 0$ is incompatible with $r(\tau) \rightarrow 0$.

By shifting the origin of time, it may now be assumed that $r(\tau) \leq r_0, \nu(\tau) \leq -\nu_1$ for all $\tau \geq 0$. It follows that the exponential estimate $r(\tau) \leq r_0 \exp(-\nu_1 \tau)$ holds. This can be used to show that $\nu(\tau)$ converges to a limit. If $h \geq 0$, $\nu(\tau)$ is increasing and the limit exists by monotonicity. So suppose $h = -|h| < 0$. Let $-\nu_0 = \limsup \nu(\tau) \leq -\nu_1$. To see that $-\nu_0$ is actually the limit, it must be shown that the negative variations of $\nu(\tau)$ tend to zero. Since

$$\nu' = \frac{1}{2}\|w\|^2 + rh \geq rh \geq -r_0 \exp(-\nu_1 \tau)|h|$$

the change of ν over any interval $[\tau_1, \tau_2]$ satisfies

$$\nu(\tau_2) - \nu(\tau_1) = \int_{\tau_1}^{\tau_2} \nu'(\tau) d\tau \geq -\frac{r_0|h|}{\nu_1} \exp(-\nu_1 \tau_1).$$

This converges to zero as $\tau_1 \rightarrow \infty$ as required.

Since $\nu(\tau) \rightarrow -\nu_0$ it follows that $-2\nu_0 \leq \nu(\tau) \leq -\nu_0$ for τ sufficiently large. Since $r = \nu r$, this gives exponential upper and lower bounds for $r(\tau)$ and, in particular, it follows that the interval of existence for $\gamma(\tau)$ must be $[0, \infty)$.

So far, it has been shown that $\gamma(\tau)$ converges to a level set of ν in the collision manifold. To get the result about the omega limit set, it will be shown that $U(s(\tau))$ has an upper bound, that is, $s(\tau)$ avoids the singular normalized configurations (which would correspond to collisions of a proper subset of the bodies). First note that if $U(s) \geq C$, $r \leq r_0$ and $-2\nu_0 \leq \nu(\tau) \leq -\nu_0$, then

$$\nu' = U(s) - \frac{1}{2}\nu^2 + 2rh \geq C - 2\nu_0^2 - 2|h|r_0.$$

Then it will certainly be true that $\nu' \geq C/2$ for all C sufficiently large. Since $\nu(\tau)$ has a limit, it cannot be that $U(s(\tau)) \geq C$ continues to hold for all $\tau \geq \tau_1$. From this, it will be shown that $U(s(\tau)) \leq 2C$ holds for all sufficiently large τ . If not, the configuration $s(\tau)$ would have to travel between the level sets $U = C$ and $U = 2C$ infinitely often. Let $\delta > 0$ be the distance between these two compact sets, using the mass metric. The energy equation gives

$$\|s'\| = \|w\| = \sqrt{2U(s) + 2rh - \nu^2} \leq \sqrt{C + 2r_0|h|}$$

The time required for U to increase from $U = C$ to $U = 2C$ is at least $\Delta\tau = \delta/\sqrt{C + 2r_0|h|}$. During this time, ν increases by at least

$$\Delta\nu \geq C\delta/2\sqrt{C + 2r_0|h|} > 0.$$

Thus if this happened infinitely often, ν could not converge.

So it has finally been shown that $\gamma(\tau)$ converges to the set $\{r = 0, \nu = -\nu_0, U(s) \leq 2C\}$. The energy equation gives a bound $\frac{1}{2}\|w\|^2 \leq 2C - \frac{1}{2}\nu_0^2$ so $\gamma(\tau)$ converges to a compact subset of \mathcal{M}_0 . Therefore the limit set $\omega(\gamma)$ is a nonempty compact, invariant subset. On the collision manifolds $\nu' = \frac{1}{2}\|w\|^2$. Since $\omega(\gamma)$ is invariant and contained in a level set of ν , it must be contained in the set $\nu' = w = w' = 0$. Since $r' = 0$ and $s' = w = 0$, this is the set of equilibrium points.

Finally, consider the angular momentum $C(q, v)$. Recall that this is generally a rank-two tensor with components $C_{\alpha\beta}(q, v) = \sum m_i(q_{i\alpha}v_{i\beta} - q_{i\beta}v_{i\alpha})$. Setting $q_i = rs_i$ and $v_i = r^{-\frac{1}{2}}z_i = r^{-\frac{1}{2}}(\nu s_i + w_i)$ shows that $C_{\alpha\beta}(q, v) = \sqrt{r}C_{\alpha\beta}(s, w)$. For any collision orbit, $s(\tau), w(\tau)$ remain bounded as $\tau \rightarrow \infty$ and hence $|C_{\alpha\beta}(s(\tau), w(\tau))|$ is bounded. Since $\sqrt{r(\tau)} \rightarrow 0$, $C_{\alpha\beta}(q, v) \rightarrow 0$. But $C_{\alpha\beta}(q, v)$ is constant along solutions, so it must be 0, as required. QED

The restpoints of (70) are exactly the ones found already in connection with the homothetic orbits, namely $(r, s, \nu, w) = (0, s_0, \pm 2\sqrt{U(s_0)}, 0)$ where the normalized configuration satisfies $\tilde{\nabla}U(s_0) = 0$. In other words, s_0 is a normalized central configuration. Therefore Proposition 7.5 gives

Proposition 7.6. *Suppose $q(t)$ is a solution of the n -body problem for $t \in [0, t_0)$ which experiences a total collision at $t = t_0$ and let $\gamma(\tau) = (r(\tau), s(\tau), \nu(\tau), w(\tau))$ be the corresponding solution in McGehee coordinates. Then $s = q/\|q\|$ converges*

to the set of normalized central configurations with $U(s_0) = \frac{1}{2}\nu_0^2$, where $-\nu_0 = \lim \nu(\tau)$.

Finding the central configurations of the n -body problem for given masses m_i involves solving a set of complicated algebraic equations. Some of the known results about this will be given in the next section, but there are still many open problems.

Because of the change of timescale, the total collision solutions slow down as they approach $r = 0$ and converge asymptotically as $\tau \rightarrow \infty$. In the usual timescale, the collision occurs in finite time. Exercise 7.5 gives some details about the rate of approach to collision, which turns out to be the same as for the two-body and Kepler problems.

Exercise 7.4. Show that if q is a CC then the center of mass is at the origin and $\lambda = U(q)/\|q\|^2 > 0$. Moreover if q is a CC then so are all of the configurations obtained from q by scaling and rotation, that is, $\tilde{q} = kRq$ where $k > 0$ and $R \in \mathbf{SO}(d)$ (acting on each q_i as usual).

Exercise 7.5. Suppose $\gamma(\tau) = (r(\tau), s(\tau), \nu(\tau), w(\tau))$ is a solution of (70) which exists for $\tau \in [0, \infty)$ and as $r(\tau) \rightarrow 0$ as $\tau \rightarrow \infty$. Then, as shown in this section, $\nu(\tau) \rightarrow -\nu_0 < 0$. Also, recall that the timescales are related by $dt/d\tau = r^{\frac{3}{2}}$.

- i. Use this to show that $t(\tau)$ converges to a finite limit $t(\tau) \rightarrow t_0 < \infty$ as $\tau \rightarrow \infty$. Thus the collision happens in finite time in the usual timescale.
- ii. Also show that the collision happens with asymptotic rate $|t - t_0|^{\frac{2}{3}}$, that is, the ratio

$$\frac{r(\tau)}{|t(\tau) - t_0|^{\frac{2}{3}}}$$

converges to a finite, nonzero limit. Hint: Apply L'Hospital's rule to the ratio $r^{\frac{3}{2}}/|t - t_0|$.

Compare Exercise 1.5.

7.2. Central Configurations. Clearly, central configurations play an important role in the study of total collision. In this section, some specific examples of CCs will be analyzed.

Equation 75 has a simple, geometrical interpretation. Let $A_i = \frac{1}{m_i} \nabla_i U(q)$ be the acceleration vector of the i -th body produced by the gravitational attraction of the other bodies. The (75) gives

$$A_i = -\lambda q_i \quad i = 1, \dots, n.$$

Since $\lambda > 0$, this means that the all of the acceleration vectors are pointing at the origin (the center of mass) and that their sizes are proportional to the distance from the origin. Figure 34 illustrates this for the case of 8 equal masses. While it is clear from symmetry that the accelerations for the left-hand configuration will satisfy the required conditions, this is far from obvious for the right-hand configuration which was found numerically.

In addition to this intuitive interpretation, Equation 75 also has a variational interpretation which will be useful later.

Proposition 7.7. *A configuration $q \in \mathbb{R}^{dn} \setminus \Delta$ is a central configuration if and only if it is a constrained critical point of $U(q)$ with the constraint that $\mathcal{I}(q) = \|q\|^2$ be constant. This is true with or without fixing the center of mass at the origin.*

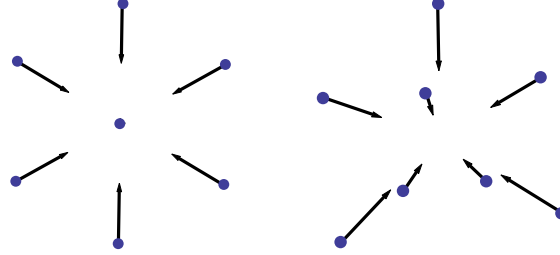


FIGURE 34. Two central configurations of 8 equal masses.

Proof. Suppose q_0 is a CC, that is, $\nabla U(q_0) + \lambda M q_0 = 0$ holds for some λ . Let $k = \mathcal{I}(q_0)$. The constraint $\mathcal{I}(q) = k_0$ defines an ellipsoid in \mathbb{R}^{dn} . Since $\mathcal{I}(q) = q^T M q$, the gradient is $\nabla \mathcal{I}(q) = 2Mq$ and (75) means that

$$\nabla U(q) + (\lambda/2) \nabla \mathcal{I}(q) = 0.$$

Interpreting $\lambda/2$ as a Lagrange multiplier, this is exactly the condition for a constrained critical point. As noted already, all of these critical points lie in the zero center of mass subspace X . Moreover, for $q_0 \in X$, it is easy to see that both of the gradient vectors are automatically tangent to X . This implies that adding the additional constraint $q \in X$ would make no difference. QED

In particular, the equation $\tilde{\nabla} U(s) = 0$ means that the normalized configuration s is a critical point of U restricted to the ellipsoid \mathcal{E} . Since the set of CCs is invariant under scaling, the choice of normalization is somewhat arbitrary. Another useful choice is to normalize so the the constant in (75) is $\lambda = 1$. The following result, whose proof is an exercise, gives a variational interpretation of these as well as another for unnormalized CCs.

Proposition 7.8. *A configuration $q \in \mathbb{R}^{dn} \setminus \Delta$ is a central configuration with $\lambda = U(q)/\|q\|^2 = 1$ if and only if it is an unconstrained critical point of $F(q) = U(q) + \mathcal{I}(q)$. Alternatively, q is a CC (with no particular normalization) if it is an unconstrained critical point of $G(q) = U(q)^2\|q\|^2 = U(q)^2\mathcal{I}(q)$.*

Note that $G(q)$ is homogeneous of degree 0, that is, $G(kq) = G(q)$. So if q is a critical point, so is kq for every $k > 0$.

Using these alternative characterizations of CCs, one can give some existence proofs for CCs and begin to work out some examples.

Proposition 7.9. *For every choice of masses in the n -body problem, at least one central configuration exists.*

Proof. Consider the restriction of the potential $U(s)$ to the ellipsoid \mathcal{E} . \mathcal{E} is a compact subset of \mathbb{R}^{dn} . The potential defines a smooth function $U : \mathcal{E} \setminus \Delta \rightarrow \mathbb{R}$ where Δ is the singular set. Since $U \rightarrow \infty$ on Δ , $U(s)$ must achieve its minimum at some point $s_0 \in \mathcal{E} \setminus \Delta$ and this will be a (normalized) CC. In a bit more detail, choose any point $s \in \mathcal{E} \setminus \Delta$ and let $K = U(s)$. The set $S_K = \{s \in \mathcal{E} : U(s) \leq 2K\}$ is compact and so U achieves its minimum at some point s_0 . Since the minimum is at most K , s_0 is not a boundary point of S_K so it must be a critical point and hence a CC. QED

Turning to examples, consider the two-body problem in \mathbb{R}^d . Using the coordinate $q = q_2 - q_1 \in \mathbb{R}^d$ to parametrize the center of mass zero subspace X , the mass norm becomes $\|q\|^2 = \mu|q|^2$ where $\mu = \frac{m_1 m_2}{m_1 + m_2}$ and $|q|$ is the Euclidean norm. In this case, the ellipsoid of normalized configurations is the Euclidean sphere $\mathcal{E} = \{s \in \mathbb{R}^d : |s|^2 = \mu^{-1}\}$. Furthermore the potential

$$U(s) = \frac{m_1 m_2}{|s|}$$

is constant on this sphere. Therefore every normalized configuration $s \in \mathcal{E}$ is a critical point of the restriction of U to \mathcal{E} , that is, $\tilde{\nabla}U(s) = 0$ for all s . It follows that every configuration $q \neq 0$ is a central configuration. In this case, all of the nonzero configurations are equivalent up to scaling and rotation – they are all just line segments of various sizes and orientations. It follows that, starting from any initial condition in X , one can find homothetic solutions as in Example 7.1.

Next consider the three-body problem in \mathbb{R}^d . A simple argument shows that it suffices to consider the planar case, $d = 2$. To see this note that the three bodies either form a triangle or else are all contained in a line. If the center of mass is at the origin, the configuration can always be rotated into the plane $\mathbb{R}^2 \times 0 \subset \mathbb{R}^d$. For such a configuration, the gradient $\nabla U(q)$ is also in \mathbb{R}^2 . It follows that the last $d - 2$ component of (75) are automatically zero and it suffices to check the first two. A similar argument shows that for the n -body problem, it suffices to consider the case $d = n - 1$. Indeed, this is the largest possible dimension for the subspace, call it $\mathcal{C}(q)$, spanned by the n bodies.

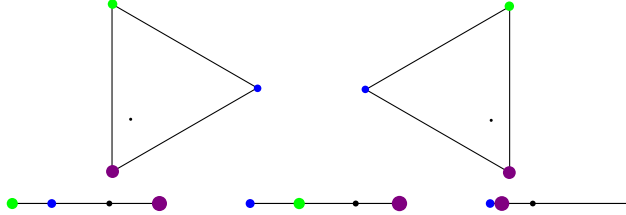


FIGURE 35. Central configurations of the planar three-body problem with masses $m_1 = 1$ (blue), $m_2 = 2$ (green), $m_3 = 5$ (purple). The small black dots show the center of mass.

It turns out that the study of CCs of the planar three-body problem is analogous to that of the Lagrange points of the PCR3BP. Namely, up to rotation and scaling there are exactly five CCs, three collinear and two equilateral triangles (see Figure 35). A nice way to handle the noncollinear case is to prove a more general result.

Proposition 7.10. *Consider the n -body problem with arbitrary masses $m_i > 0$. Then the only central configurations such that the subspace $\mathcal{C}(q)$ spanned the configuration has the maximum possible dimension $n - 1$ are the regular simplices (that is, all of the mutual distances r_{ij} are equal).*

So, for example, equilateral triangles are the unique noncollinear CCs of three bodies and regular tetrahedra are the unique nonplanar CCs of four bodies. It's

remarkable that these configurations are CCs for all choices of the masses, since the center of mass is not the geometric center of the configuration (see Figure 36).

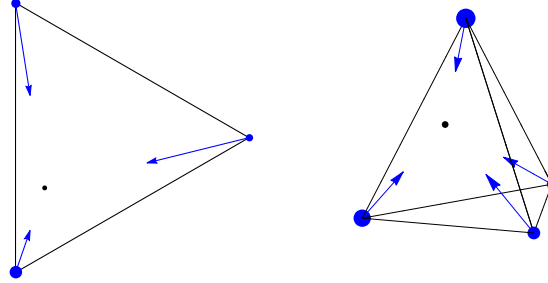


FIGURE 36. Regular simplex CCs with unequal masses – 3 bodies in \mathbb{R}^2 and 4 bodies in \mathbb{R}^3 .

Proof. The proof will use the characterization of the CCs with $\lambda = 1$ as critical points of $F(q) = U(q) + \mathcal{I}(q)$ from Proposition 7.8. Assume without loss of generality that the configuration lies in \mathbb{R}^d with $d = n - 1$. The key to this proof is the introduction of *mutual distance coordinates*, $r_{ij} = |q_i - q_j|$, $1 \leq i < j \leq n$. Note that the function F can be expressed as a function of the r_{ij} :

$$F = \sum_{i < j} \frac{m_i m_j}{r_{ij}} + \frac{1}{m} \sum m_i m_j r_{ij}^2.$$

The claim is that q is a CC of maximal dimension (that is, $\mathcal{C}(q) = \mathbb{R}^{n-1}$) if and only if all of the partial derivatives

$$\frac{\partial F}{\partial r_{ij}} = m_i m_j \left(-\frac{1}{r_{ij}^2} + 2r_{ij} \right) = 0.$$

This would mean that all of the mutual distances are equal to $2^{-\frac{1}{3}}$ as required.

First of all, if all of these partial derivatives are zero, then q must be a critical point of F because for each $k = 1, \dots, n$ the chain rule shows that

$$\frac{\partial F}{\partial q_k} = \sum_{i < j} \frac{\partial F}{\partial r_{ij}} \frac{\partial r_{ij}}{\partial q_k} = 0.$$

This part does not use the assumption that q_0 has maximal dimension. For the converse, assume that q is a critical point and also has maximal dimension. It will be shown that given any pair of indices (i, j) with $1 \leq i < j \leq n$, it is possible to vary r_{ij} while keeping all of the other r_{kl} constant to produce a smooth curve of configurations $q(r_{ij})$. Then the chain rule will give

$$\frac{\partial F}{\partial r_{ij}} = \nabla F(q) \cdot \frac{dq(r_{ij})}{dr_{ij}} = 0.$$

Before going into the proof, note that for $n = 3$, the claim amounts to the elementary assertion that if q describes a noncollinear triangle, it is possible to

smoothly vary one of the three sides while holding the others fixed. Similarly, the fact that one can vary one edge of a (nonplanar) tetrahedron without changing the other edges is intuitively obvious. Exercise 7.7 shows that this is not possible without the assumption that the configuration has maximal dimension.

To prove the analogous statement for n bodies in \mathbb{R}^{n-1} , suppose $q = (q_1, \dots, q_n) \in \mathbb{R}^{n(n-1)} \setminus \Delta$ is a configuration with maximal dimension $n-1$. Using rotational and translational symmetry, one may assume that $q_i \in \mathbb{R}^{n-1} \times 0$ for $i = 1, \dots, n-1$. The last point q_n lies in the intersection of $n-1$ spheres $S_i = \{x \in \mathbb{R}^{n-1} : |x - q_i| = r_{in}\}$, $i = 1, \dots, n-1$. The unit normal vectors of these spheres at q_n are the vectors $(q_n - q_i)/r_{in}$ and by the assumption that q has maximal dimension, these $n-1$ vectors are linearly independent. Now consider the intersection of the last $n-2$ of these spheres S_i , $i = 2, \dots, n-1$. The linear independence of the normal vectors and the implicit function theorem shows that the intersection is a smooth curve through q_n . Moving q_n along this curve, all of the mutual distances are constant, except r_{1n} . Since the sphere S_n meets the curve transversely, r_{1n} can be used as a smooth parameter along the curve. Permuting the indices shows that any one of the r_{ij} could be varied holding the others constant. QED

Turning now to the collinear CCs of the three-body problem, first discovered by Euler in 1767 [10],

Proposition 7.11. *Up to rotation and scaling, there is a unique collinear central configuration of the three-body problem for each ordering of the bodies along the line.*

Proof. Assume without loss of generality that the configuration is in \mathbb{R}^1 . The normalized configuration space

$$\mathcal{E} = \{q \in \mathbb{R}^3 : m_1 q_1 + m_2 q_2 + m_3 q_3 = 0, m_1 q_1^2 + m_2 q_2^2 + m_3 q_3^2 = 1\}$$

is the curve of intersection of a plane and an ellipsoid. The collision set consist of three planes:

$$\Delta = \{q_1 = q_2\} \cup \{q_1 = q_3\} \cup \{q_2 = q_3\}$$

which divide the curve into 6 arcs corresponding to the different orderings of the three masses along the line (see figure 37). Since $U \rightarrow \infty$ at these points, there must be at least one critical point in each of the arcs. To see that there is only one requires more work.

The three mutual distances provide convenient coordinates, but as Exercise 7.7 shows, they are not independent. Instead they are subject them to a collinearity constraint. If we fix the ordering of the bodies to be $q_1 < q_2 < q_3$ then the constraint is $r_{12} + r_{23} - r_{13} = 0$. Looking for critical points of the homogeneous function $G = U(r_{ij})^2 I(r_{ij})$ with this constraint and then normalizing by setting $r_{12} = 1, r_{13} = 1 + r, r_{23} = r$ gives a fifth-degree polynomial equation for r :

$$(76) \quad \begin{aligned} & (m_1 + m_2)r^5 + (3m_1 + 2m_2)r^4 + (3m_1 + m_2)r^3 \\ & - (m_2 + 3m_3)r^2 - (2m_2 + 3m_3)r - (m_2 + m_3) = 0. \end{aligned}$$

Fortunately there is a single sign change so Descartes' rule of signs implies there is a unique positive real root. All of this is very similar to what happened for the PCR3BP. Of course there is no simple formula for how this root changes as a function of the masses. QED

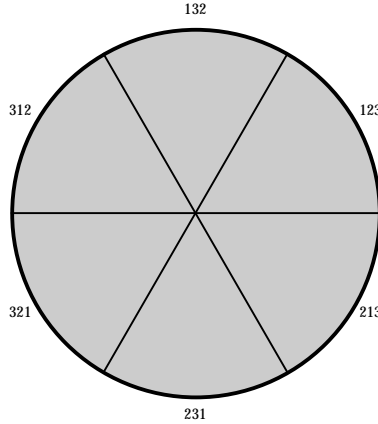


FIGURE 37. Normalized configuration space for the collinear three-body problem consists of 6 arcs of an ellipse. Here the shaded plane represents configurations with fixed center of mass, the three lines represent the collisions and the boundary circle represents fixing $\|q\|$.

Euler's example illustrates the complexity of the CC equation. Even in the simplest nontrivial case, finding CC's for given masses involves solving complicated polynomial equations. Figure 38 shows the beautiful surface defined by Euler's quintic when one of the masses is normalized to 1. The surface lies over the mass parameter space in a complicated way making the uniqueness result for fixed positive masses all the more remarkable.

Using rotations in the plane, one can flip over the collinear configurations. So, for example, the orderings 123 and 321 are the same up to rotations in the plane. Counting this way there will be three distinct collinear CCs for each choice of the masses. There are two distinct equilateral triangles distinguished the cyclic order of the three bodies around the triangle. While these could be flipped over using rotations in \mathbb{R}^3 , they should be viewed as distinct for the planar three-body problem as in Figure 35.

It turns out that Proposition 7.11 can be generalized to the collinear n -body problem, a result of F.R. Moulton [20].

Proposition 7.12. *Given masses $m_i > 0$, there is a unique normalized collinear central configuration for each ordering of the masses along the line.*

Before moving on to the proof of Moulton's theorem consider the geometry of the next case, $n = 4$. This time the set of normalized configurations

$$\mathcal{E} = \{q \in \mathbb{R}^4 : m_1 q_1 + \dots + m_4 q_4 = 0, m_1 q_1^2 + \dots + m_4 q_4^2 = 1\}$$

is the intersection of a hyperplane and an ellipsoid in \mathbb{R}^4 . So it is a two-dimensional surface diffeomorphic to \mathbb{S}^2 . There are six collision planes which divide the sphere into $4! = 24$ triangles. Figure 39 shows the how the collision planes divide the sphere.

Proof of Moulton's theorem. The collision set Δ divides the ellipsoid \mathcal{E} of normalized centered configurations into $n!$ components, one for each ordering of the bodies

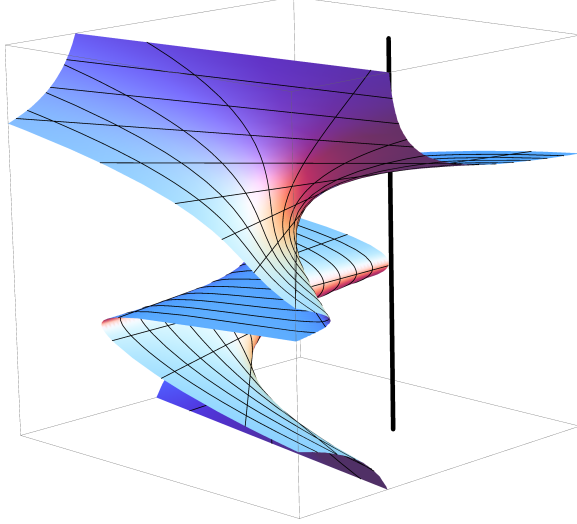


FIGURE 38. Surface defined by Euler's quintic equations in the product space of masses and configurations. After normalizing $m_3 = 1$, there are two mass parameters (horizontal) and one configuration variable r (vertical). Fixing the masses means looking for intersections of the surface with a vertical fiber, here a line segment. For positive masses, the segment cuts the surface just once but nonpositive masses can give several roots.

along the line. Let \mathcal{V} denote any one of these components. \mathcal{V} is an open set whose boundary is contained in Δ . The Newtonian potential gives a smooth function $U|_{\mathcal{V}} : \mathcal{V} \rightarrow \mathbb{R}$ and $U(q) \rightarrow \infty$ as $x \rightarrow \partial\mathcal{V}$. Hence $U|_{\mathcal{V}}$ attains its minimum at some $q_0 \in \mathcal{V}$ and q_0 is a CC with the given ordering of the bodies along the line.

Instead of working on the normalized space where $I(x) = 1$ the uniqueness proof will use the function $F(q) = U(q) + I(q)$ on the cone $\tilde{\mathcal{V}}$ of all rays through the origin passing through \mathcal{V} (in figure 37 this would be an infinite triangular wedge based on one of the six arcs). Let $x, y \in \tilde{\mathcal{V}}$ and consider a line segment $p(t) = (1-t)x + ty, 0 \leq t \leq 1$. Note that since the ordering is fixed, the sign of $p_i(t) - p_j(t) = (1-t)(x_i - x_j) + t(y_i - y_j)$ is equal to the common sign of $x_i - x_j$ and $y_i - y_j$. It follows that $p(t) \in \tilde{\mathcal{V}}$ for all t and so $\tilde{\mathcal{V}}$ is a convex set. It will be shown that if $x \neq y$ then $F(p(t))$ has a strictly positive second derivative. It follows that x, y cannot both be critical points of $F(x)$.

First consider $F(r_{ij})$ as a function of the mutual distances r_{ij} on $(\mathbb{R}^+)^{\frac{n(n-1)}{2}}$. The second partial derivative is

$$\frac{\partial^2 F}{\partial r_{ij}^2} = \frac{2m_i m_j}{r_{ij}^3} + \frac{2m_i m_j}{m} > 0.$$

Now since the configurations x, y are collinear, the mutual distances reduce to $r_{ij}(t) = |p_i(t) - p_j(t)|$ and as the ordering is constant along the segment, this is a

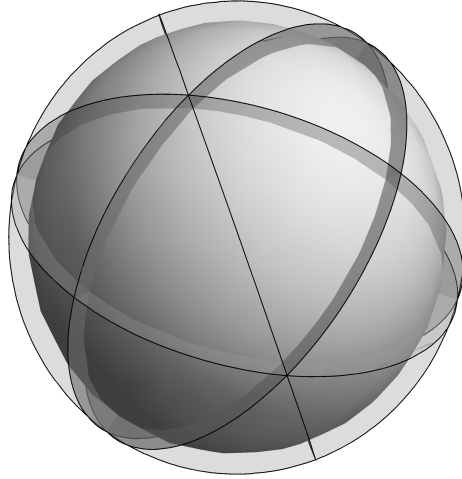


FIGURE 39. Normalized configuration space for the collinear four-body problem. The collision planes divide the sphere into triangles representing the possible orderings of the bodies.

linear function of t . It follows that $F(p(t))''$ is a sum of terms

$$\frac{\partial^2 F}{\partial r_{ij}^2}(p(t)) (r'_{ij}(t))^2.$$

These terms are all nonnegative and at least one is positive if $x \neq y$. QED

Exercise 7.6. Prove Proposition ??.

Exercise 7.7. Suppose $q = (q_1, q_2, q_3) \in \mathbb{R}^6$ is a configuration of three bodies in the plane which happens to be collinear, say $q_i = (x_i, 0)$. Prove that, in contrast to the noncollinear case, it is not possible to find a smooth curve $q(r_{ij})$ with all of the other distances r_{kl} held constant. Hint: You can move r_{12} , say, without changing r_{13}, r_{23} but the resulting curve cannot be parametrized as a smooth curve $q(r_{12})$.

Exercise 7.8. Redo the proof of Euler's Proposition 7.11 using the idea of the proof of Proposition 7.12.

Exercise 7.9. Use symmetry to prove the a regular n -gon is a central configuration of n equal masses. Similarly, show that a regular n -gon of n equal masses with another mass of possibly different size at the origin, is a central configuration of $n+1$ masses. Hint: Rotate so that one of the bodies, say q_1 , is on the x -axis and show that $\nabla_1 U(q)$ points along the x -axis. Then use rotational symmetry.

7.3. Homographic Solutions and Relative Equilibria. Central configurations first came up in Section 7.1 in connection with the homothetic solutions. Proposition 7.4 shows that every CC q gives rise to a homothetic solution $q(t) = r(t)q$ where $r(t)$ is any solution of the collinear Kepler problem. If $q = (q_1, \dots, q_n)$, $q_i \in \mathbb{R}^2$ is a *planar CC* then it also gives rise to a family of so-called *homographic*

solutions. These are constructed from the solutions of the planar Kepler problem, that is, the familiar ellipses, hyperbolas and parabolas.

It's convenient to express the planar Kepler problem using complex coordinates. Write the position as a complex number $z(t) = r(t) \exp(i\theta(t)) \in \mathbb{C}$. Then the differential equation is

$$(77) \quad \ddot{z}(t) = -\frac{\lambda z}{r(t)^3}$$

and the energy equation is $\frac{1}{2}(r^2 + r^2\dot{\theta}^2) - \frac{\lambda}{r} = h$.

Based on this, one can construct analogous solutions of the n -body problem. Starting from some initial configuration, each of the n bodies will move on its own conic section as in Figure 40. The shape of the configuration will remain the same; only the size and the rotation angle of the configuration will change. As was the case for the homothetic solution, this is only possible if the initial configuration is a central configuration.

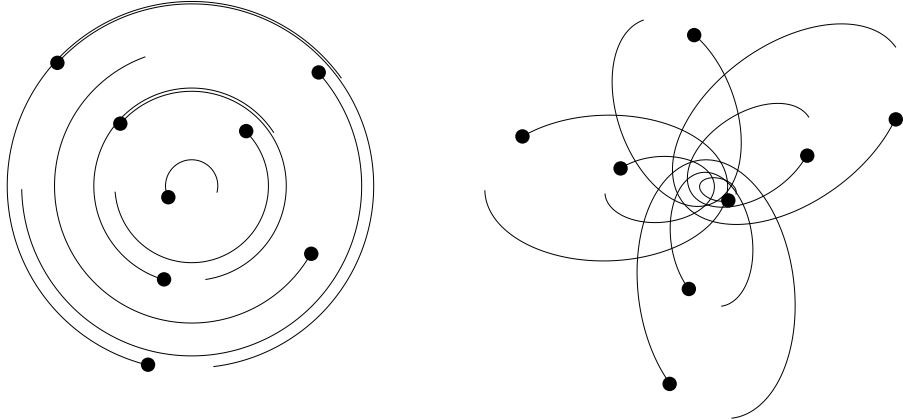


FIGURE 40. Two homographic solutions based on the CC of 8 equal mass of Figure 34 (right). In the left solution, the bodies move on circular orbits of the Kepler problem (this is a relative equilibrium solution). On the right, they move on similar ellipses.

Proposition 7.13. *Let $q_0 \in \mathbb{R}^{2n}$ be a planar configuration of n bodies in \mathbb{R}^2 . Then $q(t) = z(t)q_0$, $z(t) \in \mathbb{C}$ is a solution of the n -body problem if and only if q_0 satisfies the CC equation (75) with constant λ and $z(t)$ is a solution of the planar Kepler problem (77). Here $q_0 = (q_1, \dots, q_n)$ is regarded as a complex vector with $q_i \in \mathbb{C}$.*

Proof. Let $q(t) = z(t)q_0$. Then $q(t)$ solves Newton's equation if and only if

$$M\ddot{z}(t)q_0 = \nabla U(z(t)q_0) = z(t)r(t)^{-3}\nabla U(q_0)$$

where both the homogeneity and the rotation invariance of the potential have been used. Writing this as $(r(t)^3\ddot{z}(t)/z(t))Mq_0 = \nabla U(q_0)$, the right-hand side is a constant vector so the left-hand side must also be constant. Writing $(r(t)^3\ddot{z}(t)/z(t)) = -\lambda$ for some λ gives both equations (77) and (75). QED

There are two notable special cases of homographic solutions. The planar Kepler problem with zero angular momentum gives rise to solutions $z(t) = r(t) \exp(i\theta_0)$ moving along a ray of constant angle θ_0 . The resulting homographic solution is one of the homothetic, total collision solutions. On the other hand, one could choose a circular solution $z(t) = r_0 \exp(i\omega t)$ with constant radius r_0 as in Figure 40 (left). In a uniformly rotating coordinate system, this would appear as an equilibrium points, so it is a *relative equilibrium (RE)* solution, similar to those of the PCR3BP. The stability of these RE will be discussed later.

The starting point for the homographic solutions is a planar CC. What about nonplanar central configurations such as the regular tetrahedron in Figure 36? While it is not possible to find homographic motions of the tetrahedron in \mathbb{R}^3 , it turns out that it is possible in \mathbb{R}^4 . It's also possible to find homographic motions in \mathbb{R}^4 starting from a four-dimensional CC. Three-dimensional CCs can be seen as special cases of four-dimensional ones.

Proposition 7.14. *Let $q_0 \in \mathbb{R}^{4n}$ be a CC of n bodies in \mathbb{R}^4 which satisfies the CC equation (75) with constant λ . Let $J \in \mathbf{so}(4)$ be any antisymmetric 4×4 matrix with $J^2 = -\mathbf{Id}$. Finally, let $z(t) = r(t) \exp(\theta(t))$ be any solution of the planar Kepler problem (77). Then*

$$q(t) = r(t) \exp(\theta(t)J) q_0$$

is a homographic solution of the n -body problem in \mathbb{R}^4 . Here $\exp(\theta(t)J) \in \mathbf{SO}(4)$ is the matrix exponential.

Proof. The left-hand side of Newton's equation is

$$\begin{aligned} M\ddot{q} &= M(\ddot{r} + r\dot{\theta}^2 J^2) \exp(\theta J) q_0 + (r\ddot{\theta} + 2r\dot{\theta}\dot{r}) M \exp(\theta J) J q_0 \\ &= (\ddot{r} - r\dot{\theta}^2) \exp(\theta J) M q_0 + (r\ddot{\theta} + 2r\dot{\theta}\dot{r}) \exp(\theta J) J M q_0 \end{aligned}$$

where since the matrices J and $\exp(\theta(t)J)$ act on each body separately, they commute with the mass matrix M . On the other hand, the homogeneity and rotation invariance of the potential and the CC equation imply that the right-hand side is

$$\nabla U(r \exp(\theta J) q_0) = r^{-2} \exp(\theta J) \nabla U(q_0) = -\lambda r^{-2} \exp(\theta J) M q_0.$$

Comparing the two sides of the equation, one sees that q will be a solutions provided

$$\ddot{r} - r\dot{\theta}^2 = -\frac{\lambda}{r^2} \quad r\ddot{\theta} + 2r\dot{\theta}\dot{r} = 0.$$

But this is just the planar Kepler problem in polar coordinates. QED

Using the series formula for the matrix exponential shows $\exp(\theta J) = \cos \theta \mathbf{Id} + \sin \theta J$ so the i -th body of the homographic solution moves in the plane spanned by q_i, Jq_i according to

$$q_i(t) = r(t) \cos \theta(t) q_i + r(t) \sin \theta(t) J q_i$$

where the CC is $q_0 = (q_1, \dots, q_n)$, $q_i \in \mathbb{R}^4$. Thus each body is moving on its own Keplerian ellipse, parabola or hyperbola, but these conic sections lie in different planes in \mathbb{R}^4 . Figure 41 shows a 3D projection of a 4D homographic motion of the regular tetrahedron CC. In fact, it's a RE solution obtained by choosing a circular solution of the Kepler problem. Each body is rotating uniformly in some plane in \mathbb{R}^4 .

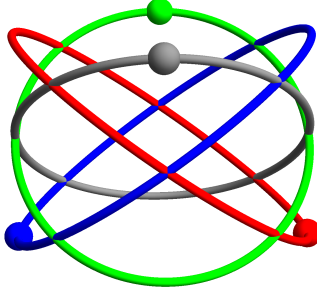


FIGURE 41. Three-dimensional projection of a relative equilibrium motion in \mathbb{R}^4 . The configuration is the regular tetrahedron with four equal masses. As the tetrahedron rotates in \mathbb{R}^4 , each body sweeps out a circle in its own plane. In the projection, these appear as ellipses.

It turns out that it's possible to find RE solutions (but not more general homographic ones) starting from certain configurations which are not CCs. For example, this is possible for any isosceles triangle in the three-body problem with two equal masses, say $m_1 = m_2$. Recall that this is not a CC unless it is equilateral. For this, one needs a rotation in \mathbb{R}^4 which rotates two orthogonal planes at two different angular velocities ω_1, ω_2 . See Exercise 7.11. In order to find these generalized RE, the initial shape has to be a so-called *balanced configuration* [2, 16].

Exercise 7.10. Suppose $q(t) = r_0 \exp(i\omega t)q_0$ is a RE solution of the n body problem based on a CC q_0 . Suppose q_0 solves the CC equation (75) with a certain constant λ . Find formulas for the energy h , angular momentum C and period T of the periodic solution $q(t)$.

Exercise 7.11. Consider the 3BP with masses $m_1 = m_2$ and a possibly different mass m_3 . Let $q_0 = (q_1, q_2, q_3)$ be an isosceles triangle configuration in \mathbb{R}^4 with $q_1 = (-x, 0, z, 0)$, $q_2 = (x, 0, z, 0)$ and $q_3 = (0, 0, z_3, 0)$ where $(m_1 + m_2)z + m_3 z_3 = 0$. Show that there is a block-diagonal 4×4 rotation matrix $R(t) = \text{diag}(\begin{bmatrix} \cos \omega_1 t & -\sin \omega_1 t \\ \sin \omega_1 t & \cos \omega_1 t \end{bmatrix}, \begin{bmatrix} \cos \omega_2 t & -\sin \omega_2 t \\ \sin \omega_2 t & \cos \omega_2 t \end{bmatrix})$ such that $q(t) = R(t)q_0$ solves the 3BP in \mathbb{R}^4 .

7.4. Restpoints on the Collision Manifold. Using McGehee coordinates, solutions which experience a total collision at some finite time are transformed into solutions converging to the set of restpoints on the collision manifold. These are the points (r, s, ν, w) with

$$r = w = 0 \quad s = \text{normalized CC} \quad \nu = \pm \sqrt{U(s)}$$

where the negative value for ν corresponds to collisions in forward time and the positive sign to collisions in backward time. In this section, the eigenvalues of the restpoints will be studied. Typically, the restpoints are hyperbolic except for the inevitable presence of zero eigenvalues due to rotational symmetry. In this case, it will be shown that the collision solutions converge to just one restpoint, rather than just to the set of restpoints.

Consider the linearized differential equations of (70) at an equilibrium point $(0, s_0, \nu_0, 0)$, $\nu_0 = \pm\sqrt{2U(s_0)}$:

$$(78) \quad \begin{bmatrix} \delta r' \\ \delta \nu' \\ \delta s' \\ \delta w' \end{bmatrix} = \begin{bmatrix} \nu_0 & 0 & 0 & 0 \\ 0 & \nu_0 & -\nabla U(s_0) & 0 \\ 0 & 0 & 0 & I \\ 0 & 0 & D\tilde{\nabla}U(s_0) & -\frac{1}{2}\nu_0 I \end{bmatrix} \begin{bmatrix} \delta r \\ \delta \nu \\ \delta s \\ \delta w \end{bmatrix}$$

where I denotes the $dn \times dn$ identity matrix. Recall that s, w are not indendent variables in \mathbb{R}^{dn} but rather, they are subjected to the constraints $\|s\|^2 = s^T M s = 1$, $\langle\langle s, w \rangle\rangle = s^T M w = 0$ as well as the center of mass constraints. If the energy is fixed, the variables also satify (72). Since these equations define invariant sets for (70), differentiation gives the following invariant subspace S for the linearized ODE (78)

$$(79) \quad \begin{aligned} \langle\langle s_0, \delta s \rangle\rangle &= \langle\langle s_0, \delta w \rangle\rangle = 0 & \nu_0 \delta \nu &= h \delta r \\ m_1 \delta s_1 + \dots + m_n \delta s_n &= m_1 \delta w_1 + \dots + m_n \delta w_n = 0. \end{aligned}$$

Note that in the derivative of the energy equation, the term $\nabla U(s_0) \cdot \delta s$ has been dropped since at a CC, $\nabla U(s_0) = U(s)Ms_0$ and therefore $\nabla U(s_0) \cdot \delta s = \langle\langle s_0, \delta s \rangle\rangle = 0$. For a similar reason, the entry $\nabla U(s_0)$ in (78) can be dropped when working on S .

The invariant subspace S has dimension $2 + 2dn - 2n - 3 = 2d(n - 1) - 1$, the same as the energy manifolds. Let A be the matrix of the linearized ODE. The goal is to find the eigenvalues and eigenvectors of A . First note that the $(\delta r, \delta \nu)$ plane consists of eigenvectors with eigenvalue $\lambda = \nu_0$, but only the line spanned by $(\delta r, \delta \nu) = (h, \nu_0)$ lies in S . The rest of the eigenvectors will lie be of the form $(0, 0, \delta s, \sigma w)$. The following lemma relates these to the eigenvectors of $D\tilde{\nabla}U(s_0)$.

Lemma 7.1. *Let δs be an eigenvector of the second derivative matrix $D\tilde{\nabla}U(s_0)$ with eigenvalue α . Then $(\delta r, \delta \nu, \delta s, \delta w) = (0, 0, \delta s, \lambda_{\pm} \delta s)$ are two eigenvectors of A with eigenvalues*

$$\lambda_{\pm} = \frac{-\nu_0 \pm \sqrt{\nu_0^2 + 16\alpha}}{4}.$$

Note that $D\tilde{\nabla}U(s_0) = M^{-1}(D\nabla U(s_0) + M)$. The second derivative matrix $D\nabla U(s_0)$ and the mass matrix M are symmetric and it follows that $D\tilde{\nabla}U(s_0)$ is symmetric with respect to the mass inner product. That is $\langle\langle v, D\tilde{\nabla}U(s_0)w \rangle\rangle = \langle\langle D\tilde{\nabla}U(s_0)v, w \rangle\rangle$. Just as for ordinary symmetric matrices, it follows that all of the eigenvalues α are real and, moreover, $D\tilde{\nabla}U(s_0)$ has a basis of eigenvectors (see Exercise 7.13). So $D\tilde{\nabla}U(s_0)$ has $d(n - 1) - 1$ eigenvectors with zero center of mass and $\langle\langle s_0, \delta s \rangle\rangle = 0$ and then the lemma provides $2d(n - 1) - 2$ eigenvectors of A in S . Together with the eigenvector $(\delta r, \delta \nu, \delta s, \delta w) = (h, \nu_0, 0, 0)$ with $\lambda = \nu_0$, this accounts for all of the eigenvectors of A in S .

Due to the rotational symmetry of the potential, it is inevitable that some of eigenvalues of $D\tilde{\nabla}U(s_0)$ are $\alpha = 0$. By the lemma, the two corresponding eigenvalues of A are $\lambda_{\pm} = 0, \nu_0/2$. This means that the restpoints on the collision manifold are degenerate. It is easy to check that if $\alpha \neq 0$ then the eigenvalues $\lambda_{\pm} \neq 0$ and, in fact, λ_{\pm} always have nonzero real parts. So except for the zero eigenvalues, the restpoints on the collision manifold are hyperbolic.

For CCs of the n -body problem in \mathbb{R}^d there can be as many as $(d - 1)(d - 2)/2$ zero eigenvalues arising from rotational symmery. To see this, recall that $d(d - 1)/2$

is the dimension of the rotation group $\mathbf{SO}(d)$. If s_0 is a normalized CC and a is any anti-symmetric matrix then the curve of configurations $s(t) = \exp(ta)s_0$ consists entirely of normalized CCs (where the rotation acts on each component of $s_0 = (s_1, \dots, s_n)$). Thus $U(s(t)) = U(s_0)$ is constant and $\tilde{\nabla}U(s(t)) = 0$. Therefore

$$\frac{d}{dt}|_{t=0}\tilde{\nabla}U(s(t)) = D\tilde{\nabla}U(s_0)as_0 = 0$$

which shows that the vector $\delta s = (a\delta s_1, \dots, a\delta s_n)$ is in the kernel of $D\tilde{\nabla}U(s_0)$ and $(\delta r, \delta\nu, \delta s, \delta w) = (0, 0, \delta s, 0)$ is in the kernel of A . There are $d(d-1)/2$ linearly independent choices for the antisymmetric matrix a . If the vectors as_0 are also linearly independent, $d(d-1)/2$ is the dimension of the kernels.

For example, consider the planar n -body problem ($d = 2$, $n \geq 2$). The rotation group $\mathbf{SO}(2)$ has dimension $d(d-1)/2 = 1$, $a = \begin{bmatrix} 0 & -1 \\ 1 & 0 \end{bmatrix}$ is a nonzero antisymmetric matrix and $as_0 = (as_1, \dots, as_n) \neq 0$ for every $s_0 \neq 0$. So the kernels of $D\tilde{\nabla}U(s_0)$ and A always have dimension at least one. For the spatial problem ($d = 3$, $n \geq 2$) $\mathbf{SO}(3)$ has dimension $d(d-1)/2 = 3$. As long as s_0 is not a collinear configuration, the dimensions of the kernels of $D\tilde{\nabla}U(s_0)$ and A are indeed 3, but if s_0 is collinear, this drops to 2 because rotation around the line of the bodies fixes s_0 .

Definition 7.2. *A normalized central configuration is called nondegenerate if the dimension of the kernel of $D\tilde{\nabla}U(s_0)$ (and of A) is the minimum permitted by rotational symmetry.*

Let s_0 be a nondegenerate, normalized CC. Because of the action of the rotation group, s_0 is part of a compact manifold of normalized CCs obtained by rotating s_0 in all possible ways. This is called the *rotation group orbit* of s_0

$$\text{Orb}(s_0) = \{Rs_0 : R \in \mathbf{SO}(d)\}.$$

Similarly, the equilibrium points $p = (r, s, \nu, w) = (0, s_0, \pm\sqrt{U(s_0)}, 0)$ are part of compact manifolds of equilibrium points $\text{Orb}(p)$. An equivalent definition of nondegeneracy is that the dimension of the kernel of $D\tilde{\nabla}U(s_0)$ is the same as the dimension of the manifold $\text{Orb}(s_0)$. Using this, one can show

Proposition 7.15. *Suppose s_0 is a nondegenerate CC. Then the rotation group orbit $\text{Orb}(s_0)$ is an isolated within the set of normalized CCs (that is, some neighborhood of $\text{Orb}(s_0)$ contains no other equilibria). If a restpoint $p = (r, s, \nu, w) = (0, s_0, -\sqrt{U(s_0)}, 0)$ is in the omega limit set $\omega(\gamma)$ of some total collision solution, γ , then $\omega(\gamma) = \{p\}$. In other words, $\gamma(\tau)$ converges to one restpoint rather than just to the set of restpoints.*

This rules out the possibility of *infinite spin* for total collision orbits converging to nondegenerate CCs.

Proof. The rotation group orbit of p is a manifold of restpoints. The tangent space to the orbit is an eigenspace of the linearized ODE with eigenvalue $\lambda = 0$, but all of the other eigenvalues have nonzero real parts, so for the linearized flow, they are either attracting or repelling. The rest of the proposition follows from some general facts from dynamical systems theory.

For an ODE in \mathbb{R}^n , suppose p is part of a compact manifold \mathcal{M} of restpoints of dimension k and suppose that all of these restpoints have $n - k$ eigenvalues with

nonzero real parts. Furthermore suppose that of these $m - k$ eigenvalues l have $\text{Re}(\lambda) < 0$ and m have $\text{Re}(\lambda) > 0$. Let $W^s(\mathcal{M})$, $W_u(\mathcal{M})$ be the local stable and unstable sets of the manifold \mathcal{M} , that is, the sets of initial conditions near \mathcal{M} whose orbits converge to \mathcal{M} in forward and backward time, respectively. Then it can be shown that $W^s(\mathcal{M})$ has dimension $k + l$, each point $p \in \mathcal{M}$ has its own stable manifold of dimension l and that $W^s(\mathcal{M}) = \cup_{p \in \mathcal{M}} W^s(p)$. A similar result holds for the unstable manifolds. In other words, instead of just converging to \mathcal{M} , solutions in $W^s(\mathcal{M})$ converge to just one point of \mathcal{M} . One says that the convergence happens with a well-defined *asymptotic phase*. This is basically a variation on the usual stable manifold theorems for hyperbolic restpoints or hyperbolic periodic orbits. Clearly this is just what is needed to get the proposition. QED

Exercise 7.12. Prove Lemma 7.1. Hint: Eigenvectors and eigenvalues satisfy $\delta w = \lambda \delta s$ and $D\tilde{\nabla}U(s_0)\delta s - \frac{1}{2}\nu_0\delta w = \lambda\delta w$.

Exercise 7.13. Let S be a real $k \times k$ matrix which is symmetric with respect to some inner product on \mathbb{R}^k , that is, $\langle\langle v, Sw \rangle\rangle = \langle\langle Sv, w \rangle\rangle$. Show that all of the eigenvalues of S are real, that the eigenvectors corresponding to distinct eigenvalues are orthogonal (with respect to the mass inner product) and that S is diagonalizable. Hint: recall the proof for ordinary symmetric matrices.

Exercise 7.14. Here is a simple example of convergence with asymptotic phase. Consider an ODE in \mathbb{R}^2 of the form $\dot{x} = f(x, y)y$, $\dot{y} = -y$ where $f(x, y)$ is a bounded, smooth function. Show that the x axis $\mathbb{R} \times 0$ consists entirely of equilibrium points, that $W^s(\mathbb{R} \times 0)$ is the whole plane and that every solution actually converges to a unique restpoint $(x_0, 0) \in \mathbb{R} \times 0$. Hint: for the last part, show that the improper integral $\int_0^\infty \dot{x}(t) dt$ is convergent.

7.5. Total Collision for $n = 2$. The last few sections provide a lot of theoretical results about total collisions and restpoints on the collision manifold. The simplest example is the planar two-body problem. Parametrizing the center of mass subspace by $q = q_2 - q_1 \in \mathbb{R}^2$, the mass metric becomes

$$\|q\|^2 = \mu|q|^2 \quad \mu = \frac{m_1 m_2}{m_1 + m_2}$$

where $|q|$ is the Euclidean norm. The size of the configuration is $r = |q|/\sqrt{\mu}$ and the normalized configuration $s = s_2 - s_1$ lies on the circle $|s| = \mu^{-1/2}$ which represents the ellipsoid \mathcal{E} . The potential on this ellipsoid is $U(s) = m_1 m_2/|s| = m_1 m_2 \sqrt{\mu}$ which will be called U_0 . Since the ellipsoid \mathcal{E} is a circle, it can be parametrized by an angle, θ . The tangential velocity w can be replaced by $\theta' = \omega$. Using these variables, the McGeehee equations (70) become

$$(80) \quad \begin{aligned} r' &= \nu r \\ \nu' &= \frac{1}{2}\nu^2 + \omega^2 - U_0 \\ \theta' &= \omega \\ \omega' &= -\frac{1}{2}\nu\omega. \end{aligned}$$

The energy and angular momentum equations are

$$\frac{1}{2}\nu^2 + \frac{1}{2}\omega^2 - U_0 = rh \quad C = \sqrt{r}\omega.$$

Even though this is the simplest case, it is still an ODE in \mathbb{R}^4 with a 3D energy manifold. A convenient way to reduce the dimension is to quotient by the rotational symmetry. In this case, this amounts to just ignoring the angular variable θ and considering the other three ODEs in (r, ν, ω) -space. The energy equation defines 2D surfaces which are paraboloids for $h \neq 0$ and a cylinder for $h = 0$. Figure 42 shows the parts of these surfaces in the physically relevant region $r \geq 0$. All of the energy surfaces intersect along the collision manifold, a circle in the plane $r = 0$, which forms their common boundary. The figure also shows the level curve of

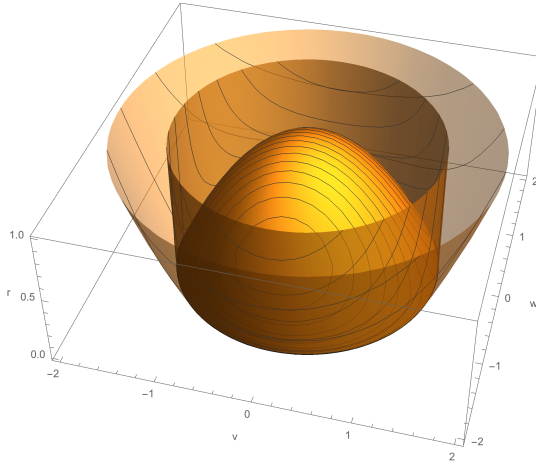


FIGURE 42. Energy surfaces for the two-body problem in blown-up coordinates with rotational symmetry quotiented out. One surface is shown for each of the cases $h > 0, h = 0, h < 0$. The contours show curves of constant angular momentum.

the angular momentum. Since this is a constant of motion, these level curves are exactly the orbits of the equations (80). In other words, these are the familiar orbits of the Kepler problem (ellipses, parabolas and hyperbolas) as viewed in blown-up coordinates.

Figure 43 shows the flow in more detail for the negative energy case, including the flow on the collision manifold itself. Recall that the solutions for fixed energy are a family of ellipses, all with the same major semiaxes and periods as in Figure 8. It's interesting to see how these appear in the figure. There are two circular orbits with the given energy, one clockwise and one counterclockwise. Since the angle has been quotiented out, these appear as two restpoints on the paraboloid, one in front and one in back. Similarly, there are two families of elliptical orbits with eccentricities $0 < e < 1$ filling out the front and back of the surface. As $e \rightarrow 1$ these converge to the collinear, collision solution moving in and out along a line segment and beginning and ending at total collision. This is an example of a homothetic orbit as in Proposition 7.4 and Figure 33. However, the new figure shows not just the two limiting restpoints, but the whole flow of the collision manifold.

Apparently the flow on the quotiented collision manifold consists of two orbits connecting the restpoints in the opposite direction from the homothetic orbit. The homothetic orbit has a total collision in forward time, converging to the restpoint

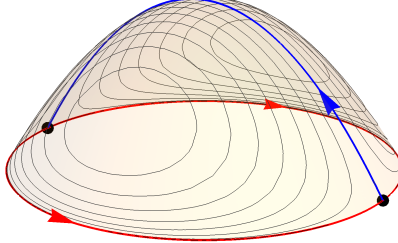


FIGURE 43. Flow on a negative energy surface of two-body problem in blown-up coordinates with rotational symmetry quotiented out. Also shown is the flow on the collision manifold (red) with its restpoints and the homothetic orbit (blue) connecting them.

with $\nu = -\sqrt{2U_0} < 0$, and a total collision in backward time, converging to a restpoint with $\nu = \sqrt{2U_0} > 0$. The solutions on the collision manifold connect these restpoints in the direction of increasing ν . Taken together, there are two *restpoint cycles*, one representing the limit of elliptical orbits with angular momentum $C > 0$ as $e \rightarrow 1$ and the other the limit of the orbits with $C < 0$. One can understand the orbits in the collision manifold as limits of the rapid spinning around the origin which the elliptical orbits exhibit near $r = 0$. Whereas the $e = 1$ orbit just moves in and out, the nearby elliptical ones move in, spin around, and then move out. In blown-up coordinates, the limit of the spinning behavior produces the orbits in $r = 0$.

Before moving on to the 3BP, the flow on the unquotiented energy manifold will be described. To make a 3D visualization of the energy manifold, use the energy equation $\frac{1}{2}\nu^2 + \frac{1}{2}\omega^2 - U_0 = rh$ in the negative energy case $h < 0$ to eliminate r via

$$r = \frac{1}{2|h|}(2U_0 - \nu^2 - \omega^2).$$

Since $r \geq 0$, the variables (ν, ω) lie in the closed disk $\nu^2 + \omega^2 \leq 2U_0$ with the boundary circle $\nu^2 + \omega^2 = 2U_0$ representing the collision manifold. Including the angular variable θ , one finds that the energy manifold is a solid torus with the boundary torus representing the collision manifold. Figure 44 shows the some features of the resulting flow. Comparing with the quotient flow in Figure 43, the full flow has two circles of restpoints $(\theta, \nu, \omega) = (\theta, \pm\sqrt{2U_0}, 0)$, $0 \leq \theta \leq 2\pi$. These are connected by a family of homothetic orbits (blue arrows) and also by two families of orbits in the collision manifold (red). The homothetic orbits have constant θ , while along the orbits in the collision manifold θ changes by $\pm 2\pi$ where the sign depend on that of ω .

Finally, it's instructive to interpret the general results about the eigenvalues of the restpoints from Section 7.4 for this simple case. In the four-dimensional (r, ν, θ, ω) space there will be four eigenvectors, but only three of them are tangent

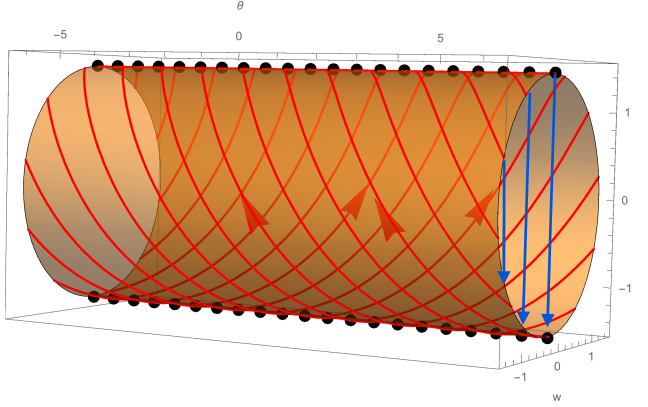


FIGURE 44. Flow on a 3D negative energy surface of two-body problem in blown-up coordinates. The coordinates in this projection are (θ, ν, ω) . The manifold is a solid torus with the collision manifold $r = 0$ represented by the boundary surface. The collision manifold has two circles of restpoints which are connected pairs of orbit running between the circles at $\nu = \pm\sqrt{2U_0}$. Also shown are some of the homothetic orbit (blue) connecting them in the opposite direction.

to the energy manifold. The linearized system is

$$\begin{bmatrix} \delta r' \\ \delta \nu' \\ \delta \theta' \\ \delta \omega' \end{bmatrix} = \begin{bmatrix} \nu_0 & 0 & 0 & 0 \\ 0 & \nu_0 & 0 & 0 \\ 0 & 0 & 0 & 1 \\ 0 & 0 & 0 & -\frac{1}{2}\nu_0 \end{bmatrix} \begin{bmatrix} \delta r \\ \delta \nu \\ \delta \theta \\ \delta \omega \end{bmatrix}.$$

As always, there is the eigenvector $(h, \nu_0, 0, 0)$ with $\lambda = \nu_0$. In the 3D projection of Figure 44, this is the vertical vector $(\nu_0, 0, 0)$ tangent to the homothetic orbits. It's an attracting direction for the restpoints with $\nu_0 < 0$ and repelling for those with $\nu_0 > 0$. By Lemma 7.1, the eigenvalues, α , of $D\nabla\tilde{U}(s_0)$ determine the other eigenvalues. Since $U(s)$ is constant on the one dimensional ellipsoid \mathcal{E} , $D\nabla\tilde{U}(s_0) = 0$ (this is the 0 in the (4, 3) position in the matrix). Its only eigenvalue is $\alpha = 0$. The corresponding eigenvectors and eigenvalues of the linearized system are

$$(\delta r, \delta \nu, \delta \theta, \delta \omega) = (0, 0, 1, 0), \lambda = 0 \quad (\delta r, \delta \nu, \delta \theta, \delta \omega) = (0, 0, 1, -\frac{1}{2}\nu_0), \lambda = -\frac{1}{2}\nu_0.$$

In the 3D projection of Figure 44, the first eigenvector is tangent to the line of restpoints and the second is tangent to the red connecting orbits in the collision manifold. The latter are repelling for $\nu_0 < 0$ and attracting for $\nu_0 > 0$ as seen in the figure.

Exercise 7.15. Consider the solutions on the collision manifold $r = 0$ for the 2BP. For each restpoint $p = (r, \nu, \theta, \omega) = (0, -\sqrt{2U_0}, \theta_0, 0)$ there is a pair of solutions starting at p and converging to a restpoint $q = (r, \nu, \theta, \omega) = (0, \sqrt{2U_0}, \theta_1, 0)$ (see Figure 44). Show that the change in the angle $\theta(t)$ along these solutions is $\pm 2\pi$ where the sign depends on the sign of ω along the orbit. Hint: Consider $\frac{d\theta}{d\nu} = \frac{\theta'}{\nu'}$.

7.6. Total collision and relative equilibria for $n = 3$. For the planar 3BP, the translation-reduced phase space has dimension $4(n - 1) = 8$ and the energy manifolds have dimension 7. By forming a quotient space, the dimension can be reduced to 5. It will not be possible to visualize these directly, but some of the features encountered above, such as homothetic orbits and circles of restpoints on the collision manifold, as well as homographic orbits, will be present there.

For the study of triple collision, the restriction to the planar problem is no loss of generality. By Proposition 7.5, the angular momentum of any total collision solution must be zero. It turns out that for the 3BP, orbits with zero angular momentum are always planar (see Exercise 7.18).

To understand triple collision, the main task will be to find the eigenvalues of the restpoints. Lemma 7.1 shows that the key is to understand the eigenvalues of $D\tilde{\nabla}U(s_0)$ whose eigenvectors satisfy

$$(81) \quad \langle\langle s_0, \delta s \rangle\rangle = 0 \quad m_1\delta s_1 + m_2\delta s_2 + m_3\delta s_3 = 0.$$

Since the dimensions are large, some tricks will be used to simplify the computations.

It is easy to guess several eigenvectors of $D\tilde{\nabla}U(s_0)$. First consider the configuration vector $s_0 = (s_1, s_2, s_3)$. Since U is homogeneous of degree -1 , ∇U is homogeneous of degree -2 and therefore $D\nabla U(s)s = -2\nabla U(s)$. Since s_0 is a normalized central configuration, $\nabla U(s_0) + U(s_0)Ms_0 = 0$ and therefore

$$D\tilde{\nabla}U(s_0)s_0 = M^{-1}D\nabla U(s_0)s_0 + U(s_0)s_0 = 3U(s_0)s_0.$$

In other words, s_0 is an eigenvector with eigenvalue $\alpha = 3U(s_0)$. However, s_0 does not satisfy the normalization conditions (81).

Next, consider translation vectors of the form $w = (k, k, k)$ where $k \in \mathbb{R}^2$. Since $\nabla U(s)$ is translation invariant, we have $D\nabla U(s_0)w = 0$ and $D\tilde{\nabla}U(s_0)w = U(s_0)w$. There are two independent eigenvectors of this type with $\alpha = U(s_0)$, but these also do not satisfy (81).

Finally, the rotational symmetry of $U(s)$ implies that s_0^\perp is an eigenvector of $D\tilde{\nabla}U(s_0)$ with eigenvalue $\alpha = 0$ where $s_0^\perp = (s_1^\perp, s_2^\perp, s_3^\perp)$, the vector with each s_i rotated by 90° in the plane. s_0^\perp does satisfy the normalization conditions. Lemma 7.1 gives eigenvalues $\lambda = 0, -\frac{\nu_0}{2}$ for the linearized ODE. There are two more eigenvectors satisfying (81) and they will determine what will be called the “nontrivial” eigenvalues of $D\tilde{\nabla}U(s_0)$. Here is the result for the equilateral CCs.

Proposition 7.16. *The nontrivial eigenvalues of $D\tilde{\nabla}U(s_0)$ at an equilateral central configuration are*

$$\alpha_1, \alpha_2 = \frac{3U(s_0)}{2} \left(1 \pm \sqrt{k} \right)$$

where

$$(82) \quad k = \frac{(m_1 - m_2)^2 + (m_1 - m_3)^2 + (m_2 - m_3)^2}{2(m_1 + m_2 + m_3)^2}.$$

The four corresponding nontrivial eigenvalues at one of the Lagrangian restpoints at triple collision are

$$\lambda = \frac{-\nu_0}{4} \left(1 \pm \sqrt{13 \pm 12\sqrt{k}} \right)$$

The proof will be given at the end of this section. An important corollary is the fact the the triple collision orbits form submanifolds in the phase space, a result first proved by C.L.Siegel [21, 22].

Corollary 7.1. *There are two circles of equilateral restpoints on the collision manifold with $\nu_0 < 0$ and two with $\nu_0 > 0$. Up to symmetry these are nondegenerate. In each manifold of constant energy, each restpoint with $\nu_0 < 0$ has an analytic stable manifold of dimension 3. These are the initial conditions leading to triple collision in forward time. Similarly, each restpoint with $\nu_0 > 0$ has a three-dimensional analytic unstable manifold consisting of all initial conditions leading to triple collision in backward time. These manifolds are entirely contained in the zero-angular-momentum submanifold.*

Proof. In the energy manifold, the seven eigenvalues at each equilateral restpoint are $\nu_0, 0, -\frac{1}{2}\nu_0$ and the four nontrivial eigenvalues from Proposition 7.16. If $\nu_0 < 0$, the three “trivial” ones are real and have signs $-, 0, +$ with the negative eigenvalue ν_0 having a nonzero δr component. One can show that the constant k in the proposition satisfies $0 \leq k < 1$ (see Exercise 7.16). Then a moments thought shows that the nontrivial eigenvalues are all real and have signs given by the choice of \pm outside the square root in the formula. Therefore, two of them are positive and two are negative. There are a total of three attracting eigenvalues. Since 0 is a simple eigenvalues, the equilateral restpoints are nondegenerate in the sense of Definition 7.2. It follows that the stable manifold of the corresponding circle of restpoints is the union of the stable manifolds of the individual restpoints (the stable manifold orbits have asymptotic phase) and the dimension of these individual manifolds is 3. A similar discussion applies near the restpoints with $\nu_0 > 0$. QED

Next consider one of the Euler configurations, say the configuration for which m_2 lies between m_1 and m_3 . Recall that the distance ratio $r = r_{23}/r_{12}$ for this configuration is the unique positive root to the fifth degree equation (76). Let

$$(83) \quad \kappa = \frac{m_3(1 + 3r + 3r^2) + m_1(3r^3 + 3r^4 + r^5)}{(m_1 + m_3)r^2 + m_2(1 + r)^2(1 + r^2)}.$$

Proposition 7.17. *The nontrivial eigenvalues of $D\tilde{\nabla}U(s_0)$ at the collinear central configuration with m_2 between m_1, m_3 are*

$$\alpha_1, \alpha_2 = -U(s_0)\kappa, U(s_0)(3 + 2\kappa)$$

with κ given by (83). The four corresponding nontrivial eigenvalues at the Eulerian equilibrium points at triple collision or at infinity are

$$(84) \quad \lambda = \frac{-\nu_0}{4} (1 \pm \sqrt{1 - 8\kappa}), \frac{-\nu_0}{4} (1 \pm \sqrt{25 + 16\kappa}).$$

The values at the other Eulerian restpoints are found by permuting the subscripts on the masses.

The restpoints corresponding to the collinear restpoints have stable and unstable manifolds of dimension two for $\nu_0 < 0$ and $\nu_0 > 0$, respectively.

Corollary 7.2. *There are six circles of collinear restpoints on the collision manifold with $\nu_0 < 0$ and six with $\nu_0 > 0$. Up to symmetry these are nondegenerate. In each manifold of constant energy, each restpoint with $\nu_0 < 0$ has an analytic stable manifold of dimension 2. Similarly, each restpoint with $\nu_0 > 0$ has a two-dimensional analytic unstable manifold.*

In addition to having zero angular momentum, it turns out that these collinear triple collision orbits are entirely contained in the invariant submanifolds of solutions which are collinear for all time (the collinear 3BP). Namely, for each ordering of the bodies along a line, there is an invariant submanifold of such solutions. This will be discussed in detail in Section 7.7. For now, the relevant point is that, inside the collinear 3BP energy manifolds, the stable and unstable manifolds of the collinear restpoints also have dimension 2. Since the dimensions are the same, it follows that the stable manifolds from the planar 3BP are identical to those of the collinear problem. As a result, triple collision with a collinear asymptotic shape is only possible if the solution is actually collinear for all time.

Another interesting feature of the collinear restpoints is the presence of nonreal eigenvalues. If the constant $\kappa > \frac{1}{8}$ then there is a pair of nonreal eigenvalues with $\text{Re}(\lambda) > 0$ at the restpoints with $\nu_0 < 0$. These unstable eigenvalues have eigenvectors transverse to the collinear 3BP submanifolds. This causes the nearby solutions to spiral around the collinear manifolds near triple collision. This phenomenon has important implications for the existence of chaotic motions near triple collision, but this will not be discussed here [18, 17].

The results of Propositions 7.16 and 7.17 can also be applied to analyze the linear stability of the relative equilibrium solutions of the planar 3BP corresponding to the five types of CCs. Recall that in the PCR3BP, the collinear RE were unstable but that the equilateral ones could have all imaginary eigenvalues if one of the two primaries is much larger than the other. Similar results will now be obtained for the planar 3BP. Since the RE solutions rotate at a constant angular speed, they will become equilibria in rotating coordinates. Since the size variable r is constant, the rotation rate will also be constant using the McGehee timescale, τ . Let

$$R(\tau) = \begin{bmatrix} \cos \omega\tau & -\sin \omega\tau \\ \sin \omega\tau & \cos \omega\tau \end{bmatrix}$$

be the rotation matrix with angular velocity ω and period $2\pi/\omega$. Starting from McGehee variables (r, ν, s, w) introduce new, rotating coordinates S, W with $s = R(\tau)S, w = R(\tau)W$ where the rotation acts on each components $S_i, W_i \in \mathbb{R}^2$ separately, as usual. Then the ODE (70) becomes

$$\begin{aligned} r' &= \nu r \\ \nu' &= \frac{1}{2}\nu^2 + \|W\|^2 - U(S) \\ S' &= W - \omega KS \\ W' &= \tilde{\nabla}U(S) - \frac{1}{2}\nu W - \|W\|^2 S - \omega KW \end{aligned} \tag{85}$$

where K is the block-diagonal 6×6 matrix $K = \text{diag}(\begin{bmatrix} 0 & -1 \\ 1 & 0 \end{bmatrix}, \begin{bmatrix} 0 & -1 \\ 1 & 0 \end{bmatrix}, \begin{bmatrix} 0 & -1 \\ 1 & 0 \end{bmatrix})$.

The energy equation is

$$\frac{1}{2}\nu^2 + \frac{1}{2}\|W\|^2 - U(S) = rh.$$

A RE solution will have some constant radius $r = r_0$ and so must have $\nu = 0$. The normalized configuration will be some constant CC S_0 with $\tilde{\nabla}U(S_0)$. The ODE gives

$$W = \omega KS \quad \|W\|^2 = \omega^2 = U(S_0).$$

With $\omega = \pm\sqrt{U(S_0)}$, there is an equilibrium point at $(r, \nu, S, W) = (r_0, 0, S_0, \omega K S_0)$. The energy equation shows that the size r_0 satisfies

$$r_0 h + \frac{1}{2} \omega^2 = 0.$$

Although the angular velocity in the rescaled time is uniquely determined up to sign by the CC, the angular velocity $\hat{\omega}$ in the usual timescale depends on the size via

$$\hat{\omega} = r_0^{-\frac{3}{2}} \omega = \pm r_0^{-\frac{3}{2}} \sqrt{U(S_0)}.$$

To analyze stability, the eigenvalues of the linearized system will be found. The linearized ODE at the restpoint $(r, \nu, S, W) = (r_0, 0, S_0, \omega K S_0)$ is

$$(86) \quad \begin{bmatrix} \delta r' \\ \delta \nu' \\ \delta S' \\ \delta W' \end{bmatrix} = \begin{bmatrix} 0 & r_0 & 0 & 0 \\ 0 & 0 & -\nabla U(S_0) & 2W^T M \\ 0 & 0 & -\omega K & I \\ 0 & 0 & D\tilde{\nabla}U(S_0) & -\omega K \end{bmatrix} \begin{bmatrix} \delta r \\ \delta \nu \\ \delta S \\ \delta W \end{bmatrix}$$

Since $S = (S_1, S_2, S_3)$, $W = (W_1, W_2, W_3)$ have dimension 6, the matrix is 14×14 . As before, only the eigenvectors with

$$\begin{aligned} \langle\langle S_0, \delta S \rangle\rangle &= \langle\langle S_0, \delta W \rangle\rangle = 0 \\ m_1 \delta S_1 + \dots + m_n \delta S_n &= m_1 \delta W_1 + \dots + m_n \delta W_n = 0 \end{aligned}$$

are relevant. This time, the energy equation gives

$$\langle\langle W, \delta W \rangle\rangle = \langle\langle \omega K S_0, \delta W \rangle\rangle = h \delta r.$$

There will be seven eigenvectors satisfying these constraints (the dimension of the energy manifold).

First note that the vector $(\delta r, \delta \nu, \delta S, \delta W) = (0, 0, K S_0, -S_0)$ (tangent to the circle of restpoints) is an eigenvector with eigenvalue $\lambda = 0$. Next, the vectors $(\delta r, \delta \nu, \delta S, \delta W) = (\omega, 0, 0, h K S_0), (0, 2h\omega, h K S_0, h\omega S_0)$ satisfy the constraints and form an invariant two-dimensional plane with matrix $\begin{bmatrix} 0 & -\omega^2 \\ 1 & 0 \end{bmatrix}$. The restriction of the linearized ODE to this plane has two imaginary eigenvalues $\lambda = \pm\omega$. The other four eigenvectors will satisfy $\delta r = \delta \nu = 0$ and $\langle\langle K S_0, \delta S \rangle\rangle = 0$. They will be related to the nontrivial eigenvectors of $D\tilde{\nabla}U(S_0)$ from Propositions 7.16 and 7.17.

Lemma 7.2. *Let v_1, v_2 be the eigenvectors associated to the nontrivial eigenvalues α_1, α_2 of $D\tilde{\nabla}U(S_0)$. Then, up to a scalar multiple, $v_2 = K v_1$.*

Proof. Consider the 6×6 matrices $D\tilde{\nabla}U(S_0)$ and K . The first is symmetric and the second is antisymmetric with respect to the mass metric, that is, for all $v, w \in \mathbb{R}^6$

$$\langle\langle v, D\tilde{\nabla}U(S_0)w \rangle\rangle = \langle\langle D\tilde{\nabla}U(S_0)v, w \rangle\rangle \quad \langle\langle v, Kw \rangle\rangle = -\langle\langle Kv, w \rangle\rangle.$$

As noted above, it follows that the eigenvectors of $D\tilde{\nabla}U(S_0)$ are orthogonal (meaning, with respect to the mass metric). If $\mathcal{S} \subset \mathbb{R}^6$ is an invariant subspace for $D\tilde{\nabla}U(S_0)$ then its orthogonal complement (with respect to the mass metric) is also invariant. This is a standard fact about ordinary symmetric matrices which generalizes to this case. Similarly, if \mathcal{S} is invariant for the antisymmetric matrix K , then its orthogonal complement is also K -invariant. Now the four-dimensional subspace \mathcal{S} spanned by $(1, 0, 1, 0, 1, 0), (0, 1, 0, 1, 0, 1), S_0, K S_0$ is invariant for both $D\tilde{\nabla}U(S_0)$ and K . It follows that its orthogonal complement, a two-dimensional subspace \mathcal{S}^\perp , is also invariant for both linear maps. There will be two eigenvectors

in \mathcal{S}^\perp and these must be the vectors v_1, v_2 . Now the antisymmetry of K implies that $\langle\langle v_1, Kv_1 \rangle\rangle = 0$. But also $\langle\langle v_1, v_2 \rangle\rangle = 0$, since they are both eigenvectors. Since \mathcal{S}^\perp has dimension two, it must be that $v_2 = cKv_1$ for some scalar $c \neq 0$. QED

Corresponding to the invariant subspace \mathcal{S}^\perp with basis $v_1, v_2 = Kv_1$ there is a four-dimensional invariant subspace for the linearized ODE. Namely, with $\delta r = \delta\nu = 0$, let $(\delta S, \delta V) = (v_1, 0), (v_2, 0), (0, v_1), (0, v_2)$. With respect to this basis, the 4×4 matrix of the restriction of the linearized ODE to this subspace is

$$\begin{bmatrix} 0 & \omega & 1 & 0 \\ -\omega & 0 & 0 & 1 \\ \alpha_1 - \omega^2 & 0 & 0 & \omega \\ 0 & \alpha_2 - \omega^2 & -\omega & 0 \end{bmatrix}$$

and the characteristic polynomial is

$$\lambda^4 + (4\omega^2 - \alpha_1 - \alpha_2)\lambda^2 + \alpha_1\alpha_2.$$

For the equilateral restpoints, this becomes

$$\lambda^4 + \omega^2\lambda^2 + \omega^4 \frac{27(m_1m_2 + m_1m_3 + m_2m_3)}{4(m_1 + m_2 + m_3)^2}$$

where the equations $\omega^2 = U(S_0)$ and $\alpha_1, \alpha_2 = \frac{3}{2}U(s_0)(1 \pm \sqrt{k})$ have been used. For spectral stability, the solutions of this quadratic equation for λ^2 should both be real and negative. Since the coefficients are positive, this will be true if and only if the discriminant is nonnegative, that is

Proposition 7.18. *The Lagrange equilateral triangle relative equilibria are spectrally stable if and only if*

$$27(m_1m_2 + m_1m_3 + m_2m_3) \leq (m_1 + m_2 + m_3)^2.$$

This is Routh's stability criterion. Just as for the PCR3BP, the inequality fails to hold for most masses. In fact it only holds when one mass is much larger than the other two. For example, suppose the masses are normalized so that $m_3 = 1$ is the largest mass. Then Figure 45 shows the masses m_1, m_2 for which the equilateral triangle is spectrally stable.

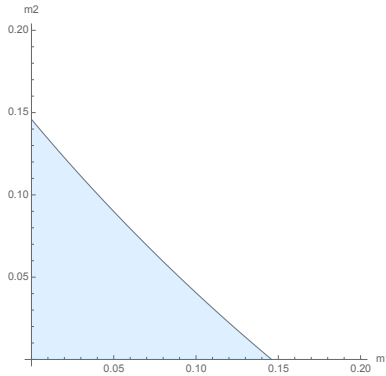


FIGURE 45. The shaded region show the masses (m_1, m_2) for which the equilateral relative equilibrium of the planar 3BP is spectrally stable, assuming that $m_3 = 1$ is the largest mass.

Just as for the PCR3BP, the collinear RE solutions are unstable. Their eigenvalues can be computed in a similar way. Then the eigenvectors with eigenvalues $\lambda = 0, \pm i\omega$ are as for the equilateral case. Lemma 7.2 applies and one obtains the same 4×4 matrix as before. This time, Proposition 7.17 shows that $\alpha_1 = -U(S_0)\kappa$, $\alpha_2 = U(S_0)(3 + 2\kappa)$ and the characteristic polynomial of the 4×4 matrix is

$$\lambda^4 + \omega^2(1 - \kappa)\lambda^2 - \omega^4(3\kappa + 2\kappa^2).$$

Since the constant term is negative, the values of λ^2 are real with opposite signs. The positive root gives a pair of real eigenvalues $-\lambda < 0 < \lambda$ which means that the collinear RE are always unstable.

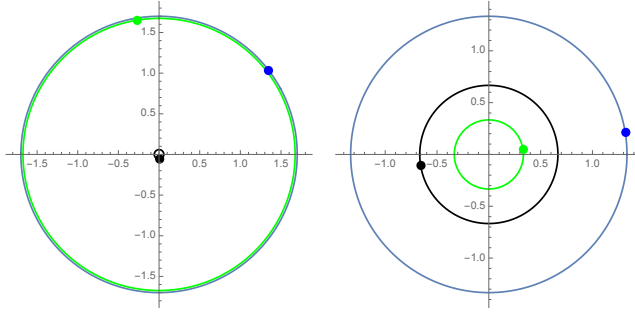


FIGURE 46. Relative equilibria of the 3BP. Lagrange RE for $m_1 = 1, m_2 = 10, m_3 = 300$ is spectrally stable (left). Euler RE for masses $m_1 = 1, m_2 = 2, m_3 = 3$ is unstable (right).

7.6.1. How to compute the eigenvalues. To prove propositions 7.16 and 7.17 one has to find the nontrivial eigenvalues α_1, α_2 of $D\tilde{\nabla}U(s)$ for the equilateral and collinear central configurations of the three-body problem. It is straightforward to calculate the 6×6 matrix $D\nabla U(s)$ with the result

$$(87) \quad D\nabla U(s) = \begin{bmatrix} D_{11} & D_{12} & D_{13} \\ D_{21} & D_{22} & D_{23} \\ D_{31} & D_{32} & D_{23} \end{bmatrix}$$

where the 2×2 blocks are

$$D_{ij} = \frac{m_i m_j}{r_{ij}^3} (I - 3u_{ij}u_{ij}^t), \quad u_{ij} = \frac{q_i - q_j}{r_{ij}} \quad \text{for } i \neq j$$

and

$$D_{ii} = - \sum_{j \neq i} D_{ij}.$$

It is more convenient to work with the matrix

$$P = \frac{I(s)}{U(s)} M^{-1} D\nabla U(s).$$

Since P is invariant under scaling and translation, it can be computed without imposing the normalizations $\|s\| = 1$ and $m_1 s_1 + m_2 s_2 + m_3 s_3 = 0$. If β is an eigenvalue of P then $\alpha = U(s)(\beta + 1)$ is an eigenvalue of $D\tilde{\nabla}U(s)$ for the corresponding normalized s . So one is reduced to finding the nontrivial eigenvalues β_1, β_2 of P .

Proof of Proposition 7.16. Consider an equilateral triangle configuration s . Working with P one can use the unnormalized configuration

$$s_1 = (1, 0) \quad s_2 = \left(-\frac{1}{2}, \frac{\sqrt{3}}{2}\right) \quad s_3 = \left(-\frac{1}{2}, -\frac{\sqrt{3}}{2}\right)$$

for which

$$U(s_0) = \frac{m_1 m_2 + m_1 m_3 + m_2 m_3}{\sqrt{3}} \quad I(s_0) = \frac{3(m_1 m_2 + m_1 m_3 + m_2 m_3)}{m}.$$

Using these together with (87) gives

$$P = \frac{1}{4m} \begin{bmatrix} 5(m_2 + m_3) & 3\sqrt{3}(m_3 - m_2) & -5m_2 & 3\sqrt{3}m_2 & -5m_3 & -3\sqrt{3}m_3 \\ 3\sqrt{3}(m_3 - m_2) & -(m_2 + m_3) & 3\sqrt{3}m_2 & m_2 & -3\sqrt{3}m_3 & m_3 \\ -5m_1 & 3\sqrt{3}m_1 & 5m_1 - 4m_3 & -3\sqrt{3}m_1 & 4m_3 & 0 \\ 3\sqrt{3}m_1 & m_1 & -3\sqrt{3}m_1 & -m_1 + 8m_3 & 0 & -8m_3 \\ -5m_1 & -3\sqrt{3}m_1 & 4m_2 & 0 & 5m_1 - 4m_2 & 3\sqrt{3}m_1 \\ -3\sqrt{3}m_1 & m_1 & 0 & -8m_2 & 3\sqrt{3}m_1 & -m_1 + 8m_2 \end{bmatrix}$$

One can guess 4 of the 6 eigenvalues of P . If $e_1 = (1, 0)$, $e_2 = (0, 1)$ then (e_1, e_1, e_1) and (e_2, e_2, e_2) are eigenvectors with eigenvalue $\beta = 0$. Also s_0, s_0^\perp are eigenvectors with eigenvalues $\beta = 2, -1$ respectively. Since the trace of P is 2, the remaining eigenvalues satisfy $\beta_1 + \beta_2 = 1$. Alternatively, the numbers $\gamma_i = \beta_i + 1$ satisfy $\gamma_1 + \gamma_2 = 3$. One can also find the product $\gamma_1 \gamma_2$ as follows. We have

$$(\text{tr } P)^2 - \text{tr } P^2 = (1 + \beta_1 + \beta_2)^2 - (5 + \beta_1^2 + \beta_2^2) = 2\beta_1\beta_2 - 2 = 2\gamma_1\gamma_2 - 6.$$

With some computer assistance, this gives

$$\gamma_1\gamma_2 = \frac{27(m_1 m_2 + m_1 m_3 + m_2 m_3)}{4(m_1 + m_2 + m_3)^2}$$

Solving the quadratic equation $\gamma^2 - 3\gamma + \gamma_1\gamma_2 = 0$ gives the eigenvalues $\alpha_i = U(s)\gamma_i = \nu_0^2\gamma_i/2$ of $D\tilde{\nabla}U(s)$ listed in the proposition. Then Lemma 7.1 gives the nontrivial eigenvalues λ of the restpoint. QED

Proof of proposition 7.17. Consider a normalized collinear central configuration such that $s_i = (x_i, 0) \in \mathbb{R}^2$. Then the unit vectors $u_{ij} = (\pm 1, 0)$ so the 2×2 matrices D_{ij} reduce to

$$D_{ij} = \frac{m_i m_j}{r_{ij}^3} \begin{bmatrix} -2 & 0 \\ 0 & 1 \end{bmatrix} \quad i \neq j.$$

Rearranging the variables as $q = (x_1, x_2, x_3, y_1, y_2, y_3)$ produces a block structure

$$(88) \quad M^{-1} D \nabla U(s_0) = \begin{bmatrix} 2C & 0 \\ 0 & -C \end{bmatrix}$$

where C is the $n \times n$ matrix

$$C = \begin{bmatrix} \frac{m_2}{r_{12}^3} + \frac{m_3}{r_{13}^3} & -\frac{m_2}{r_{12}^3} & -\frac{m_3}{r_{13}^3} \\ -\frac{m_1}{r_{12}^3} & \frac{m_1}{r_{12}^3} + \frac{m_3}{r_{23}^3} & -\frac{m_3}{r_{23}^3} \\ -\frac{m_1}{r_{13}^3} & -\frac{m_2}{r_{23}^3} & \frac{m_1}{r_{13}^3} + \frac{m_2}{r_{23}^3} \end{bmatrix}.$$

An eigenvalue μ of C determines two eigenvalues

$$\alpha = -\mu + U(s_0), 2\mu + U(s_0)$$

for $D\tilde{\nabla}U(s_0) = M^{-1} D \nabla U(s_0) + U(s_0)I$.

It is possible to guess two eigenvectors of C . First of all $v_1 = (1, 1, 1)$ is an eigenvector with eigenvalue 0. Next, let $v_2 = (x_1, x_2, x_3)$ be the vector of x -coordinates of the collinear central configuration. Then it is easy to see that

$$Cv_2 = -M_0^{-1} \nabla_x U$$

where ∇_x is the partial gradient with respect to the x -coordinates and $M_0 = \text{diag}(m_1, m_2, m_3)$. Since s is a normalized central configuration, we have $Cv_2 = U(s_0)v_2$, so v_2 is also an eigenvector, with eigenvalue $U(s_0)$. The remaining, non-trivial eigenvalue of C can now be found as $\mu = \tau - U(s_0)$ where $\tau = \text{tr}(C)$, i.e.,

$$\tau = \left(\frac{m_1 + m_2}{r_{12}^3} + \frac{m_1 + m_3}{r_{13}^3} + \frac{m_2 + m_3}{r_{23}^3} \right).$$

Therefore the nontrivial eigenvalues of $D\tilde{\nabla}U(s_0)$ are

$$\alpha = 2\tau - U(s_0), 2U(s_0) - \tau.$$

To get the form shown in the proposition, let κ be the translation and scale invariant quantity

$$\kappa = \frac{I(s)}{U(s)}\tau - 2.$$

Then for the normalized configuration $\alpha_1, \alpha_2 = -U(s_0)\kappa, U(s_0)(3 + 2\kappa)$ and it remains to show that κ has the indicated form.

Here is a computer assisted way to prove it. Using the configuration $s_1 = (0, 0), s_2 = (1, 0), s_3 = (1 + r, 0)$ we have

$$r_{12} = 1 \quad r_{23} = r \quad r_{13} = 1 + r.$$

Substituting these into the formulas for $I(s), U(s), \tau$ expresses $\kappa = \frac{I(s)}{U(s)}\tau - 2$ as a rational function $\kappa(r)$. Subtracting the expression (83) and factorizing the difference reveals that there is a factor of $g(r)$ in the numerator, where $g(r)$ is the fifth degree polynomial (76) giving the location of the central configuration. So $\kappa(r)$ is indeed given by (83) at the central configuration. QED

Exercise 7.16. Prove that the constant k in (?? satisfies $0 \leq k < 1$ for all masses $m_i > 0$. Hint: the question can be reduced to finding the maximum of the numerator of (?? on the simplex where $m_1 + m_2 + m_3 = 1$.

Exercise 7.17. Suppose $m_1 = m_3 = 1$ and $m_2 > 0$. For which values of m_2 do the collinear restpoints of Proposition 7.17 have nonreal eigenvalues (so there is spiralling) ?

Exercise 7.18. Suppose $q(t) = (q_1(t), q_2(t), q_3(t)) \in \mathbb{R}^9$ is a solution of the 3BP in \mathbb{R}^3 with center of mass at the origin and angular momentum vector $C = (0, 0, 0)$. Show that $q(t)$ is planar, that is, all of the positions $q_i(t)$ lie in some fixed plane for all time. Hint: In Jacobi coordinates, $x_1, x_2 \in \mathbb{R}^3$, the angular momentum is $C = \mu_1 x_1 \times u_1 + \mu_2 x_2 \times u_2$ where $u_i = \dot{x}_i$. Show that if $x_i \in \mathbb{R}^2 \times 0$ then the velocities are also in $\mathbb{R}^2 \times 0$. The case when the positions are collinear requires some care.

7.7. The Collinear Three-Body Problem. The planar 3BP is difficult to visualize due to the high dimensions of the phase space. The collinear 3BP is an interesting special case where the phase space has dimension 4 and the energy manifolds have dimension 3, just like the planar 2BP. It was the first case studied by McGehee and provides a nice application of the blow-up method [13]. The details here differ somewhat from McGehee's presentation.

Consider the collinear three-body problem with masses m_1, m_2, m_3 and positions be $q_i \in \mathbb{R}$. Here it will be assumed that the order of the bodies along the line is $q_1 < q_3 < q_2$. Since the bodies are all on a line, binary collisions are inevitable but they will be regularized such that the solutions continue after a "bounce". Figure ?? shows a spacetime plot of typical solution. For each time, t , the positions of bodies are shown along a vertical line. The solution features several collisions, after which m_2, m_3 go off together in a tight binary while m_1 moves off in the other direction.

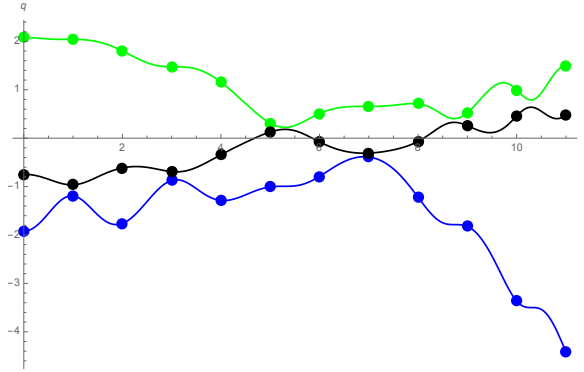


FIGURE 47. Spacetime diagram for a typical solution of the collinear 3BP. The points $(t, q_i(t))$, $i = 1, 2, 3$, are plotted in the (t, q) plane.

Assume without loss of generality that total momentum is zero and that the center of mass is at the origin and introduce Jacobi variables

$$(89) \quad x_1 = q_2 - q_1 \quad x_2 = q_3 - (\alpha_1 q_1 + \alpha_2 q_2) \quad \alpha_i = \frac{m_i}{m_1 + m_2}$$

and their velocities $u_i = \dot{x}_i$. This is like Example 3.2 except that here the variables are all scalars.

Then the equations of motion are the Euler-Lagrange equations for $L = \frac{1}{2}K + U$ where

$$(90) \quad \begin{aligned} K &= \frac{1}{2}\mu_1|u_1|^2 + \frac{1}{2}\mu_2|u_2|^2 \\ U &= \frac{m_1 m_2}{r_{12}} + \frac{m_1 m_3}{r_{13}} + \frac{m_2 m_3}{r_{23}} \end{aligned}$$

and where $\mu_1 = \frac{m_1 m_2}{m_1 + m_2}$, $\mu_2 = \frac{(m_1 + m_2)m_3}{m_1 + m_2 + m_3}$. The mutual distances are given by

$$(91) \quad \begin{aligned} r_{12} &= |x_1| \\ r_{13} &= |x_2 + \alpha_2 x_1| \\ r_{23} &= |x_2 - \alpha_1 x_1| \end{aligned}$$

and the mass norm is given by

$$r^2 = \|x\|^2 = \mu_1 x_1^2 + \mu_2 x_2^2.$$

The use of Jacobi coordinates eliminates the translational symmetry of the problem and reduces the number of degrees of freedom from 3 to 2.

Here it will be assumed that the order of the bodies along the line is $q_1 < q_3 < q_2$. Then $x_1 \geq 0$ and $-\alpha_2 x_1 \leq x_2 \leq \alpha_1 x_1$. The normalized configuration $s = x/r$ satisfies $\mu_1 s_1^2 + \mu_2 s_2^2 = 1$. Define an angle variable such that

$$(92) \quad x_1 = \frac{1}{\sqrt{\mu_1}} r \cos \theta \quad x_2 = \frac{1}{\sqrt{\mu_2}} r \sin \theta$$

and let $\omega = \dot{\theta}$. The choice of ordering implies that $-\frac{\pi}{2} < \theta_1 \leq \theta \leq \theta_2 < \frac{\pi}{2}$ where

$$\tan \theta_1 = -\alpha_2 \sqrt{\frac{\mu_2}{\mu_1}} \quad \tan \theta_2 = \alpha_1 \sqrt{\frac{\mu_2}{\mu_1}}.$$

Then the blown-up equations (70) become

$$(93) \quad \begin{aligned} r' &= \nu r \\ \nu' &= \frac{1}{2} \nu^2 + \omega^2 - V(\theta) \\ \theta' &= \omega \\ \omega' &= V_\theta - \frac{1}{2} \nu \omega. \end{aligned}$$

where

$$V(\theta) = \frac{m_1 m_2}{r_{12}} + \frac{m_1 m_3}{r_{13}} + \frac{m_2 m_3}{r_{23}}$$

and the mutual distances are

$$(94) \quad \begin{aligned} r_{12} &= \left| \frac{1}{\sqrt{\mu_1}} \cos \theta \right| \\ r_{13} &= \left| \frac{1}{\sqrt{\mu_2}} \sin \theta + \alpha_2 \frac{1}{\sqrt{\mu_1}} \cos \theta \right| = A_1 \sin(\theta - \theta_1) \\ r_{23} &= \left| \frac{1}{\sqrt{\mu_2}} \sin \theta - \alpha_1 \frac{1}{\sqrt{\mu_1}} \cos \theta \right| = A_2 \sin(\theta_2 - \theta) \end{aligned}$$

where

$$A_1 = \sqrt{\frac{m_1 + m_3}{m_1 m_3}} \quad A_2 = \sqrt{\frac{m_2 + m_3}{m_2 m_3}}.$$

The energy equations is

$$\frac{1}{2} \nu^2 + \frac{1}{2} \omega^2 - V(\theta) = rh.$$

The triple collision has been blown up into the invariant manifold $\{r = 0\}$ but the differential equations are still singular due to the double collisions at $\theta = \theta_1, \theta_2$. There are several ways to regularize these collisions. One way is just to introduce a new timescale by multiplying the vectorfield by a factor of

$$\phi(\theta) = \sin(\theta - \theta_1) \sin(\theta_2 - \theta)$$

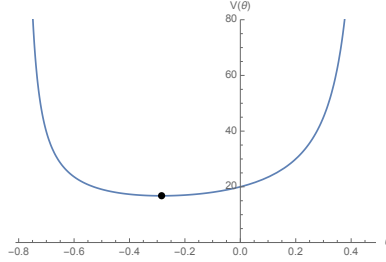


FIGURE 48. The potential $V(\theta)$ for the collinear 3BP with $m_1 = 1, m_2 = 2, m_3 = 3$. V is convex on (θ_1, θ_2) . There is a unique critical point at the Euler central configuration around $\theta = -0.284895$.

and a new velocity variable γ such that $\gamma = \omega\phi(\theta)$.

$$\begin{aligned}
 r' &= \phi\nu r \\
 \nu' &= W - \frac{1}{2}\phi\nu^2 + 2rh\phi \\
 \theta' &= \gamma \\
 \gamma' &= \phi W_\theta - \frac{1}{2}\phi\nu\gamma + \phi_\theta(2rh\phi + W - \phi\nu^2)
 \end{aligned} \tag{95}$$

where $W(\theta) = \phi(\theta)V(\theta)$, that is,

$$W(\theta) = \frac{m_1 m_2 \sqrt{\mu_1} \sin(\theta - \theta_1) \sin(\theta_2 - \theta)}{\cos \theta} + \frac{m_1 m_3 \sin(\theta_2 - \theta)}{A_1} + \frac{m_2 m_3 \sin(\theta - \theta_1)}{A_2} \tag{96}$$

In deriving the differential equations, the energy relation

$$\frac{1}{2}\phi^2\nu^2 + \frac{1}{2}\gamma^2 - \phi W(\theta) = rh\phi^2 \tag{97}$$

has been used. Since the rescaled potential $W(\theta)$ is smooth for $\theta_1 \leq \theta \leq \theta_2$, the double collisions have been regularized.

Equations 95 have a time-reversal symmetry which will be important later.

Proposition 7.19. *If $(r(\tau), \theta(\tau), \nu(\tau), \gamma(\tau))$ is a solution of the collinear 3BP, then so is $(r(-\tau), \theta(-\tau), -\nu(-\tau), -\gamma(-\tau))$.*

In other words, reflecting the velocity variables and reversing time takes solutions to solutions. In particular, this operation will take solutions having a triple collision in forward time to those having a triple collision in backward time.

Figure 49 shows the projection of the collision manifold to (θ, ω, ν) space. The solid inside the surface represents a manifold of fixed negative energy. The size variable r could be recovered via $r = \frac{1}{2|\hbar|\phi}(2W - \phi^2\nu^2 - \gamma^2)$ which gives a unique value except on the double collision set. On the collision manifold, $r = 0$, the equation for ν' can be written $\nu' = \frac{1}{2}\gamma^2/\phi \geq 0$ showing that ν is an increasing Lyapunov function, as expected. In the figure, the level curves of ν are shown. The θ variable is monotonically increasing on the $\omega > 0$ half of the surface and decreasing on the other half. So the general character of the solutions on the collision manifold is to wind around the surface while spiraling upward. Inside the

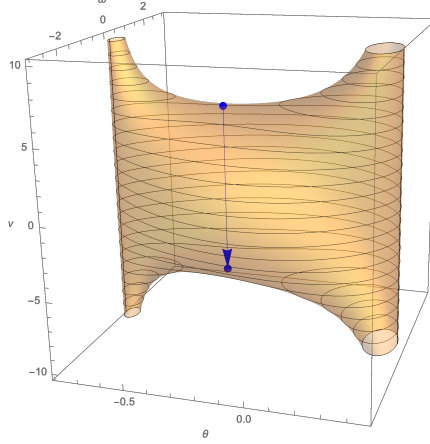


FIGURE 49. The collision manifold for the collinear 3BP with $m_1 = 1, m_2 = 2, m_3 = 3$. A manifold of fixed negative energy could be viewed as the solid inside the collision manifold. The variables are (θ, ω, ν) with the Lyapunov function ν vertical. Also shown are level curves of ν , the restpoints on the collision manifold and the homothetic orbit (blue arrow) connecting them.

surface, the homothetic solution generated by the Euler CC is shown, connecting the restpoints in the direction of decreasing ν .

To understand the flow near triple collision, the eigenvalues of the restpoints will be needed. Since the eigenvalues will be independent of the choice of coordinates, the unregularized ODE (93) can be used. Then the linearized ODE at the restpoint $(r, \nu, \theta, \omega) = (0, \nu_0, \theta_0, 0)$ is

$$\begin{bmatrix} \delta r' \\ \delta \nu' \\ \delta \theta' \\ \delta \omega' \end{bmatrix} = \begin{bmatrix} \nu_0 & 0 & 0 & 0 \\ 0 & \nu_0 & 0 & 0 \\ 0 & 0 & 0 & 1 \\ 0 & 0 & V_{\theta\theta}(\theta_0) & -\frac{1}{2}\nu_0 \end{bmatrix} \begin{bmatrix} \delta r \\ \delta \nu \\ \delta \theta \\ \delta \omega \end{bmatrix}.$$

Here θ_0 is the Euler central configuration with $V_\theta(\theta_0) = 0$. $V_{\theta\theta}(\theta_0) > 0$ is the second derivative which plays the role of the tangential gradient $\tilde{\nabla}U(s_0)$ in the general theory. So $\alpha = V_{\theta\theta}(\theta_0) > 0$ is the only eigenvalue and the general theory shows that the three eigenvalues and eigenvectors of the linearized ODE which are tangent to the energy manifold are

$$(\nu_0, h, 0, 0), \lambda = \nu_0 \quad (0, 0, 1, \lambda_{\pm}), \lambda_{\pm} = \frac{-\nu_0 \pm \sqrt{\nu_0^2 + 16\alpha}}{4}.$$

Since $\alpha > 0$ the eigenvalues λ_{\pm} with eigenvectors tangent to the collision manifold are real and have opposite signs. So both restpoints are saddle points in the collision manifold. In the 3D energy manifold, the restpoint $p_- = (0, -\sqrt{2U(s_0)}, \theta_0, 0)$ has an additional stable direction in $r > 0$ (tangent to the homothetic orbit). So there is a 2D stable manifold of orbits tending to triple collision in forward time. Similarly, the restpoint $p_+(0, \sqrt{2U(s_0)}, \theta_0, 0)$ gets an additional unstable direction so there is also a 2D unstable manifold of orbits tending to triple collision in backward time. Figure 50 shows several orbits in the 2D manifold $W^u(p_+)$. Each of these

solutions tends to the triple collision restpoint p_+ in backward time. Evidently, they spread out dramatically in forward time. Because of the time-reversal symmetry, the manifold $W^s(p_-)$ of solutions ending in triple collision can be obtained by reversing the velocities. In the figure, this would just be reflection through the horizontal axis.

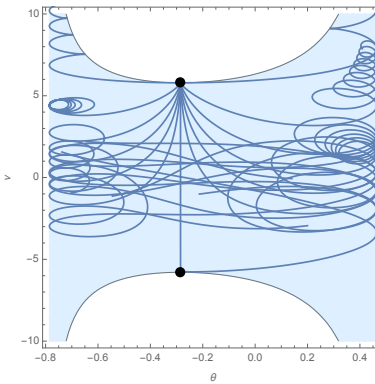


FIGURE 50. Orbits beginning at triple collision for a masses $m_1 = 1, m_2 = 2, m_3 = 3$. The 2D unstable manifold $W^u(p_+)$ contains many solutions with $r > 0$, projected here to the (θ, ν) plane.

The fact that $W^u(p_+)$ and its reflection $W^s(p_-)$ are 2D justifies the observation from the previous section that triple collision in the general 3BP with a collinear asymptotic shape is only possible for orbits which are collinear for all time. Namely, the corresponding manifolds for the general problem were also 2D, so must be identical to those found here for the collinear problem.

7.7.1. Flow on the Collision Manifold and Nonregularizability. Following McGehee, one can try to understand solutions which approach triple collision but do not actually collide. In other words, consider initial conditions close to but not actually on the stable manifold $W^s(p_-)$. Now the unstable manifold $W^u(p_-)$ has dimension 1. It lies entirely in $\{r = 0\}$ and consists of the two unstable branches of the saddle (see Figure 51). An orbit starting close to $W^s(p_-)$ will pass near p_0 and then leave close to the collision manifold along one of these two branches. For example, a solution approaching triple collision in forward time, but not actually colliding would pass close to the restpoint p_- and then follows one of the branches of $W^u(p_-)$ (blue or green curves in the figure) close to the collision manifold.

Figure 52 shows the behavior of the branches for several choices of the masses. Evidently, they typically wind around the collision manifold a variable number of times and then spiral up one of the two “arms”.

If the two branches of $W^u(p_-)$ end up in different arms on the collision manifold, then the behavior of orbits near triple collision will depend on which branch they follow. After the close approach to the triple collision, orbits which follow one branch will end up in a tight binary configuration with m_1, m_3 close together while for orbits which follow the other branch, m_3, m_2 will be close. This proves the nonregularizability of the triple collision. More precisely, suppose there were a way to extend solutions in $W^s(p_-)$ through the triple collision which was continuous

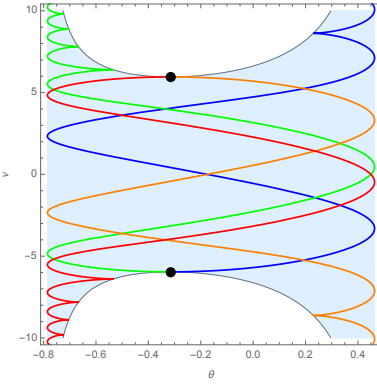


FIGURE 51. Branches of $W^u(p_-)$ (blue, green) and $W^s(p_+)$ (red, orange) for masses $m_1 = 1, m_2 = 2, m_3 = 3$, projected to the (θ, ν) plane. The two manifolds are related by reflection through the horizontal axis.

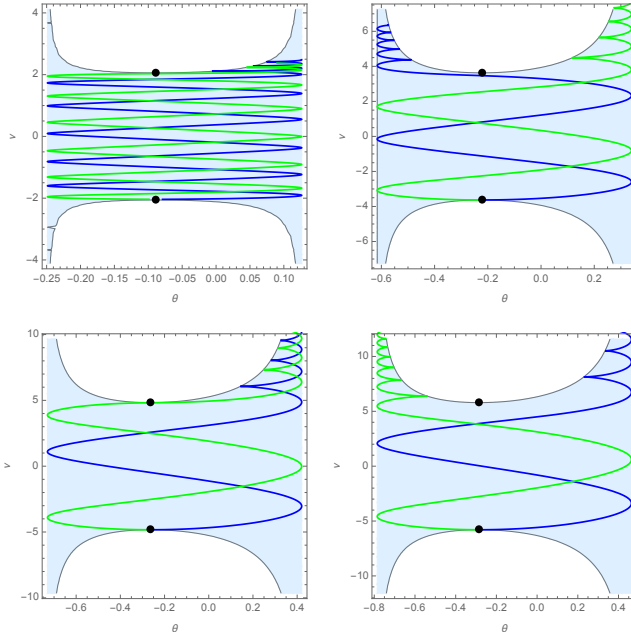


FIGURE 52. Branches of the unstable manifold of the rest point p_- for masses $m_1 = 1, m_2 = 2, m_3$ for $m_3 = 0.1, 1, 2, 3$. These orbits lie in the collision manifold but this is the projection to the (θ, ν) plane. For 3 of these four cases, the two branches spiral up opposite “arms”. This is the key point in the proof of nonregularizability of triple collision.

with respect to initial conditions. Then solutions near $W^s(p_-)$ should emerge from their near collisions close to the extended collision solutions. For example, in the Kepler problem, solutions near the collinear collision solutions are on highly

eccentric conics and remain close to the regularized collision orbits. But for the collinear 3BP, the near-collision solutions will be far part if they follow different branches of $W^u(p_-)$.

A crucial point in McGehee's proof is to prove that the behavior of the branches of $W^u(p_-)$ changes as the masses change. More precisely, the number of times that the branches wind around the collision manifold as ν increases from $-\nu_0$ to ν_0 can be arbitrarily large.

Proposition 7.20. *If $m_3 \rightarrow 0$ with $m_1 = m_2 = 1$ fixed, the number of binary collisions of the branches of $W^u(p_-)$ as ν increases from $-\nu_0$ to ν_0 tends to infinity.*

Proof. Let $m_1 = m_2 = 1$ and $m_3 = \epsilon^2$ where $\epsilon > 0$ is small. The normalized mutual distances become

$$r_{12} = \sqrt{2} \cos \theta \quad r_{13} = \frac{\sqrt{1+\epsilon^2}}{\epsilon} \sin(\theta + \theta^*) \quad r_{23} = \frac{\sqrt{1+\epsilon^2}}{\epsilon} \sin(\theta^* - \theta)$$

where $\tan \theta^* = \frac{\epsilon}{\sqrt{2+\epsilon^2}}$. Then $\theta^* = \epsilon/\sqrt{2} + O(\epsilon^2)$.

Define a new shape variable ξ such that $\theta = \theta^* \xi$. Then the relevant interval for ξ is $[-1, 1]$ and the mutual distances are

$$r_{12} = \sqrt{2} + O(\epsilon) \quad r_{13} = \frac{1}{\sqrt{2}}(1 + \xi)f_{13} \quad r_{23} = \frac{1}{\sqrt{2}}(1 - \xi)f_{23}$$

where $f_{ij}(\xi, \epsilon)$ are smooth functions with $f_{ij}(\xi, \epsilon) = 1 + O(\epsilon)$. The potential is

$$V = (1 - \xi^2)^{-1} \left(\frac{1}{\sqrt{2} + O(\epsilon)} + \frac{\sqrt{2}\epsilon^2(1 - \xi)}{f_{13}} + \frac{\sqrt{2}\epsilon^2(1 + \xi)}{f_{23}} \right).$$

The central configuration is at $\theta = \xi = 0$ and $\nu_0^2 = 2V(0) = 1/\sqrt{2} + O(\epsilon)$.

On the collision manifold, the differential equation for ν can be written $\nu' = \gamma^2/(2\phi)$ and also $\xi' = \gamma/\theta^*$ so

$$\frac{d\nu}{d\xi} = \frac{\theta^* \gamma}{2\phi}.$$

Now $\theta^* = O(\epsilon)$ and the energy equation shows that that

$$\left| \frac{\gamma}{\phi} \right| \leq \sqrt{2W/\phi} = \sqrt{2V} \leq \frac{K}{\sqrt{1 - \xi^2}}$$

for some constant K .

Since this upper bound is integrable on $[-1, 1]$ it follows that as ξ increases from -1 to 1 or decreases from 1 to -1 , the change in the increasing function ν is $O(\epsilon)$. Thus the number of oscillations of ξ over this interval in order that ν increases from $-\nu_0$ to ν_0 tends to infinity like $O(1/\epsilon)$ as $\epsilon \rightarrow 0$ QED

Suppose the masses are such that at least one of the branches of $W^u(p_-)$ winds up one of the arms of the collision manifold. Along the branch the size variable $r(\tau) = 0$ while the size velocity $\nu(\tau) \rightarrow \infty$. It follows that, given any constant N , there exist near-collision solutions reach $\nu(\tau) = N$ with $r(\tau) > 0$ arbitrarily small. It's interesting to consider what happens to the three bodies for such a solution.

Consider an initial condition with $\nu(0) = N, r(0) = r_0 > 0$ and suppose for definiteness that the solution has followed a branch of $W^u(p_-)$ near $\theta = \theta_1$. If N is sufficiently large, this implies that m_1, m_3 form a tight binary, relatively far

from m_2 . To see this note that, assuming that $r_{min} = r_{13}$ is the smallest of the (normalized) mutual distances, the energy equation gives

$$\frac{1}{2}\nu^2 - r_0 h \leq V = \frac{m_1 m_2}{r_{12}} + \frac{m_1 m_3}{r_{13}} + \frac{m_2 m_3}{r_{23}} \leq \frac{K}{r_{13}} \quad K = m_1 m_2 + m_1 m_3 + m_2 m_3.$$

If $\nu \geq N$ this implies $r_{min} \leq 2K/(N^2 - 2r_0 h)$. If N is large, r_{13} will be small. Now the normalization equation implies that the largest normalized distance, $r_{max} = r_{12}$ in this case, satisfies

$$1 = \frac{1}{m}(m_1 m_2 r_{12}^2 + m_1 m_3 r_{13}^2 + m_2 m_3 r_{23}^2) \leq \frac{K}{m} r_{max}^2$$

where $m = m_1 + m_2 + m_3$. Therefore the ratio

$$\frac{r_{min}}{r_{max}} = \frac{r_{13}}{r_{12}} \leq \frac{2K^{\frac{3}{2}}}{\sqrt{m}(N^2 - r_0 h)}$$

which is small when N is large. Then since $r_{23} = r_{12} - r_{13} = r_{max} - r_{min}$, the ratio r_{13}/r_{23} is also small. Of course these statements about ratios also apply to the mutual distances of the unnormalized configuration.

Next it will be shown that if N large, the lone body m_2 moves away from the binary formed by m_1, m_3 at high velocity. For this it's convenient to introduce another set of Jacobi coordinates $y_1 = q_3 - q_2$, $y_2 = q_2 - \beta_1 q_1 - \beta_3 q_3$ where $\beta_i = m_i/(m_1 + m_3)$. It will be shown that \dot{y}_2 is large and positive.

The size variable r satisfies

$$r^2 = \mu_1 y_1^2 + \mu_2 y_2^2 \quad r\dot{r} = \mu_1 y_1 \dot{y}_1 + \mu_2 y_2 \dot{y}_2$$

where now $\mu_1 = m_1 m_3 / (m_1 + m_3)$ and $\mu_2 = m_2 (m_1 + m_3) / (m_1 + m_2 + m_3)$. In terms of the blown-up variables, $\dot{r} = \nu / \sqrt{r}$ so $r\dot{r} = \sqrt{r}\nu$. If $|y_1| = rr_{13}$ is the smallest of the unnormalized mutual distances, the unnormalized energy equation gives

$$\mu_1 \dot{y}_1^2 \leq 2h + \frac{2K}{|y_1|}$$

so $\mu_1 y_1^2 \dot{y}_1^2 \leq (2h|y_1| + 2K)|y_1|$ and

$$\mu_2 y_2 \dot{y}_2 \geq \sqrt{r}\nu - \sqrt{\mu_1(2h|y_1| + 2K)|y_1|}.$$

Recall that with fixed $r_0 > 0$, one can arrange that the ratios $r_{13}/r_{12}, r_{13}/r_{23}$ can be made arbitrarily small by choose $\nu \geq N$ with N sufficiently large. This implies that the ratios $|y_1|/|y_2|, |y_1|/r$ can also be made arbitrarily small, say less than some $\delta > 0$. Then r_0 and $y_2 > 0$ are related by $r_0 \leq Cy_2$, where $C = \sqrt{\mu_1 \delta^2 + \mu_2}$. Then

$$\mu_2 \dot{y}_2 \geq \frac{CN}{\sqrt{r_0}} - C \sqrt{\mu_1(2h\delta + 2K/r_0)}.$$

For fixed $r_0 > 0$, one can make \dot{y}_2 arbitrarily large.

To summarize: if the branches of the saddles in the collision manifold spiral up the arms then one can find near collision solutions which emerge from their close encounter with collision in an arbitrarily tight binary configuration. Moreover, the velocity of separation between the binary and the third mass can be made arbitrarily large.

Exercise 7.19. Prove Proposition 7.19.

REFERENCES

- [1] Albert, A.A., *An inductive proof of Descartes' rule of signs*, Amer.Math.Monthly (1943), 178–180.
- [2] A. Albouy and A. Chenciner, *Le problème des n corps et les distances mutuelles*, Inv. Math., **131** (1998) 151–184.
- [3] Arnold, V. I., *Geometrical methods in the theory of ordinary differential equations*. Vol. 250. Springer Science & Business Media, 2012.
- [4] V.I. Arnold, *Mathematical Methods of Classical Mechanics*, 2nd ed., Springer-Verlag, New York, 1989.
- [5] R.Broucke, *Regularization of the plane restricted three-body problem*, Icarus, **4**, (1965) 8–18.
- [6] Conkwright, N.B., *Theory of equations*. Ginn and Co., Boston, 1957.
- [7] C.C. Conley, *The retrograde circular solutions of the restricted three-body problem via a submanifold convex to the flow*, SIAM J. Appl. Math., **16**, (1968) 620–625.
- [8] C.C. Conley, *Isolated Invariant Sets and the Morse Index*, CBMS Regional Conference Series, 38, American Mathematical Society (1978).
- [9] C.C. Conley and R.W. Easton, *Isolated invariant sets and isolating blocks*, Trans. AMS, **158**, 1 (1971) 35–60.
- [10] L. Euler, *De motu rectilineo trium corporum se mutuo attrahentium*, Novi Comm. Acad. Sci. Imp. Petrop. **11** (1767) 144–151.
- [11] Hill, G. W., *Researches in the lunar theory* Amer.J.Math. 1,1 (1878), 5–26.
- [12] Laskar, J., *Andoyer construction for Hill and Delaunay variables*, Cel.Mech.Dyn.Astr. 128,4 (2017), 475–482.
- [13] R. McGehee, *Triple collision in the collinear three-body problem*, Inv. Math., **27**, (1974) 191–227.
- [14] R. McGehee, *Singularities in classical celestial mechanics*, Proc.Int.Cong.Math., Helsinki, (1978), 827–834.
- [15] K. Meyer, G.Hall and D.Offin *Introduction to Hamiltonian Dynamical Systems and the N-body Problem*, Springer-Verlag, New York (2009).
- [16] Lectures on Central Configurations
- [17] R. Moeckel, *Chaotic dynamics near triple collision*, Arch. Rat. Mech, v. 107, no. 1, 37–69, 1989.
- [18] R. Moeckel, *Heteroclinic phenomena in the isosceles three-body problem*, SIAM Jour. Math. Anal., v. 15, 857–876, 1984.
- [19] Moser, J., *Regularization of Kepler's problem and the averaging method on a manifold*, Comm.PureAppl.Math. 23 (1970), 609–636.
- [20] F. R. Moulton, *The Straight Line Solutions of the Problem of n Bodies*, Ann. of Math. **12** (1910) 1–17.
- [21] C.L. Siegel, *Der dreierstoss*, Ann.Math, **42** (1941) 127–168.
- [22] C.L. Siegel and J. Moser, *Lectures on Celestial Mechanics*, Springer-Verlag, New York (1971).
- [23] NASA data,
https://nssdc.gsfc.nasa.gov/planetary/factsheet/planetfact_notes.html
- [24] Souriau, J.M., *Sur la variété de Kepler*, Symp.Math, 14 (1974) 343–360.